Analysis and Development of Energy Efficient Techniques for 5G Green Cognitive Radio Network

Ph.D. Thesis

by

Akanksha Srivastava

DEPARTMENT OF ELECTRONICS & COMMUNICATION ENGINEERING

Delhi Technological University

(Formerly Delhi College of Engineering)

Shahbad Daulatpur, Bawana Road-Delhi-42 (India)

October, 2023

Analysis and Development of Energy Efficient Techniques for 5G Green Cognitive Radio Network

A Thesis submitted
in partial fulfillment of the requirements
for the Degree of

Doctor of Philosophy

in

Electronics & Communication Engineering

by

Akanksha Srivastava

(Enrollment No. : 2K19/Ph.D./EC/10)

Under the guidance of
Dr. Gurjit Kaur
Professor

DEPARTMENT OF ELECTRONICS & COMMUNICATION ENGINEERING
Delhi Technological University
(Formerly Delhi College of Engineering)
Shahbad Daulatpur, Bawana Road-Delhi-42 (India)

October, 2023

DELHI TECHNOLOGICAL UNIVERSITY
(Formerly Delhi College of Engineering)
Shahbad Daulatpur, Bawana Road- Delhi-42
Electronics & Communication Engg. Deptt.

CERTIFICATE

I hereby certify that the work which is being presented in Thesis entitled **"Analysis and Development of Energy Efficient Techniques for 5G Green Cognitive Radio Network,"** in partial fulfillment of the requirements for the Degree of **Doctor of Philosophy** submitted in Department of Electronics & Communication Engineering, Delhi Technological University, Delhi, is an authentic record of my own work carried out under the supervision of **Dr. Gurjit Kaur, Professor**, Department of Electronics & Communication Engineering, Delhi Technological University Delhi during a period from July 2019 to February 2023.

The matter presented in this thesis has not been submitted by me for the award of any other degree elsewhere.

Akanksha Srivastava
03/10/2023

Signature of Candidate
Akanksha Srivastava
Enrollment No. : 2K19/Ph.D./EC/10

This is to certify that the above statement made by the candidate is correct to the best of my knowledge.

Gurjit Kaur
03/10/2023

Signature of Supervisor
Dr. Gurjit Kaur
Professor, ECE Department

Acknowledgment

My Ph.D. journey comprises a lot of learning and achievements which I culminate with this thesis. The credit for its success is the people who always stood by me and encouraged me during the journey. I am very grateful to have them in my life. I want to express my gratitude to all of them.

I feel immense pleasure in expressing my profound gratitude to my thesis supervisor Dr. Gurjit Kaur, whose inspiring guidance and supervision I had the privilege to carry out my research work. I am indebted to her for her constant and ungrudging encouragement, ingenious ideas, and valuable suggestions. She showed me different ways to approach a research problem and the need to be persistent to accomplish any goal. I also appreciate her enthusiasm, insights, and productive suggestions on this research. I admire many of her qualities and seek to learn from her. The way she keeps raising the research standards and devotes herself to whatever she works on will continue to inspire me all along my life. Her immense patience and advice have had a positive influence on not only my research but also on my further career.

I express my thanks to the Head of the Department and office staff of the Department of ECE for all kinds of support provided. I thankfully acknowledge the support and inspiration that I received from Prof. S. Indu, Prof. Neeta Pandey, Prof. Poornima Mittal, and Prof. Jeebananda Panda. Their useful suggestions and feedback helped me a lot in improving my research work in the present thesis I also wish to express sincere gratitude to all the other faculty members of the ECE department, DTU, Delhi, for their support and encouragement. I am deeply appreciative of DTUs support in providing lab facilities and infrastructure. Furthermore, I extend my sincere thanks to the Department of Science and Technology, Government of India, for their essential financial assistance.

I also express my thanks to my husband Dr. Mani Shekhar Gupta for the beautiful partnership of responsibilities that we share and supported me so strongly that I could focus on my research work. His valuable suggestions helped me a lot in my Ph.D work.

Though it is beyond the scope of any acknowledgment for all that I have received from my beloved parents Sh. Dinesh Kumar Srivastava and Smt. Manorama Srivastava, by the way of inspiration, patience, and encouragement at all times but most conspicuously during this period, yet I make an effort to express my heartfelt and affectionate gratitude to them. I also owe an extreme debt of gratitude to Mrs. Astha Srivastava, Mr. Ajitesh Ranjan, and Atharv Srivastava who helped me by giving me time to complete my thesis.

I wish to acknowledge the enjoyable company rendered by my friends Puja Priya, Asbah Masih, Bhawna Rawat, Snehlata Yadav, Kirti Dalal, and Shikha Singhal. I would also like to acknowledge Dr. Ashok Kumar and Mr. Monish Bhatia who helped me many times with software-related issues.

Above all, thanks to the Almighty for granting me wisdom health, and strength to undertake this research task and enabling me to its completion.

Akanksha Srivastava
03/10/2023

Akanksha Srivastava

Abstract

WITH the growing cognizance of environmental concerns and global warming related to communication technologies, researchers have been seeking some solutions to minimize the consumption of energy in the telecommunication industry. There is a remarkable advancement in mobile communication from simple voice-based devices to ubiquitous data-hungry smart phones. The telecommunication industry expressions a serious energy consumption challenge. The existing static spectrum allocation-based technologies are not in a position to fulfill this extra spectrum requirement and handle this future traffic load. This volatile evolution of global traffic data urges research attention globally and can be handled by future cognitive radio networks (CRNs). This directed to the development of the idea of inclusion of CR technology with green networking. The Green Cognitive Radio Networks (GCRNs) are able to remove this limitation related to spectrum scarcity. The application of CR technology will be utilized to make the green (radiation free) environment in order to increase the spectrum resource opportunities available for next generation (6G) networking. We analyse that the energy- efficient green communication and seamless networking are very important pillars of smart city construction, and connect the different essential elements of smart cities. Emerging technologies such as green communication, artificial intelligence, cognitive technology, Internet of Things, machine learning and cloud computing are now being used in a significant manner to convert cities into ”smart cities”.

As a consequence, the main objective of the thesis is to investigate the schemes to allocate the resources/power efficiently in cognitive radio technology-enabled green networks to support intelligent telecommunication systems.

To start with, this thesis provides an introduction, subsequently by a overview of CRNs, spectrum management, energy efficiency measurement and power allocation. A detailed review of the current literature on the concerned has been presented.

The first objective of the thesis is to investigate various next generation green wireless communication networking techniques, with consideration of energy-efficient transmission. The futuristic technologies like cognitive radio, carrier aggregation, Terahertz communication, Internet of Things (IoT), massive MIMO (multiple-input multiple-output) and mm wavelength are briefly reviewed to prepare for advancing recent research contributions. It is followed by a discussion on the green CRN architecture and cognitive cycle. Further, the challenges related to green CRN and spectrum management are also reviewed.

The second objective examines two proposed channel selection strategies: probability-based and sensing-based channel selection strategies. The proposed channel selection methods evenly allocate the CU's traffic load among various applicant channels. Results of the work present that in the circumstances of huge traffic, SCSS reduces the total network time, while in the situation of low traffic, PCSS gives better results. These observations offer a vital perception in designing of traffic-adaptive channel selection strategy in the existence of PU's interruptions and sensing errors. The proposed strategies can minimize the total network time by 60% as compared to non-load balancing strategy for $\lambda_{cu} = 0.05$. Next, we calculate the total energy consumption at various operational modes in GCRN. The results indicate that the arrival rate of the CUs and the time spent on channel scanning affect the energy consumption of the network. The proposed channel selection strategies reduce energy consumption by 75% as compared to non-load balancing strategy.

The third objective analyzes the benefits of cooperation between SUs for detecting the PU's spectrum, through which the rapidity of the network can be improved. Two cases (having a distinct level of cooperation) have been exploited to reduce the sensing time. The first one is non-cooperative, in which all SUs independently sense the PU, and the first user who senses first, informs the presence of the PU to the other SUs via a central controller. The second is cooperative, in which SUs follow the protocols of Amplify-and-Forward cooperation to minimize the sensing time. The results show that the proposed joint cooperation spectrum sensing (JCSS) scheme increases the sensing probability for a vacant spectrum by as much as 34%. After this, we propose two distinct spectrum sensing schemes preset spectrum sensing (PSS) and viscous spectrum sensing (VSS) that presents the energy savings percentage in GCRNs under specific conditions.

These results conclude that the energy consumed by the user's contention increases due to the increase in sensing time. The proposed schemes are better in terms of scalability because it is not essential to sense all spectrums in these schemes.

The fourth objective has analysed a cooperation-based energy-efficient scheme for cognitive users in GCRN to improve the energy efficiency of CU. The proposed cooperation-based energy-aware reward (CEAR) scheme supports CUs to actively cooperate by utilizing temporal and antenna diversity to improve energy efficiency. The proposed CEAR scheme is compared with other existing schemes, and it is presented that the CEAR scheme provides up to 28% improvement in energy efficiency. In this work, the optimal stopping protocol is used for problem formulation, and the backward induction method is employed for solving the decision problem. This chapter has contributed significant insight in terms of energy efficiency, spectral efficiency, throughput, and consumed energy, which motivates the design of future green communications systems.

In the final objective,a real-time learning-based scheme has been proposed to control transmission power and decrease the overall network power consumption while supporting QoS for multilayers. The reinforcement learning method takes into account the influence of cognitive transmitters' actions on the transmission power policy that has been chosen. In addition to this, the proposed ROPC scheme is based on the upgradation method for the Q-value. This feature of scheme helps to decrease the state/action pair and improves convergence speed. The suggested scheme's performance is proved by simulation, which shows that it achieves faster convergence and higher EE, SNIR, and SE than existing schemes.

In the end, the thesis briefs the research objective findings and come up with the proposal for the future aspect of the research work.

Contents

List of Figures

List of Tables

Nomenclature

List of Abbreviations

AMPS	Advanced Mobile Phone Service
APs	Access Points
ASIC	Application-specific integrated circuit
CRB	CR Base Station
CRNs	Cognitive Radio Networks
IoT	Internet of Thing
IPR	Interference Power Restraint
LTE-A	Long Term Evolution Advanced
MIMO	Multiple-Input Multiple-Output
OFDM	Orthogonal Frequency Division Multiplexing
PoA	Plan of Action
QoE	Quality of Experiance
SAR	Specific Absorption Rate
SDR	Software Defined Radios
SE	Stackelberg Equilibrium
SG	Stackelberg Game
SINR	Signal to Interference Noise Ratio
SM	Spatial Multiplexing
UDN	Ultra Dense Network

Chapter 1

Introduction

This chapter briefly explained the overview of the thesis followed by motivation, research gap, objectives and research methodology.

1.1 Motivation

WITH the growing cognizance of environmental concerns and global warming related to communication technologies, researchers have been seeking some solutions to minimize the energy consumption in the telecommunication industry. There is a remarkable advancement in mobile communication from simple voice-based devices to ubiquitous data-hungry smartphones. The telecommunication industry expressions a serious energy consumption challenge. The existing static spectrum allocation-based technologies are not in a position to fulfill the extra spectrum requirement and handle this future traffic load. This volatile evolution of global traffic data urges research attention globally and can be handled by future cognitive radio networks (CRNs). Thus, CR technology and green networking can be combined for designing of next generation networks. The Green Cognitive Radio Networks (GCRNs) are able to remove this limitation related to spectrum scarcity. The application of CR technology will be utilized to make the green (radiation free) environment in order to increase the spectrum resource opportunities available for next generation (5G and beyond) networking. We analyse that the energy-efficient green communication and seamless networking are very important pillars of smart city construction. Emerging technologies such as green communication, artificial intelligence, cognitive technology and Internet of Things are now being used in a significant manner to convert cities into ”smart cities”.

1.2 Objectives

The key objective of the thesis is to develop and analyses the schemes to support energy efficient transmission and management of the spectrum in GCRN to support next generation (5G and beyond) wireless networks.

To achieve this, the given sub-objectives are framed as follows:

1. To analyse the various energy efficient transmission schemes and develop the improved schemes to solve the issues like traffic imbalance problem, blocking probability, power management and also improve the energy efficiency for 5G green cognitive radio network.

2. To propose a scheme based on resource management to solve the traffic imbalance problem for 5G green cognitive radio network.

3. To develop a scheme based on cooperative cognitive radio which can reduce the blocking probability and improve the energy efficiency of 5G green cognitive radio network.

4. To develop a scheme based on heterogeneous network architecture to solve the issue of adaptive power management for 5G green cognitive radio network.

5. To propose a machine learning based spectrum management scheme for 5G green cognitive radio network.

1.3 Challenges

1. The surge of EE at a single stage of the communication system might be the reason for the decline at another stage of the system. For instance, the usage of a cognitive radio system may decrease the transmission energy by using proper bandwidth but drain additional power in the process of sensing the spectrum hole of the second network.

2. A trade-off between EE and QoS.

3. A traffic imbalance (load balancing) problem in heterogeneous networks.

4. Analysis of spectrum/power allocation issues in GCRN.

5. How to minimize the blocking probability arises due to the resource's unavailability in the network?

6. What is the minimum and maximum permissible power to the SUs to avoid interference?

7. A trade-off between flexibility and EE.

1.4 Major Contributions

The major contributions of this thesis are summarized below:

- The futuristic technologies like cognitive radio, carrier aggregation, Terahertz communication, Internet of Things (IoT), massive MIMO (multiple-input multiple-output) and mm wavelength are briefly reviewed to prepare for advancing recent research contributions. This chapter also covers challenges, applications, and research directions for next generation communication system, which contribute an overview of the active research initiatives in the area of green networks and encourage future studies and research activities.

- In the direction of next generation network, two channel selection strategies are proposed with multiuser channel decision framework. In the probability-based channel selection strategy, optimum distribution probability and busy channel probability have been derived. These calculations show the distribution of CU's traffic load among the various applicant channels. In the sensing-based strategy, the optimum number of applicant channels has been estimated, which helps to minimize the sensing time. The energy consumption is analysed in a GCRN for various operational modes like transmission mode, collision mode, receiving mode, sleep mode, channel sensing mode, and propose a channel scanning scheme, with the consideration of various parameters (like energy consumption, scanning time, and the number of PUs in a channel) as a metric.

- The advantages of cooperative communication are introduced, and a joint cooperation spectrum sensing (JCSS) scheme is proposed for GCRNs. The amplitude-

and-forward (AF) cooperative technique and the network's inherent asymmetry property are considered, which results in faster spectrum sensing with cooperation. The total sensing time and rapidity gain under the proposed cooperation scheme is investigated. The results show a significant reduction in sensing time for PU's spectrum. Based on energy harvesting, two spectrum sensing schemes are proposed named as preset spectrum sensing (PSS) and viscous spectrum sensing (VSS). These schemes are based on different parameters (i.e., energy-saving percentage and number of contending users in any spectrum).

- A novel cooperation-based energy-aware reward (CEAR) scheme has been proposed for CUs that takes antennae diversity and temporal diversity into account for improving the EE in CRNs. In antenna diversity, the PU that one has the least traffic load is selected by the CU. In temporal diversity, the CUs select a specific time slot when an immediate incentive is higher than anticipated in terms of EE. Two different cases have been considered for the analysis of the proposed CEAR scheme. In the first case, the CUs contain a fixed amount of packets to transmit. In second, the CUs contain continuously new incoming packets throughout the data transmission and decision process. In this case, the data transmission time limit is considered dynamic in nature and depends on the CUs' buffer overflow probability. For both cases, the optimal stopping protocol is implemented for decision problem analysis, and the backward induction method is exploited for determining the optimal solution.

- A reinforcement learning-based optimal power control (ROPC) scheme is proposed to address the complex power-related issues in multilayer GCRNs. The real-time learning feature is exploited in the proposed ROPC scheme. Real-time learning requires complete knowledge about all the learning agents present in dynamic environment, and this process is challenging in the context of the heterogeneous environment.In a heterogeneous CRN environment, each cognitive transmitter (CT) updates its learning information by interacting with the environment and exploiting its previous experience, without cooperating with other CTs. This feature of the proposed scheme minimizes the cooperation overhead and helps to design the energy-efficient GCRNs. A concise representation of the Q-values is considered to minimize the network's computational complexity.

1.5 Thesis Outline

The thesis is outlined as follows:

Chapter 2 (**Literature Review**) discussed about available literature and background related to advanced wireless networks. At the beginning, a brief idea about CR technology is explained. This chapter also provides the key concept of various next generation green wireless communication networking techniques, with consideration of energy-efficient transmission. The futuristic technologies like cognitive radio, carrier aggregation, Terahertz communication, Internet of Things (IoT), massive MIMO (multiple-input multiple-output) and mm wavelength are briefly reviewed to prepare for advancing recent research contributions. Further, the challenges related to green CRN and spectrum management are also reviewed.

Chapter 3, (**Resource Management for Traffic Imbalance Problem in Green Cognitive Radio Network**) deals with the unbalanced traffic load of CUs (when multiple CUs try to approach the same channel and their time and energy are wasted due to congestion). The channel decision model is proposed that is based on queuing priority for two different channel selection strategies, first probability-based channel selection strategy (PCSS) and second sensing-based channel selection strategy (SCSS). This model helps to calculate the optimum channel selection probability in PCSS and the optimum number of channels in the SCSS. By these parameters, the total network time of CUs can be minimized, and their traffic load can be distributed among multiple applicant channels. The proposed strategies minimize the total network time over 60% and energy consumption over 75% compared to the non-load balancing strategy.

Chapter 4 (**Cooperation and Energy Harvesting based Spectrum Sensing Schemes for Green Cognitive Radio Networks**) deals with multilayer heterogeneous GCRNs. The secondary users (micro users and femto users) are exploited the resources of primary users (macro users) in an underlay manner. In a multilayer heterogeneous network, efficient power control with improved quality of service (QoS) is a critical challenge. In this work total sensing time and rapidity gain under the proposed cooperation scheme is investigated. The results show a significant reduction in sensing time for PU's spectrum.

Chapter 5 (**CEAR: A Cooperation based Energy Aware Reward Scheme for Next Generation Green Cognitive Radio Networks**) studies a proposed CEAR scheme

that is based on the antenna and temporal diversity of the primary users (PUs). For providing the service to the PUs, the users of another network called cognitive users (CUs) work as a cooperative relay node, and, in return, they get more spectrum access opportunities as a reward from the primary network. The CUs with delay-tolerant data packets take a cooperative decision by recognizing the availability and traffic load of PUs, channel state information, and data transmission requirements. We utilized the optimal stopping protocol for solving the decision-making problem and use the backward induction method to obtain the optimal cooperative solution. The proposed CEAR scheme is more energy-efficient for ultra-dense network deployment because results show that the CUs EE, spectral efficiency (SE), and throughput improved with the increase of PUs.

Chapter 6 (**Machine Learning based Optimal Power Control Scheme for Next Generation Multi-layer Green Cognitive Radio Networks**) is the final contributory chapter that deals with a real-time learning-based scheme to control transmission power and decrease the overall network power consumption while supporting QoS for multi-layers. The reinforcement learning method takes into account the influence of cognitive transmitters' actions on the transmission power policy that has been chosen. In addition to this, the proposed ROPC scheme is based on the upgradation method for the Q-value. This feature of scheme helps to decrease the state/action pair and improves convergence speed. The suggested scheme's performance is proved by simulation, which shows that it achieves faster convergence and higher EE, SNIR, and SE than existing schemes.

The final chapter 7 (**Conclusions and Future Direction**) highlights the important conclusions drawn from these research objectives and gives the details of future scope of work.

1.6 Conclusions

In this chapter, a brief summary of the thesis followed by motivation, research gaps, challenges, objectives, contributions and research methodology are presented. In this thesis, green network is designed and analyzed to support intelligent telecommunication system for next generation wireless networks. The main results obtained in the work and how they contribute to the designing of energy efficient green communication are discussed.

Chapter 2

Literature Review

IN the last few years, the mobile telecommunication industry has increased exponentially. The call for wireless applications is growing because of the astronomical boom of mobile subscribers, multimedia applications, and data applications. In this thesis, the word green cognitive radio (CR) communication is used to express an efficient method of the congregation of energy-efficient technologies at different levels to reduce the unfavorable effects of technology on the environment. Globally, by the year 2022, the internet user population will be increased from 45.3% to 59.7% [1]. In addition to this, Fig. 2.1 depicts the growth rate of different parameters from 2018 to 2025 [2]. The nuts and bolts of a telecommunication network are a mobile node, access network and a backbone core network. Base Stations (BSs) are the key component of the radio access network that connects mobile phone devices to a core network. So, with a growth rate in the number of mobile subscribers per day, the growth rate of BSs is also increasing. According to [3] it is expected that during period $2017-2021$, the BS market of Long Term Evaluation (LTE) system will increase by more than 17 percent compound annual growth rate (CAGR).

2.1 Green Communication Networks

Available literature work centering on improving both quality of service (QoS) and quality of experience (QoE), while ignoring the increased demand for energy for the mobile communication system. This increasing energy demand has motivated us to work on the subject of cognitive-based green communication with the objective of energy-efficient

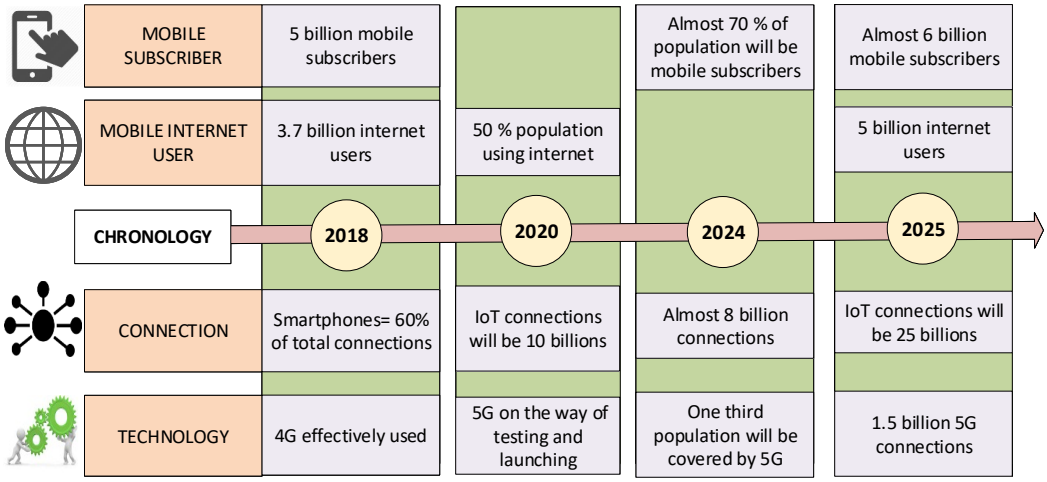

Figure 2.1: Breakthrough in the field of telecommunication industry

wireless communication. Based on our studies, we found two major goals of the green communication network. The first is to reduce the CO_2 emission from the system and second is to save energy by reducing transmitting power which will lead to reducing the operational expenditures (OPEX). The off-grid sites (to serve in remote areas) are the main cause of CO_2 emission. Mostly diesel-power generators are required for working on such sites. Presently, as the number of mobile subscribers is increasing, nearly 43% of the total CO_2 emission is contributed by the mobile communication system and this value will increase by 51% of the total in 2020 [4]. Due to the different segments of the mobile communication system, the CO_2 level is continuously increasing in the atmosphere. The electrical energy consumption by the ICT will be increased from 611 to $1,752$ Tera-watt hours by 2030 [5]. This rapid energy consumption rate by wireless communication networks will cause a serious problem in the future if no steps are taken to change the existing trend.

The telecommunication industry expressions a serious energy consumption challenge. This industry is growing rapidly to serve the smartphone user anywhere, anytime and anyone. The simple reason is that every human is using dual a SIM card enabled phone. At the end of 2019, in the Asia Pacific there were 2.9 billion (nearly the world's half population) mobile subscribers [6]. India and China are the most populous countries, which jointly covers nearly two-thirds of total mobile users. Nearly, 71.9 million mobile users are expected to be added in China by 2025, which is nearly 1.2 billion

(85%) of the total population [7]. On the other hand, in India, it is expected to be nearly 207.9 million (22% of total Asia Pacific) by 2025. So, this makes a remarkable improvement in digital literacy and advanced mobile phones. In 2018, Indonesia was developed as a third-largest mobile phone market in the world (behind India and China) [8]. The smartphone adoption rate is to be expected very high (nearly 90% of total connections) for Indonesia by the end of 2025. Fig. 2.2 depicts the technology penetration of the four fastest-growing countries. Fig shows the percentage of the population which was using the different wireless generation (2G, 3G, 4G and 5G) in 2018 and how much this percentage value will be changed when we will reach 2025. In China and Japan, the 2G population will completely remove till 2025, on the other hand, some populations will present in India and Indonesia.

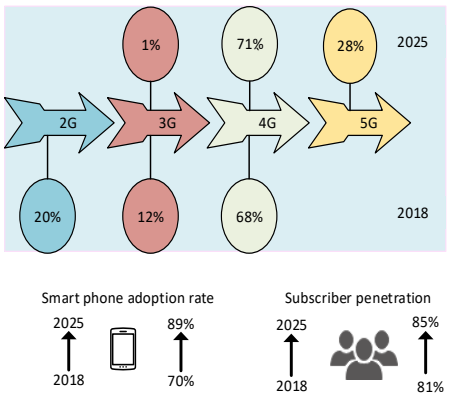

(a) Technology penetration for China

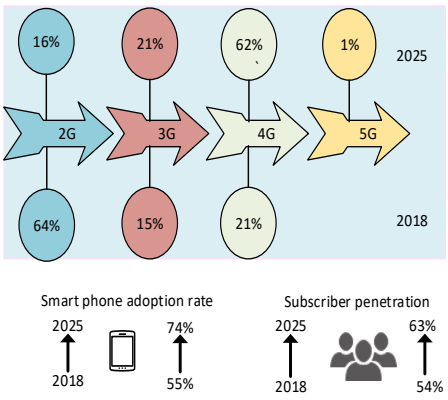

(b) Technology penetration for India

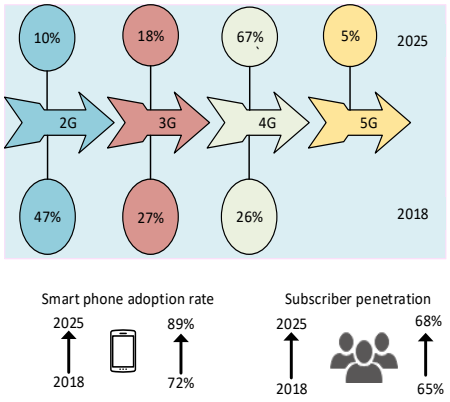

(c) Technology penetration for Indonesia

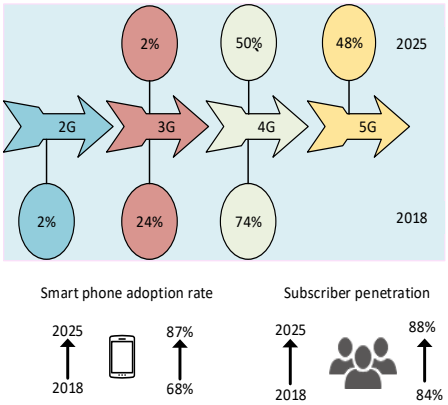

(d) Technology penetration for Japan

Figure 2.2: Technology penetration of different countries from year 2018 to 2025

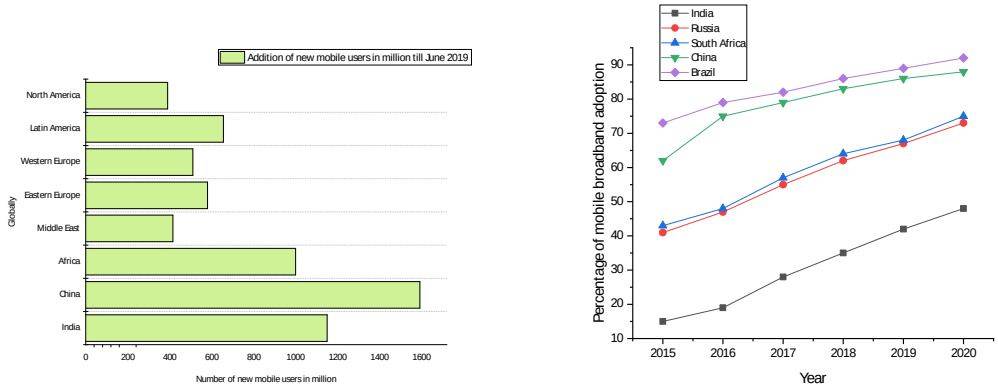

(a) Addition of new mobile users in million 2019 **(b)** Mobile broadband acquisition rate

Figure 2.3: Current global scenario of data hungry devices

In addition to this, Fig. 2.3a represents the addition of new mobile users globally till June 2019 in million [9] and Fig. 2.3b shows the mobile broadband adoption rate for different countries from 2015 to 2020. The wireless communication networks have experienced a prodigious evolution from 1G to 5G networks. Nowadays 4G is effectively in use and 5G on the way of testing and launching. Recently, during the testing of the 5G network, $100s$ of birds dropped from the sky at Hague in the Netherlands [10]. The 5G antenna was situated at the Dutch railway station, to examine how large the 5G range was. At once, birds fell dead from the sky and the ducks that were swimming in nearby ponds seemed to respond very strangely. To escape from radiation, they were instantaneously inserting their heads inside water whereas some flew away. If they all had a healthy body, healthy blood, no effect of any virus and bacterial infection then the reasonable explanation behind this incident is using of microwaves in 5G having a serious impact on birds' hearts. It highly resonates with erratic pulsed microwaves (millions per second) which harm body organs [11]. Table 2.1 represents the upgradation of the various generation of wireless networks. This table reflects different characteristics, to discuss a tangible contrast among the generations of wireless networks. In 5G a drastic growth in the CO_2 emissions is presented.

To overcome this problem a pathway is designed in Fig. 2.4 which represents greenhouse gas (GHG) deductions across different sectors to reach 2030. Fig. 2.4 shows that the amount of CO_2 was present almost 440 MMT in 2015 and the target is to reduce this value to 261 MMT till 2030. To curb such enormous emissions, various technologies have been discussed in this work.

Table 2.1: Upgradation and contrast among various generations of wireless networks in green communication aspect

Technology	1G	2G	3G	4G	5G
Frequency band	800 Mhz	900/1800 Mhz	1900/2100 Mhz	1.8/2.6 Ghz	30-300 Ghz
Power density ($Watt/meter^2$)	4	4.5-9	4.5-10	10	10
Power level of MS	Low	GSM 900:35 dBm GSM 1800:22-37 dBm	20-32 dBm	23 dBm	High
Power level of BS	Low	Macro 46 dBm, Micro 13-30 dBm	32-38 dBm	44-49 dBm	High
CO_2 emission	23 Mt CO_2	30 Mt CO_2	85 Mt CO_2	171 Mt CO_2	236 Mt CO_2
Carbon footprint per mobile	10kg	15kg	20kg	24kg	30kg
Date rate	2.4 Kbps	100 Kbps	2.4-30 Mbps	100-200 Mbps	10-50 Gbps
Access technology	AMPS	GSM-GPRS	WCDMA, UMTS	LTE-A, WiMAX	BDMA, FBMC
Spectral efficiency (bps/Hz)	0.46	1.4	2.7	4.27	10.6
MIMO/Massive MIMO	SISO	SISO	SIMO, MISO	MIMO	Massive MIMO
WLAN Technology	802.11	802.11b	802.11ag, 802.11n	802.11ac, 802.11an	802.11ad
BS density per square km	Very low	Low	4-5 BSs	8-10 BSs	40-50 BSs
OPEX	-	-	Low	High	High
SAR value	-	-	High	Higher	Expected to reduce
Used antenna	Low frequency antenna	High frequency antenna	High gain and clip antenna	Slot and Patch antenna	Phased array antennas

2.1.1 Preliminaries

As we know, the cellular system is the largest component of ICT sector. So, energy efficiency measurement (EEM) statistics have encouraged both academia and industry researchers to evolve methods to cut down the energy expenditure of cellular system and

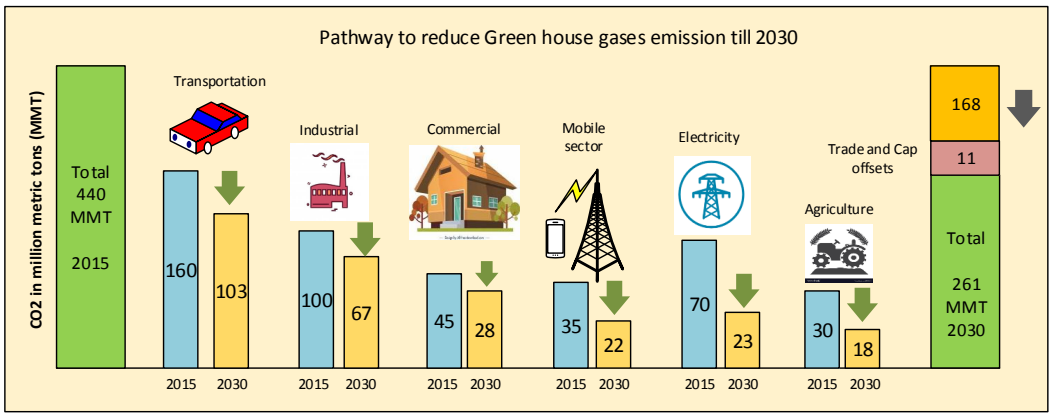

Figure 2.4: Aim to reduce GHG across various sectors to reach 2030

make the wireless network system greener. The primary goals of energy-aware green CRNs are:

- Improving EE.
- Improvement in the tradeoff between energy-saving and seamless connectivity.
- Reducing unnecessary GHG emission.
- Proper utilization of resources.

2.1.1.1 Energy Efficiency Measurement (EEM)

The number of BSs are continuously increasing to provide better QoE expected by mobile users. Thus, energy consumption will also increase proportionally. Fig. 2.5 represents that in a wireless communication network BS consumes the maximum amount of energy as compared to the other component of the network [12]. Nowadays this is a very crucial subject for research to find out some effective methods to minimize energy consumption by fixed and dynamic components of BS while maintaining the QoS. The internal components like digital signal processors, power amplifier (PA), feeder cables and cooling system of BS are considered under the fixed components while network planning, deployment and management based on proper load balancing are under the dynamic components. For the conversion of a base station into a green base station, several schemes have been suggested in [13]. A game theory-based scheme considers

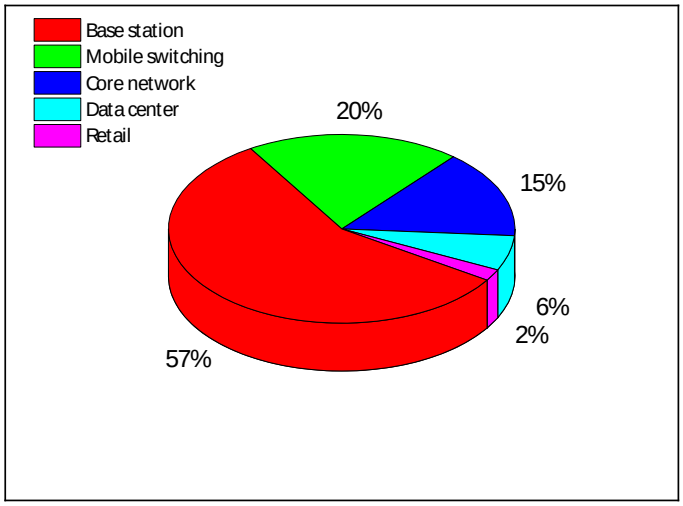

Figure 2.5: Energy consumption w.r.t. different components of communication system

heterogeneous networks for the reduction of power consumption at the base station level is discussed in [14]. A novel network architecture having energy-efficient techniques based on the physical layer and cross-layer of cellular networks is represented in [15]. Different research activities and projects based on energy- efficient communication has been considered in [16].

The various components in wireless networks consume different amounts of energy. So, for calculating and comparing the amount of energy which is consumed by the various components and a communication system as a whole, EE metrics are used. Researchers have been proposed different levels (facility, component, and system) for measuring EE metrics [17]. The high-level systems such as data centers are considered under the facility level [18]. Presently, with the upsurge in research activities on green energy efficient wireless networks, some standard organizations like European Technical Standards Institute (ETSI) and Alliance for Telecommunications Industry Solutions (ATIS) are making efforts to describe diverse EE metrics for wireless networks. The EE metrics consist of three major metrics as follows:

2.1.1.2 Energy Efficiency

EE is a very essential metric to measure in green wireless CRN [19]. This can be obtained by dividing network output energy to network input energy consumption [20]

and expressed as

$$\eta = \frac{\text{Network output energy}}{\text{Network input energy consumption}} \tag{2.1}$$

here η represent EE. The best EE can be achieved by minimizing total power consumption and maximizing the data rate.

2.1.1.3 Secrecy Energy Efficiency

This is another important metric consider under the system level. The high value of this metric provides better security in the CRN [21] [22]. This is given by

$$S_{EE} = \frac{\text{Secrecy rate}}{\text{Power consumption at network}} \tag{2.2}$$

here secrecy rate (SR) is defined as the difference of data transmission rate of the transmitter-receiver link to the transmitter-eavesdropper link and S_{EE} represents secrecy energy efficiency.

2.1.1.4 Area Energy Efficiency

The A_{EE} metric is considering for a dense deployment [14]. This can be obtained by dividing overall energy efficiency to the macro cell area and given by

$$A_{EE} = \frac{\text{Energy efficiency}}{\text{Total area of macrocell}} \tag{2.3}$$

here A_{EE} is area energy efficiency.

The readers can discover different taxonomy of green communication metrics which are summarized in Table 2.2.

2.1.2 Challenges and Existing Practical Implementations of Green Communication Networks

The framework to enhance the EE of telecommunication the system has a holistic view which considers possibly all facts and figures of an ecosystem for green communication. The several challenges related to green communication are listed as:-

- For estimating any energy efficient solution, the required energy for manufacturing of a communication system (called embodied energy) has a significant role.

Table 2.2: Summary for several EE metrics evaluation in green communication networks

Level	Metric	Remark	Unit	Reference
Facility level	Power usage efficiency	It gives the ratio of total power consumption at facility level to the total power consumption at equipment level.	PUE $\geq$1	[23, 24]
Facility level	Data center efficiency	Reciprocal of PUE	DCE in percentage	[23]
Element level	Energy consumption rating (ECR)	Ratio of energy consumed to the adequate system capacity.	$W/Gbps$	[17]
Element level	ECR-weighted (ECRW)	Evaluated in the similar manner as ECR but energy consumption is in ECRW is calculated as $0.25E_i$+$0.4E_h$+$0.35E_f$ here E_i, E_h and E_f represents energy consumption in idle mode, half and full load.	$W/Gbps$	[17]
Access point level	Energy consumption rate	Energy used to transmit a piece of information.	J/bit	[14, 25]
Access point level	Spectral efficiency	For a communication system, the transmitted information rate to a given frequency	$b/s/Hz$	[26, 27]
System level	Power per bit per area	The average power used in terms of the average transmission rate and the coverage area.	$W/bps/m^2$	[28, 29]
System level	Energy per bit per unit area	The energy consumed for transferring the bits for a particular coverage area.	$J/bit/m^2$	[24]
System level	The power consumed per unit area	Ratio of power consumed to unit area	W/km^2	[30]

- The surge of EE at a single stage of the communication system might be the reason for the decline at another stage of the system. For instance, the usage of a cognitive radio system may decrease the transmission energy by using proper bandwidth but drain additional power in the process of sensing the spectrum hole of the second network.

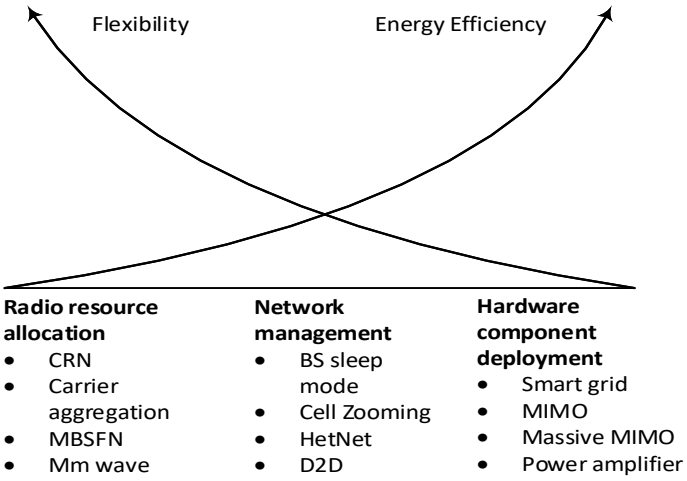

Figure 2.6: Tradeoff between flexibility and EE

- There should be a respectable trade-off between EE and QoS. Like the aforementioned usage of BS sleep modes technique, more energy can be saved during off mode of some cells. But, it is compulsory to stipulate the cell waking time in advance as well otherwise, the QoS may degrade.

- There should be also a proper trade-off between flexibility and EE which depicts in Fig. 2.6.

The energy-efficient solution depends on certain guidelines, concepts, parameters, energy consumption models and considerations. The energy consumption of the telecommunication system is load-dependent and implementation-dependent. These are the challenges for modeling the energy- efficient system. The EE metric for a green telecommunication system is generally expressed in the form of performance per unit of energy. The performance usually measured in terms of efficiency and throughput for the energy-efficient communication system. Other key challenges for designing the green energy-efficient system are cross-layer adaptation, system reconfiguration, load balancing, and multi-domain scheduling. It is necessary to gauge EE from a new perspective for designing and developing novel energy-efficient architecture.

The pathway represented in Fig. 2.7 to implement in the real world for making communication green is also having several challenges that need to be paid consideration too in this research area. Several challenges, related to green communication for

next generation networks are represented in Fig. 2.7.

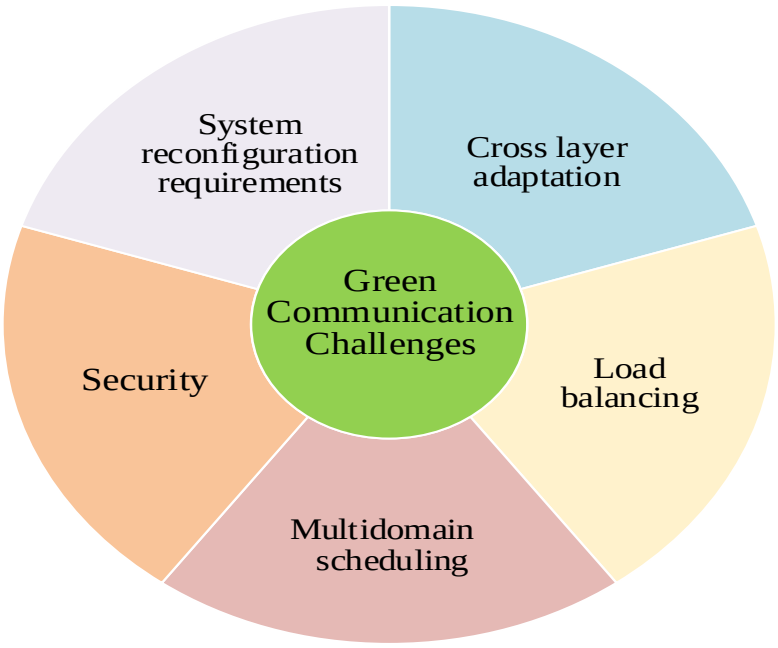

Figure 2.7: Green communication related challenges

2.2 Related Work for Proposed Objectives

In this section, several traditional and recent advanced energy efficient communication approaches for future GCRNs (5G and beyond) are considered with their detailed overview in an informational manner.

2.2.1 Related Work on Different Energy Efficient Transmission Schemes

Various energy-efficient communication approaches are highlighted in a classification tree as shown in Fig. 2.8. These different approaches are introduced by researches to handle various inspiring topics allied with GCRNs.

2.2.2 Related Work on Resource and Traffic Management in Cognitive Radio Network

In the literature, the investigations have been concentrated on various energy-related challenges of CRNs, but they are less focused on analyzing the energy consumption at different operational modes. In [31], the sensing time of CU is calculated, but with the

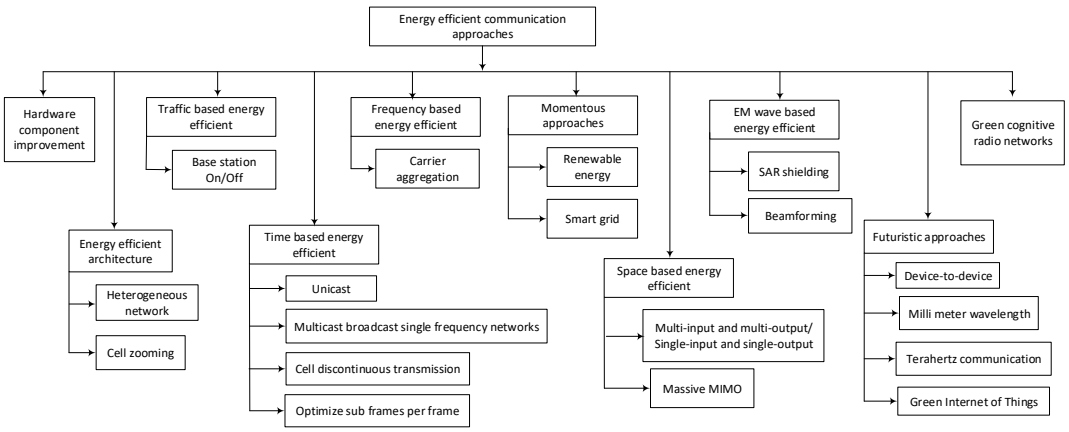

Figure 2.8: A classification tree of different energy efficient communication approaches

consideration that throughout the CU's transmission, the PU does not resume the channel. The channel assignment problem in CRN has been investigated via various optimization techniques in [32], but not consider the traffic load balancing of CUs. There are numerous issues are arisen in the non-load balancing method like, when more than one CUs approach the same channel then the confliction happens in the channel, the total network time of the CU is increased, the delay involves in the PU's transmission, no proper utilization of resources, etc. In the non-load balancing strategy, the CUs scrutinize various parameters for selecting the operating channel such as expected delay time, data traffic load, channel busy probability, channel idle time, but they avoid the requirement of sharing channels with other CUs. In [33], the authors calculate the energy consumption during the channel sensing and determine the optimal sensing interval, through which the throughput of CU's can be maximized. In [34], a joint optimization-based technique has been developed for intelligent spectrum allocation. This technique enhances the CU's throughput in a heterogeneous network. The frequency and power-based sensing techniques have been suggested in [35] but, the effects of sensing errors on CU's total network time CRN have not been discussed. A reinforcement learning based energy-efficient channel switching scheme for CUs is proposed in [36]. The authors have been presented a framework that aims to save energy the time of channel switching. In [37], authors have been focused on spectrum handoff schemes for optimum channel selection, but not consider the green communication aspect. Table 2.3 represents the comparison of various existing load-balancing channel selection strate-

gies, where "×" and "√" symbolizes that the proposed schemes "do not" and "do" examine the corresponding characteristic, respectively.

Table 2.3: Comparison of several load-balancing channel selection strategies in CRN

Channel Selection Strategies and Models	False Alarm Error	Missed Detection Error	Multiple Interruptions
Game theory based Deterministic Process [38]	×	×	×
Game theory-based M/M/1 Model [39]	×	×	√
Two-state Markov Chain Process [40]	×	×	×
Markov Chain Theory based Model [41]	×	×	√
Packet Probability based Bernoulli Process [42]	×	√	×
Learning Automata based General Distribution Approach [43]	√	×	×
Our M/G/1 based Proposed Model	√	√	√

2.2.3 Related Work on Energy Efficient Cooperative Cognitive Radio Network

Extensive studies are being carried out to maximize the sensing probability and save energy in GCRNs. We have surveyed various literature focusing on the spectrum sensing aspect of GCRNs. The sensing time of SU has been calculated in [44], but in the proposed work, there is an assumption that during the SU's transmission, the PU did not use the channel. The suggested scheme is based on orthogonal frequency division multiplexing (OFDM). In [45], authors have discussed the channel sensing technique but did not analyze the cooperative protocols like DF and AF techniques. In [46], the authors have estimated the consumption of energy at several channel decision states, but the energy dissipated in the channel sensing has not been investigated. The work presented in [38] mainly considers the different coding and modulation techniques for reducing the power consumption. In [47], a framework is proposed to calculate the energy consumption in the spectrum sensing process. They have divided the spectrum into various frequency bands. In [48], the authors proposed a receiver detection approach by utilizing the oscillator power of the PU.

In [49], the authors have presented a novel spectrum sensing energy harvesting (SSEH) scheme that is based on opportunistic relay selection (ORS) protocol. The proposed scheme is exploited cooperative communication for designing the CRNs. In [50], authors have presented frequency and time domain-based energy harvesting cognitive radio networks with the multichannel (EH-CRNsM) technique. In the suggested technique, the SUs consume harvested energy to access licensed subchannels opportunistically. An energy-efficient game-based power allocation (EGPA) scheme is suggested in [51]. The proposed scheme considers SU clustering and power allocation to improve the detection of PU's vacant spectrum in CRNs. In [52], the authors have presented an auction framework and Stackelberg game-oriented optimal network's resource selection (AFSOS) scheme to attain the acceptable interference power constraints and highest payoff in CRNs. The work presented in [53] suggests a preference relation game (PRG) scheme using a cooperative coalitional game (CCG) in hybrid NOMA (HNOMA) to maximize the energy efficiency in CRNs. In [54], authors have presented a network-assisted networks' resource selection (NANS) technique to ensure the guaranteed QoS and maintain mobility in GCRNs.

2.2.4 Related Work on Heterogeneous Green Cognitive Radio Network

In this chapter, we review the current literature based on spectrum management techniques for data communication and differentiate the proposed work from the existing works. Numerous works on energy-efficient CRNs for dissimilar networking technologies such as non-orthogonal multiple access (NOMA) assisted networks, ultra-dense networks, and cloud networks have been analyzed in several aspects. In [55], the authors presented a scheme to minimize the energy consumption of CUs from radio frequency signals. A packet error probability of CRNs is estimated considering the energy harvesting factor. The energy-harvesting-aided data transmission and channel sensing schemes are discussed in [56]. The results show that the schemes achieve high detection probability with sufficient energy harvested from the cognitive relay's RF signals. In [57], a multi-objective resource allocation problem is formulated to optimize the SE and EE in heterogeneous CRNs.

A probability-based dynamic model (PBDM) has been presented in [58], illustrat-

ing the analytical techniques for average throughput and energy harvesting. In [59], authors have proposed a novel multichannel protocol for CRNs to harvest the energy. The suggested protocol depends on the multiple channel states and intelligently selects whether to enter energy harvesting or data transmission modes. In [60], the authors have presented a joint optimization problem to maximize the sum rate of D2D users and cellular. The authors have considered channel assignment, transmission time allocation, user pairing, and power allocation for the analysis. An energy-efficient game-based power allocation (EGPA) scheme is suggested in [51]. The proposed scheme considers secondary user clustering and power allocation to improve the throughput of CRNs. A power-based pricing algorithm (PBPA) scheme is proposed in [61], which limits the PU's interference to acceptable levels and minimizes the computational complexity in down link CRNs.

2.2.5 Related Work on Different Machine Learning based Spectrum Management

In [55], the authors have proposed a power control scheme relying on BS traffic forecasting. The outcomes demonstrate the trade-off between energy usage and network rate with considering the backhaul constraint. Authors in [62], addressed an adaptive power control strategy based on the game theory technique for reducing the interference effect in heterogeneous networks. Markov decision process (MDP) based on a multi-agent distributed model has been proposed in [63]. This model optimizes the power control issue in the heterogeneous network. In [64], the authors have presented a multi-objective-based joint power and admission control (JPAC) optimization technique. The proposed technique aims to improve throughput of the network and reduce power consumption in underlay mode of operation in CRNs. In [65], authors proposed a reinforcement learning-based technique to optimize the sensing probability (SPORL). The suggested scheme enhances the EE of the system and maintains system coverage and capacity. A distributed utility function-based power control scheme (DUFPC) has been proposed in [66] to decrease the transmission power of the femtocell BS. This work aimed to maximize the utility function via regulating the transmission power of the femtocell BSs. A modified greedy algorithm (MGA) has been presented in [67] to mitigate the interference among secondary nodes while maintaining the network ca-

pacity. In [68], the authors presented a combined optimization algorithm for subcarrier allocation and power control, which minimizes cross-tier interference and maximizes the utility function of femtocell and macrocell. In addition to these works, Table 2.4 represents a comparison of existing power control schemes, models and protocols.

Table 2.4: Comparison of existing surveys

Type of machine learning	Structure	Power control	Energy efficiency	Spectral efficiency	Approach	Dynamic environment	Ref.
Supervised learning	SVM	Yes	No	No	Design SVM & DBN based learning system	Yes	[69]
Reinforcement learning	Q-learning	No	Yes	No	Q-learning based data dissemination method	Yes	[70]
Supervised learning	FNN	No	Yes	Yes	Taxonomy of feed forward neural network	Yes	[71]
Deep-learning	Q-learning	No	Yes	No	Q-learning based data dissemination method	Yes	[72]
Unsupervised Learning	K-means clustering	No	Yes	Yes	Joint genetic algorithm and unsupervised learning	Yes	[73]
Supervised learning	ANN	No	No	No	Hierarchical support vector machines	Yes	[74]

2.3 Conclusions

This chapter discussed the trends of the telecommunication system in the last decade which visualize a move towards following energy efficient green communication for the purpose of designing next-generation (5G and beyond) networks. For each energy efficient technique, an outline of the existing state of the art research, merits, demerits, open issues, challenges, and possible forward way research direction has been investigated.

Chapter 3

Resource Management for Traffic Imbalance Problem in Green Cognitive Radio Networks

THE trend of minimizing energy consumption in the field of telecommunication system encourages researchers to look for novel technologies to attain ”Green communication”. In GCRN, the cognitive user (CUs) can utilize the PU's channel opportunistically until the PU is not present at that particular geographic area and specific time slot. But, when the PU decides to send the information through the frequency band utilized by the CU, the CU should immediately leave the frequency band to avert a collision with the PU. The CUs again start the sensing of the vacant channel to complete their unfinished data transmission, at other channels, or the same channel after the end of the PU's communication. This process increases the energy consumption and total network time of CUs (defined as the entire period starts when the call for information transmission appears at the network by CU until their entire data transmission). Various parameters like multiple spectrum handoffs due to the interruptions of PUs, sensing errors like false alarm and missed detection, and different data transmission rates and capacity of the channels affect total network time. These parameters increase the total network time of CUs, which results in the wastage of network energy and increment in queue waiting time of other CUs for accessing the network services. So, it is essential to bring down the effects of these parameters. The reduced network time preserves the network's energy and increases the serving rate of the network.

By allocating the traffic load of CUs among all the applicant primary channels, the total network time of CUs can be minimized. In this chapter, two channel selection strategies are proposed and total network time of the CUs is calculated. The two strategies are, the first one is a probability-based channel selection strategy (PCSS), and the second is a sensing-based channel selection strategy (SCSS). In PCSS, the operating channel selection depends on predetermined probabilities taken from the long-term observations of the traffic statistics, while in SCSS, channel selection is based on instantaneous sensing outcomes, which are received after the wideband spectrum scanning. The proposed channel selection strategies have some design challenges like in PCSS; the main precaution is to forbid the CUs from selecting the busy channel, and in SCSS; scanning of all the applicant's channels increases the overall network time of CUs. One side where the narrowband sensing (less number of applicant channels) decreases the sensing time, but due to this the problem of finding a vacant channel among a small set of applicant channels is appeared. Hence, to find out the optimum number of applicants channel to reduce the total network time is one of the critical challenges. Therefore, in this chapter, we calculate the optimum channel selection probability in PCSS and the optimum number of channels in the SCSS with the consideration of the various interruptions from the PU, data rate, channel capacity, and sensing errors.

The energy required to transmit the CU's data via PU's vacant channels needs to be reduced under the high quality of service (QoS) demand for both primary and cognitive users. So, it requires analyzing the amount of energy used by the CUs in the network. We proposed a multiuser channel decision framework, which is enabled before the preemptive resume priority (PRP) M/G/1 based queueing model. With the help of the proposed framework, the traffic load of CUs can be evenly allocated among the multiple channels, unlike the non-load balancing strategy where different CUs approach for the same channel and waste their energy and time. The significant contributions of the work are highlighted as follows:

- Two channel selection strategies are proposed and design the multiuser channel decision framework for both strategies.
- In the probability-based channel selection strategy, optimum distribution probability and busy channel probability have been derived. These calculations show the distribution of CU's traffic load among the various applicant channels.

- In the sensing-based strategy, the optimum number of applicant channels has been estimated, which helps to minimize the sensing time.
- We compare the probability-based and sensing-based strategies and present their performances in terms of total network time for different arrival rates of CUs and other parameters.
- The energy consumption in a CRN is analyzed at various operational modes like transmission mode, collision mode, receiving mode, sleep mode, channel sensing mode, and propose a channel scanning scheme, with the consideration of various parameters (like energy consumption, scanning time, and the number of PUs in a channel) as a metric.

3.1 Network system model

In this section, we first, discuss some assumptions which are considered in this chapter. Then, the channel decision model is described. This model is adopted for evaluating the total network time of CUs in various channel selection strategies. After that, the sensing errors are discussed, and due to these sensing errors, the actual service time of CUs and PUs extends.

3.1.1 Assumption

In this chapter, a time-slotted cognitive radio network is considered, in which to detect and preserve the PU's channel. At the starting of every time slot the channel sensing must be performed by the CUs. If the detected channel is vacant, the CU sends its data (information) in the same time slot. On the other hand, if the detected channel is engaged, the CU may wait till the channel free, or it may sense the other channel. This listen-before-talk (LBT) method is followed in most of the wireless networks, like IEEE 802.11 standard-based clear channel assessment (CCA) and IEEE 802.22 standard-based quiet period [75].

3.1.2 Description of Channel Decision Model and Sensing Errors

The channel decision model is presented in Fig. 3.1, which is adopted for evaluating the total network time of CUs in various channel selection strategies. It is assumed that the traffic arrival rate for primary and cognitive users is Poisson. There is an assumption that the values of ${\lambda_{pu}}^{(j)}$, λ_{cu}, ${m_{pu}}^{(j)}(l)$, and $m_s(l)$ are known by all CUs and calculated by [76]. Hence, the service time is ${X_{pu}}^{(j)} \triangleq \frac{{B_{pu}}^{(j)}}{{D_{pu}}^{(j)}}$ and ${X_{cu}}^{(j)} \triangleq \frac{B_{cu}}{{D_{cu}}^{(j)}}$ for PU and CUs at channel j, respectively. Based on Fig. 3.1, one of the K applicant channels is selected by each CU and according to our proposed model, for proper traffic load balancing of CUs in multiple channels, all the CUs can dynamically obtain their functioning channels with appropriate probability. The probability distribution vector (written as $p = (p^{(1)}, p^{(2)}, ...p^{(K)})$ denotes the probabilities set for identifying the applicant channels, where $p^{(j)}$ represents the probability of CU obtaining channel j as its functioning channel. However, at channel j the effective arrival rate of the CU is ${\lambda_{cu}}^{(j)} = p^{(j)}\lambda_{cu}$. Note that the probability distribution vectors are different for different channel selection algorithms. The two types of sensing errors (i) missed detection (occur due to the

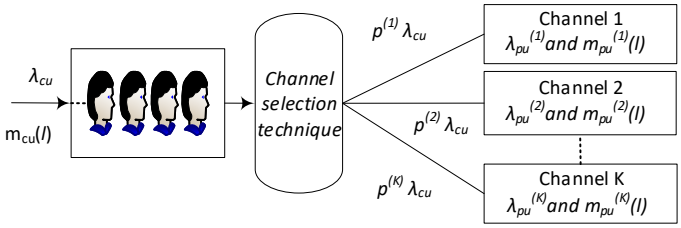

Figure 3.1: Channel decision model

interruption of cognitive connection, hence the PU has to resend the contaminated data frames in the upcoming slots) extends PU's service time from ${X_{pu}}^{(j)}$ to $\widehat{{X_{pu}}^{(j)}}$ and (ii) false alarm (when occur CU does not send data even the channel is idle) extends the service time of CU from ${X_{cu}}^{(j)}$ to $\widehat{{X_{cu}}^{(j)}}$.

3.2 Proposed Probability-based Channel Selection Strategy and Sensing-based Channel Selection Strategy

In this section, first, the total network time of CU in a network is formulated. Then, the optimum probability distribution vector in PCSS and the optimum number of applicant channels in SCSS are calculated for reducing the total network time. After this, the proposed framework for both strategies has been discussed and sensing error effects on service time of CUs and PUs have been presented. At the last, the energy consumption at different stages is analyzed.

3.2.1 Total Network Time

The total network time (indicated by A) is a significant performance metric for CU's connection-based service, and it consists of request time (R) and data transmission time (T), as represented in Fig. 3.2. The total network time in terms of expectation function is,

$$E[A] = E[R] + E[T] \tag{3.1}$$

Here, E[R] and E[T] represent the expected value of request time and data transmission time. The E[R] is the time duration, starts from the moment when the data sending petition reaches the network till the time of the beginning of data transmission. The request time interval depends on the channel selection strategy. The data transmission time (E[T]) starts at the moment of the beginning of data transmission in the initial time slot to the complete data transmission at the last slot. The data transmission time is affected by various handoffs performed in the system.

3.2.1.1 PCSS for Reducing Total Network Time

In probability-based strategy, every CU selects their communicating channel from the K applicant channels which depends on a predetermined probability distribution vector p_{pbc}. So, for this case the time minimization is formulated as, the given set of applicant channels is $\delta = \{1, 2, 3.....K\}$, our objective is to find out the optimum probability distribution vector (denoted as $\hat{p}$) to reduce the average total network time ($E[A_{pbc}]$) of CU.

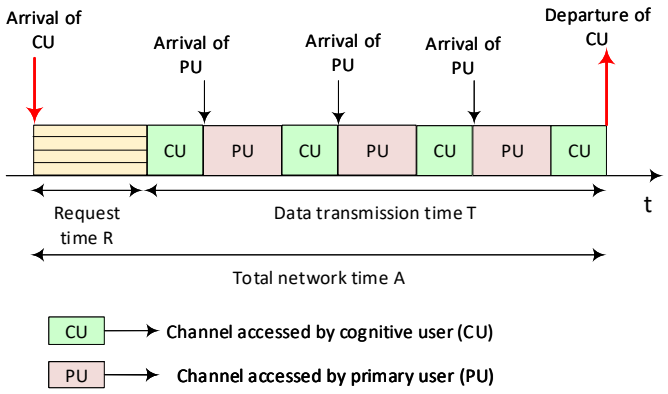

Figure 3.2: Total network time of cognitive user in CRN

Formally,

$$\hat{p} = \underset{\forall}{arg\,min}\, E[A_{pbc}(p_{pbc})] \tag{3.2}$$

s.t.

$$0 \leq {p_{pbc}}^{(j)} \leq 1, \forall j \in \delta, \tag{3.3}$$

$$\sum_{j\in\delta} {p_{pbc}}^{(j)} = \sum_{j=1}^{K} {p_{pbc}}^{(j)} = 1, \tag{3.4}$$

$$\varphi^{(j)} = {\varphi_{pu}}^{(j)} + {\varphi_{cu}}^{(j)} < 1, \tag{3.5}$$

where $\varphi^{(j)}$ shows the busy probability of j channel. Moreover, ${\varphi_{pu}}^{(j)}$ and ${\varphi_{cu}}^{(j)}$ are representing the busy probabilities obtained from the connections of PU and CUs at channel j when sensing errors are taken into the consideration. So, ${\varphi_{pu}}^{(j)} = {\lambda_{pu}}^{(j)} E[\widehat{X_{pu}}^{(j)}]$ and ${\varphi_{cu}}^{(j)} = {\lambda_{cu}}^{(j)} E[\widehat{X_{cu}}^{(j)}]$.

3.2.1.2 SCSS for Reducing Total Network Time

In sensing based strategy, wideband sensing is performed by the CUs to search out the vacant channel from the list of all available applicant channels. To minimize the total time of sensing, the CU scans only the best of n channels from K channels. Here, it is assumed that the lexicographic manner is followed by CUs for channel selection which is represented as if $i > m$, then i channel is not better than m channel. Let the total number of applicant channels are K and the set of applicant channels is $\delta = \{1, 2, 3 \ldots\ldots n\}$ where $n = |\delta| \leq K$. Now for minimizing the total network time ($E[A_{pbc}]$) in this strategy,

the objective is to search out the optimum number of applicant channels (given as $\hat{n}$)

$$\hat{n} = \underset{1 \le n \le K}{arg} \min E[A_{sbc}(n)] \tag{3.6}$$

3.2.2 Proposed Model and Total Network Time Calculation

For evaluating the total network time, the presented channel selection model is designed by including the PRP based M/G/1 queueing systems in both the channel selection strategies. Fig. 3.3 represents the probability-based model in which the CU's traffic load is immediately linked with the selected channel with the help of the predetermined probability distribution vector, while Fig. 3.4 expresses the sensing-based model in which the CU executes the spectrum sensing to search out the idle channels when CU's traffic arrives. A tapped delay circuit [[A]] is adopted to illustrate the total sensing time, and this circuit is observed as a server with constant service time. The CU can be directly served at once the idle channel is found. The proposed model describes the consequences of various sensing errors and interruptions on the total network time. Few key characteristics of this proposed queueing model are listed below.

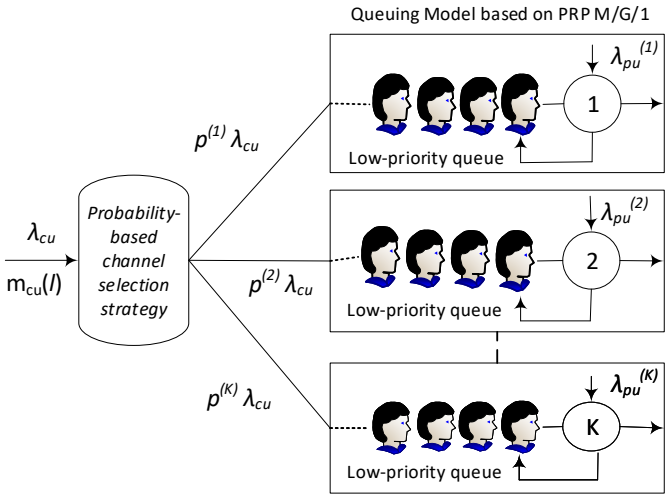

Figure 3.3: Proposed framework enabled with PRP based M/G/1 queuing theory for probability-based channel selection strategy

- The users are categorized into two types in every channel. The PUs are linked with the high priority queue, and CUs are linked with low priority queue.

- If PU interrupts the CU's transmission. Then the interrupted CU places the spare data traffic in front of the low-priority queue of current working channel. After this, when this current channel becomes idle, the CU completes its spare data transmission.

- The proposed model depicts the effects of various spectrum handoffs that may be experienced by CU during its transmission, from PU. Furthermore, the channels that have similar channel access priorities are served on the basis of first-come-first-served.

By using this proposed channel models, the total network time for both channel selection strategies is compared empirically for different traffic frameworks and sensing time. Each CU wisely selects the best strategy to reduce its total network time. Now the optimum total network time is written as-

$$\hat{A} = \min\left(E[A_{pbc}], E[A_{sbc}]\right) \tag{3.7}$$

The total network time is obtained from request time and data transmission time as mentioned in (3.7). Let R_{pbc} and R_{sbc} are average request time in case of PCSS and SCSS, respectively. Furthermore, T_{pbc} and T_{sbc} are data transmission time in case of PCSS and SCSS respectively, then the total network time is

$$E[A_{pbc}] = E[R_{pbc}] + E[T_{pbc}] \tag{3.8}$$

$$E[A_{sbc}] = E[R_{sbc}] + E[T_{sbc}] \tag{3.9}$$

Now, we illustrate the calculation of the average request time and average data transmission time.

3.2.2.1 Request Time Calculation

- Probability-based Channel Selection Strategy- This strategy suggests that the operating channel is selected on the basis of predetermined probability. In this case, a newly arrived CU is connected with the low priority queue of the channel, and this CU will be served only after providing the service to the PU, CUs of the high priority queue, and already existing users at low priority queue of that channel.

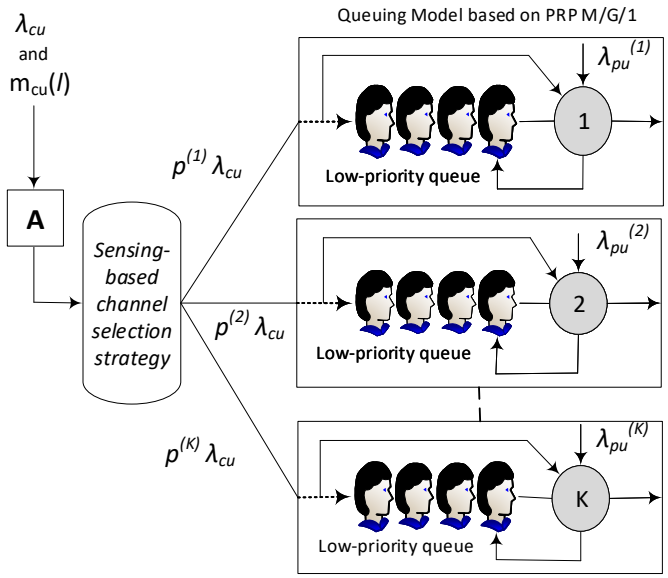

Figure 3.4: Proposed framework enabled with PRP based M/G/1 queuing theory for sensing-based channel selection strategy

Therefore, for a CU, we can define the request time as the period starts from the moment when a CU reaches the selected channel's low-priority queue until the selected channel becomes free. Hence, the request time of CU at channel j is,

$$E[R_{pbc}] = \sum_{j=1}^{K} {p_{pbc}}^{(j)} E[{R_{pbc}}^{(j)}] \tag{3.10}$$

Now apply the PRP based M/G/1 queuing theory [77]. It can be written as,

$$E[{R_{pbc}}^{(j)}] = \frac{E[S^{(j)}]}{(1-{\varphi_{pu}}^{(j)})(1-{\varphi_{pu}}^{(j)}-{\varphi_{cu}}^{(j)})} \tag{3.11}$$

where $E[S^{(j)}]$ shows the average residual time required to finish the service. Considering the [77] we get,

$$E[S^{(j)}] = \frac{1}{2}{\lambda_{pu}}^{(j)} E[(\widehat{X_{pu}}^{(j)})^2] + \frac{1}{2}{p_{pbc}}^{(j)} \lambda_{cu} E[(\widehat{X_{cu}}^{(j)})^2] \tag{3.12}$$

Put (3.11) and (3.12) into (3.10) and get $E[R_{pbc}]$.

- Sensing-based Channel Selection Strategy- In SCSS the request time R_{sbc} is obtained from the total sensing time and queue waiting time (W_{sbc}). Let sensing time

$\widehat{\theta}_{scan}$ is required to scan one applicant channel, then for scanning the n channels, the total scanning time required is $n\widehat{\theta}_{scan}$. If the CU does not find any channel idle after the wideband sensing, then it does not send its data immediately and puts the data on low priority queue of selected channel. Therefore,

$$E[R_{sbc}] = n\widehat{\theta}_{scan} + \Pr\{\alpha^c\} \times E[W_{sbc}] \tag{3.13}$$

Here, α represents the occurrence of finding at least one channel idle after sensing and its complement is represented by α^c. Now for deriving the $\Pr\{\alpha\}$ and $\Pr\{\alpha^c\}$, two observations are considered. The first one is, the channel is actually unoccupied if (i) there is no PU in the channel, and (ii) there is empty low priority queue in the channel, and the second one is, a channel is evaluated as an idle channel only if a false alarm does not happen. Therefore, it may be written by (3.14),

$$\begin{aligned} \Pr[\alpha] &= \sum_{j=1}^{n} [\Pr\{\alpha \,|\, j\, channels\ are\ actually\ idle\}\ \Pr(j)] \\ &= \sum_{j=1}^{n} \left[1 - (P_{FA})^j\right] \times \sum_{\xi \subseteq \delta, |\xi| = j} \left[\prod_{i \in \xi} (1 - \varphi^{(i)}) \prod_{m \in \delta - \xi} \varphi^{(m)} \right]. \end{aligned} \tag{3.14}$$

where $\varphi^{(j)} = {\varphi_{pu}}^{(j)} + {\varphi_{cu}}^{(j)}$, false alarm probability is P_{FA} and complement of α is represented by α^c.

$$\Pr\{\alpha^c\} = 1 - \Pr\{\alpha\} \tag{3.15}$$

When all applicant channels are busy, then ${}^1/_n$ is the probability of selecting each channel by the CU. Hence, for this case, according to PRP based M/G/1 queueing theory, the average queueing waiting time is written as [78],

$$E[W_{sbc}] = \sum_{j=1}^{n} \left[\frac{1}{n} \cdot \frac{E[S^{(j)}]}{(1 - {\varphi_{pu}}^{(j)})(1 - {\varphi_{pu}}^{(j)} - {\varphi_{cu}}^{(j)})} \right] \tag{3.16}$$

3.2.2.2 Data Transmission Time

We can calculate the CU's data transmission time by using the PRP-based M/G/1 queueing model. Let the number of interruptions are denoted by the $N^{(j)}$ for a CU on channel j. Furthermore, the busy time period (denoted by ${Y_{pu}}^{(j)}$) appears from transmissions of

PU at channel j. This period is defined as the duration that starts from when channel j is engaged by PU to the time when the high priority queue is vacant. The CU of channel j has to wait for the span of $E[{Y_{pu}}^{(j)}]$ for retransmitting its data after interruption from PU. Let $T^{(j)}$ shows the data transmission time of CU on channel j then,

$$E[T^{(j)}] = E[\widehat{{X_{cu}}^{(j)}}] + E[N^{(j)}]E[{Y_{pu}}^{(j)}] \tag{3.17}$$

where $E[N^{(j)}] = {\lambda_{pu}}^{(j)} E[\widehat{{X_{cu}}^{(j)}}]$ and $E[{Y_{pu}}^{(j)}] = \frac{E[\widehat{{X_{pu}}^{(j)}}]}{1-{\lambda_{pu}}^{(j)} E[\widehat{{X_{pu}}^{(j)}}]}$. The average data transmission time in both these strategies is written as:

$$E[T_{pbc}] = \sum_{j=1}^{K} {p_{pbc}}^{(j)} E[T^{(j)}] \tag{3.18}$$

$$E[T_{sbc}] = \sum_{j=1}^{n} {p_{sbc}}^{(j)} E[T^{(j)}] \tag{3.19}$$

By evaluating the total network time minimization problem in (3.2), the probability distribution vector p_{pbc} can be calculated in PCSS while in SCSS, the calculation of probability distribution vector p_{sbc} depends on the specified data traffic statistics. Appendix B discussed the evaluation of p_{sbc} by the given traffic pattern. Note that after spectrum sensing, the CUs prefer to approach the channels which have a higher idle probability.

Finally, by substituting (3.10) and (3.18) in (3.8), the relationship between probability distribution vector p_{pbc} and average total network time in PCSS is obtained. After this, by evaluating the total network time minimization problem by (3.2), the optimum probability distribution vector $\hat{p}$ can be obtained. In the same way, by substituting (3.13) and (3.19) in (3.9), the relationship between the number of applicant channels n and average total network time can be obtained. By this scheme we can minimize the total sensing time $n\mu$ by considering the smaller number of channels in (3.13) but it results higher value of $\Pr(\alpha^c)$ in (3.13). Now after evaluating the total network time minimization problem defined in (3.6), the optimum number of channels $\hat{n}$ can be obtained in SCSS.

3.2.3 Possession of Sensing Errors

Under this subsection the performance of real service time of PU and CU is investigated, which is caused by the false alarm and missed detection errors. Particularly, we present that how to determine the first and the second moments of $\widehat{X_{pu}}^{(j)}$ and $\widehat{X_{cu}}^{(j)}$.

3.2.3.1 False Alarm Error

In false alarm error, CU does not send data even in a empty channel. So, the real service time of CU extends up to $\widehat{X_{cu}}^{(j)}$ from ${X_{cu}}^{(j)}$. Hence, the first and the second moments of $\widehat{X_{cu}}^{(j)}$ are represented as

$$E[\widehat{X_{cu}}^{(j)}] = \sum_{z=1}^{\infty} E[\widehat{X_{cu}}^{(j)} \Big| {X_{cu}}^{(j)} = z] \Pr\{{X_{cu}}^{(j)} = z\} \tag{3.20}$$

and

$$E[(\widehat{X_{cu}}^{(j)})^2] = \sum_{z=1}^{\infty} E[(\widehat{X_{cu}}^{(j)})^2 \Big| {X_{cu}}^{(j)} = z] \Pr\{{X_{cu}}^{(j)} = z\} \tag{3.21}$$

The false alarm slot is observed as a busy slot because it cannot be used by PU and CUs.

$$E[\widehat{X_{cu}}^{(j)} \Big| {X_{cu}}^{(j)} = z] = \sum_{i=0}^{\infty} (z+i) \binom{z+i-1}{i} (1-P_{FA})^z (P_{FA})^i \tag{3.22}$$

$$E[(\widehat{X_{cu}}^{(j)})^2 \Big| {X_{cu}}^{(j)} = z] = \sum_{i=0}^{\infty} (z+i)^2 \binom{z+i-1}{i} (1-P_{FA})^z (P_{FA})^i \tag{3.23}$$

Hence ${\varphi_{cu}}^{(j)} = {\lambda_{cu}}^{(j)} E[\widehat{X_{cu}}^{(j)}]$ and the data transmission is adjourned to succeeding time slots when a false alarm takes place. Hence, in the case of z slots, for a user, the real service time is extended up to $z+i$ slots if the false alarm takes place at i slots from the first $z+i-1$ slot and not take place in $(z+i)^{th}$ slot. So for real service time, the conditional expectation follows negative binomial distribution with P_{FA} (Probability of false alarm).

Here, $m_{cu}(l)$ provides the value of $\Pr\{{X_{cu}}^{(j)} = z\}$, so the value of $E[\widehat{X_{cu}}^{(j)}]$ and $E[(\widehat{X_{cu}}^{(j)})^2]$ is obtained by substituting (3.22) into (3.20) and (3.23) into (3.21). Like, if $m_{cu}(l)$ is geometric distribution then,

$$m_{cu}(l) = \left(1 - \frac{1}{E[B_{cu}]}\right)^{z-1} \left(\frac{1}{E[B_{cu}]}\right) \tag{3.24}$$

$$E[\widehat{X_{cu}}^{(j)}] = \frac{E[X_{cu}{}^{(j)}]}{1 - P_{FA}} \tag{3.25}$$

$$E\left[(\widehat{X_{cu}}^{(j)})^2\right] = \frac{E\left[X_{cu}{}^{(j)}\right]\left(2E[X_{cu}{}^{(j)}] - 1 + P_{FA}\right)}{(1 - P_{FA})^2} \tag{3.26}$$

where $E[X_{cu}{}^{(j)}] = E[B_{cu}]/D_{cu}{}^{(j)}$.

3.2.3.2 Missed Detection

Due to the missed detection error, the transmitting data of PU is interrupted by the CU. Thus, the PU resends its interrupted data in the next time slot. Thus, the PU's real service time is extended from $X_{pu}{}^{(j)}$ to $\widehat{X_{pu}}^{(j)}$. So, the first and second moments of $\widehat{X_{pu}}^{(j)}$ are written as:

$$E[\widehat{X_{pu}}^{(j)}] = \sum_{z=1}^{\infty} E[\widehat{X_{pu}}^{(j)} \left| X_{pu}{}^{(j)} = z\right] \Pr\{X_{pu}{}^{(j)} = z\} \tag{3.27}$$

$$E[(\widehat{X_{pu}}^{(j)})^2] = \sum_{z=1}^{\infty} E[(\widehat{X_{pu}}^{(j)})^2 \left| X_{pu}{}^{(j)} = z\right] \Pr\{X_{pu}{}^{(j)} = z\} \tag{3.28}$$

Next, in this case, we consider the possibility when in the transmission slot of PU, more than one CU arrives with the probability of $1 - e^{-\lambda_{cu}{}^{(j)}\tau}$, where τ is slot duration. For these CU's arrivals, every CU accesses this busy slot as a vacant slot and missed detection error takes place. At channel j, let $L_{cu}{}^{(j)}$ represents the low-priority queue length. Therefore, in the considered slot the first arrival provides an error channel estimation with probability $P_{MD}\Pr\{L_{cu}{}^{(j)} = 0\}$ where the missed detection probability is P_{MD}. Now in the considered slot the remaining arrivals are $\Pr\left\{L_{cu}{}^{(j)} = 0\right\} = 0$ because the initial arrival is placed at the low-priority queue of j channels. By considering these observations, the conclusion is that the PU's transmission slot is interrupted by CU's arrivals with probability

$$P_I{}^{(j)} = \left(1 - e^{-\lambda_{cu}{}^{(j)}\tau}\right) P_{MD} \Pr\left\{L_{cu}{}^{(j)} = 0\right\} \tag{3.29}$$

In the same way, in false alarm error, we observe that the random variables $\widehat{X_{pu}}^{(j)}$ and $(\widehat{X_{pu}}^{(j)})^2$, follows negative binomial distribution with value $P_I{}^{(j)}$ if $X_{pu}{}^{(j)} = z$. After this, because $\Pr\{X_{pu}{}^{(j)} = z\}$ can be evaluated with the help of $m_{pu}{}^{(j)}(l)$, and the value of $E[\widehat{X_{pu}}^{(j)}]$ and $E[(\widehat{X_{pu}}^{(j)})^2]$ can be calculated by (3.27) and (3.28), respectively. If the

geometric distribution is ${m_{pu}}^{(j)}(l)$, then,

$$ {m_{pu}}^{(j)}(l) = \left(1 - \frac{1}{E[{B_{pu}}^{(j)}]}\right)^{z-1} \left(\frac{1}{E[{B_{pu}}^{(j)}]}\right) \tag{3.30} $$

we can get

$$ E[\widehat{{X_{pu}}^{(j)}}] = \frac{E[{X_{pu}}^{(j)}]}{1 - {P_I}^{(j)}} \tag{3.31} $$

and

$$ E\left[(\widehat{{X_{pu}}^{(j)}})^2\right] = \frac{E\left[{X_{pu}}^{(j)}\right]\left(2E[{X_{pu}}^{(j)}] - 1 + {P_I}^{(j)}\right)}{\left(1 - {P_I}^{(j)}\right)^2} \tag{3.32} $$

where $E[{X_{pu}}^{(j)}] = E[{B_{pu}}^{(j)}]/{D_{pu}}^{(j)}$.

3.2.4 Analysis of Energy Consumption

This subsection represents the energy consumption analyses in CRN, which is modeled as the addition of the energy required to scan a new channel, and energy required to deliver a packet on this newly detected channel. It is assumed that the various mobile nodes are scan and select the channel simultaneously for a summary of notations used). Fig. 3.5 represents the periodic scanning with two mobile nodes. The expected energy consumption per-packet of the CU can be modeled as:

$$ \widehat{E}_{cu} = \widehat{E}^{b}_{pkt} + \frac{\widehat{E}_{scan}}{\widehat{\theta}^{b}/\widehat{\theta}_{pkt}} \tag{3.33} $$

For calculating the $\widehat{E}_{cu}$ in (3.33), energy consumed by the CU at various operation modes is calculated. Therefore, first of all, we compute $\widehat{E}^{b}_{pkt}$, and afterward, suggest a channel scanning scheme and investigate the $\widehat{E}_{scan}$. Fig. 3.6, which describes the various frames involved in the communication is considered for calculating the $\widehat{E}^{b}_{pkt}$. Fig. 3.6 reveals the timing and performance of a CU that is receiving, transmitting, and simply listening to the medium with the help of a basic access mechanism without request-to-send/ clear-to-send. The short period $\widehat{\theta}_{sifs}$ is neglected for analysis simplicity.

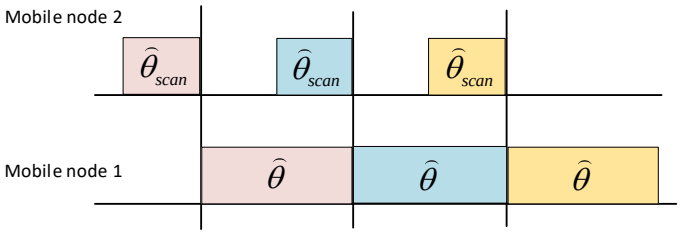

Figure 3.5: Communication model and periodic scanning with two mobile node

3.2.4.1 Transmission Mode Energy

The energy consumed in a successful packet transmission can be written as:

$$\widehat{E}_{trx} = \widehat{P}_{trx}\widehat{\theta}_{data} + \widehat{P}_{rcx}\widehat{\theta}_{ack} + \widehat{P}_{idle}\widehat{\theta}_{difs} \tag{3.34}$$

When a packet collision acquires due to false alarm error of the idle channel, then the energy consumed CU can be given as:

$$\widehat{E}_{coll} = \widehat{P}_{trx}\widehat{\theta}_{data} + \widehat{P}_{idle}\left(\widehat{\theta}_{ack} + \widehat{\theta}_{difs}\right) \tag{3.35}$$

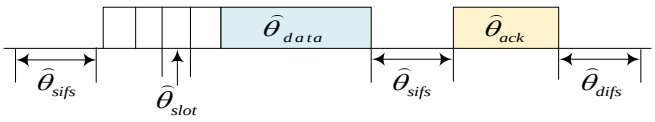

Figure 3.6: Packet Transmission Mode in the IEEE 802.11

3.2.4.2 Receiving Mode Energy

When a packet is received, then the consumed energy can be analyzed in three cases (i) packet has been received to the assigned CU (ii) packet has been jammed because of collision and (iii) packet has not been received to the assigned CU and required to be rejected. In first case energy consumed is:

$$\widehat{E}_{rcx} = \widehat{P}_{rcx}\widehat{\theta}_{data} + \widehat{P}_{trx}\widehat{\theta}_{ack} + \widehat{P}_{idle}\widehat{\theta}_{difs} \tag{3.36}$$

In the second case, the received packet is rejected because of a collision. Thus the consumed energy is expressed as:

$$\widehat{E}_{rxcol} = \widehat{P}_{rcx}\widehat{\theta}_{pkt.hdr} + \widehat{P}_{idle}\left(\widehat{\theta}_{coll} + \widehat{\theta}_{difs} - \widehat{\theta}_{pkt.hdr}\right) \tag{3.37}$$

In the third case, when packet has to be rejected, then the energy consumed is:

$$\widehat{E}_{rjt} = \widehat{P}_{rcx}\widehat{\theta}_{pkt.hdr} + \widehat{P}_{idle}\widehat{\theta}_{difs} + \widehat{P}_{sleep}\widehat{\theta}_{nav} \tag{3.38}$$

where $\widehat{\theta}_{nav} = \widehat{\theta}_{data} - \widehat{\theta}_{pkt.hdr} + \widehat{\theta}_{ack}$

3.2.4.3 Energy Consumption during Backoff

We consider [79], [80] for our analysis, which presents the idea of a tick rather than a slot to interpret the IEEE 802.11 based distributed coordination function (DCF). The energy consumed during a tick period is equal to the energy consumed between two consecutive decrements of a user's backoff counter. A user observes the tick period in the backoff mode. There are $r-1$ other possible transmitting users, where r represents the total number of CUs on the current channel. If no other user endeavors a transmission, then the backoff counters are decreased by one in each time slot. But if the channel is occupied, then the backoff counters are stopped, and it again continues when the channel is free. A couple of situations arise if a user attempts to communicate in an assigned tick time with $r-1$ different transmitters. (i) when the given user transmits, in this situation, the probability can be given as:

$$M_{\Delta} = (r-1)\,\wp(1-\wp)^{r-2} \tag{3.39}$$

where $\wp$ indicates the probability that a user transmits at an assigned tick time [81], [82]. (ii) when more than one user intends to communicate, then the probability is given as:

$$M_{\Delta\Delta} = 1 - (1-\wp)^{r} - r\wp(1-\wp)^{r-1} \tag{3.40}$$

Furthermore, per tick average energy consumption is given by (3.41),

$$\widehat{E}_{tik} = (1 - M_{\Delta} - M_{\Delta\Delta})\,\widehat{P}_{idle}\widehat{\theta}_{slot} + M_{\Delta}\left\{p_g\widehat{E}_{rcx} + \left(1-p_g\right)\widehat{E}_{rjt}\right\} + M_{\Delta\Delta}\widehat{E}_{rxcol} \tag{3.41}$$

where p_g shows the probability; that on the channel, the packet is destined to the assigned user.

3.2.4.4 Energy Consumption during Communicate through a Channel

On the basis of (3.33) and by analyzing the [83], the energy consumed to send a packet, when a total b number users contending for the same channel, can be given as,

$$\widehat{E}_{pkt}^{b} = \widehat{E}_{trx} + \frac{p_b}{1-p_b}\widehat{E}_{coll} + V\left(p_b\right)\widehat{E}_{tik} \tag{3.42}$$

where p_b is the probability with which a collision happens when there is b number of contending users. Moreover, $V\left(p_b\right)$ indicates the slots number required to be counted down before a packet is sent. It is interpreted as $V\left(p_b\right) = \left[\tilde{W}\frac{(1-p_b)-p_b(2p_b)^x}{(1-2p_b)} - 1\right]$, here the initial contention window size is $\tilde{W}$, and x represents the number of times the backoff window increases before it approaches the maximum allotted size. Importantly, $V\left(p_b\right)$ depends on the number of contending CUs b, which defines all significant values of p_b.

3.2.4.5 Energy Consumption during Channel Scanning

In this chapter, an optimum scanning scheme is proposed. Let us assumed that there is J number of channels to scan including the current channel. According to this scanning scheme, CU scans all the channels, and an optimum channel (channel on which the least number of users are contending) is selected. Hence, the energy consumption in the scanning process $\widehat{E}_{scan}$ is expressed as:

$$\widehat{E}_{scan} = \widehat{P}_{sw}\widehat{\theta}_{sw}\left(J-1\right) + \widehat{P}_{sw}\widehat{\theta}_{sw}p_{sw} + J\widehat{E}_{scan}^{ch} \tag{3.43}$$

where $\widehat{E}_{scan}^{ch}$ is the expected energy consumption for a single channel scanning, $\widehat{P}_{sw}$ is the average power consumed during channels switching, and p_{sw} indicates the probability of observing a more reliable channel than the current one. When a better channel is observed, the user will switch the channels, and (3.44) express the total energy consumption to switch between channels.

$$\widehat{E}_{scan}^{ch} = \frac{\widehat{\theta}_{scan}}{\widehat{\theta}_{tik}}\left\{\left(1 - M_{\Delta} - M_{\Delta\Delta}\right)\widehat{P}_{idle}\widehat{\theta}_{slot} + M_{\Delta}\widehat{E}_{rjt} + M_{\Delta\Delta}\widehat{E}_{rxcol}\right\} \tag{3.44}$$

3.3 Performance Evaluation

The proposed traffic load balancing strategies have been verified using the MatLab software. This software is used to analyze the system metric like total network time, probability distribution vector, optimum number of channels, and energy consumed at various stages of communication in CRN. In this chapter, the IEEE 802.11 standard protocols, and parameters are used for the simulation purpose. Table 3.1 represents the list of simulation parameters. In the proposed framework, it is considered that the service time length of the PU and CUs is geometrically distributed because this work emphasizes latency-delicate traffic.

Table 3.1: Simulation Parameters

Name of Parameter	Parameters value
False alarm probabilities (P_{FA})	0, 0.1, 0.5
Missed detection probability (P_{MD})	0, 0.1
Data rates of PU and CU	1
Total number of channels	4
Average arrival rate of the PUs in PCSS	${\lambda_{pu}}^{(1)} = 0.02,\ {\lambda_{pu}}^{(2)} = 0.02,$ ${\lambda_{pu}}^{(3)} = 0.01,\ {\lambda_{pu}}^{(4)} = 0.01$
Average service time of PU in PCSS	$E[{X_{pu}}^{(1)}]$=25, $E[{X_{pu}}^{(2)}]$= 30, $E[{X_{pu}}^{(3)}]$=25, $E[{X_{pu}}^{(4)}]$=20
Average arrival rate of the PUs in SCSS	${\lambda_{pu}}^{(1)} = 0.02,\ {\lambda_{pu}}^{(2)} = 0.25,$ ${\lambda_{pu}}^{(3)} = 0.01,\ {\lambda_{pu}}^{(4)} = 0.15$
Average service time in SCSS for any j	$E[{X_{pu}}^{(j)}]$= 20
Average service time of CU in SCSS	$E[X_{cu}] = 10, 15, 20$

3.3.1 Probability-based Channel Selection Strategy

Three different scenarios are examined for the performance evaluation of the proposed strategy as follows:

3.3.1.1 Scenario 1

In this scenario a four-applicant channel system is considered with following traffic parameters: ${\lambda_{pu}}^{(1)} = 0.02,\ {\lambda_{pu}}^{(2)} = 0.02,\ {\lambda_{pu}}^{(3)} = 0.01,\ {\lambda_{pu}}^{(4)} = 0.01$ and $E[{X_{pu}}^{(1)}]$= 25, $E[{X_{pu}}^{(2)}]$= 30, $E[{X_{pu}}^{(3)}]$= 25, $E[{X_{pu}}^{(4)}]$= 20 as well as $P_{FA} = 0.1$ and $P_{MD} = 0.1$. The optimum probability distribution vector is affected by arrival rates of the CUs, which

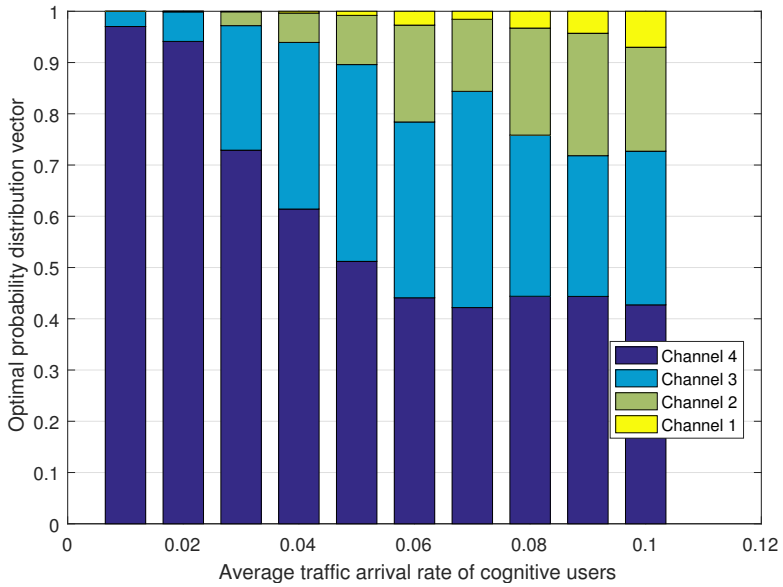

Figure 3.7: Optimum probability distribution vector in PCSS

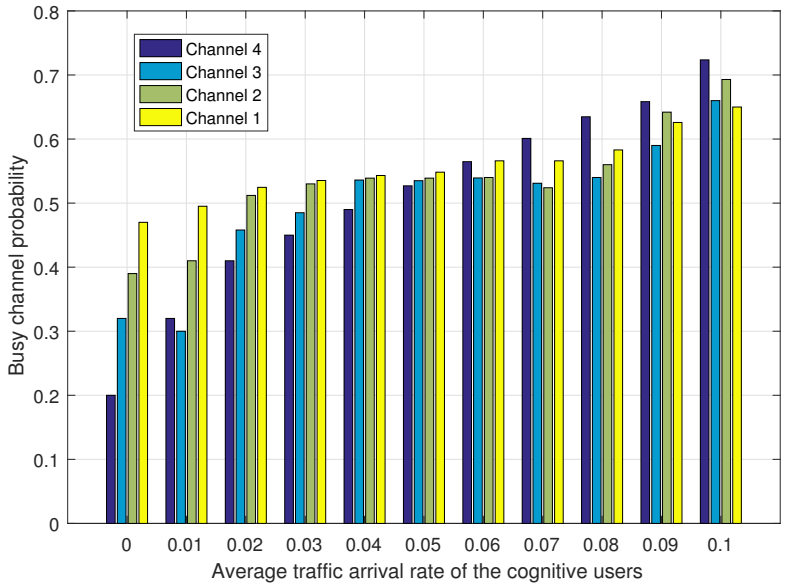

Figure 3.8: Probability of busy channel in PCSS for ($P_{FA} = 0.1$) and ($P_{MD} = 0.1$)

is presented by Fig. 3.7. It represents that at a low λ_{cu}, channel 4 has maximum selection probability but with the increase in traffic rate, the probability of this channel is decreasing, but still high than other channels. The CUs select channel 4 for communication due to its lowest traffic load. As the rate of arrival increases, other channel's selection probability also starts increasing to balance the traffic among four channels. All four channels come in the selection list when $\lambda_{cu} > 0.04$ for balancing the traffic loads in each channel. Table 3.2 shows the various values of optimum probability distribution vector at different channels for multiple values of CU's average traffic arrival

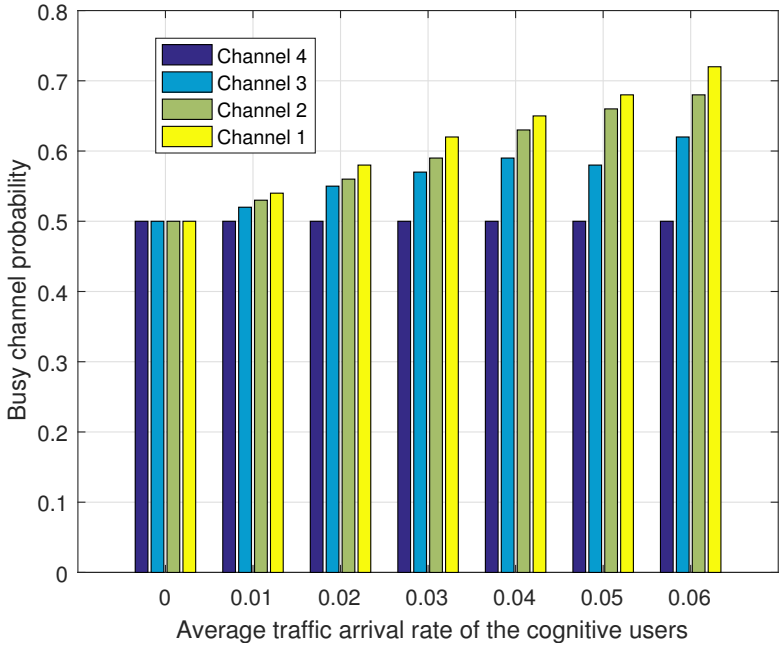

Figure 3.9: Probability of busy channel in PCSS for ($P_{FA} = 0$) and ($P_{MD} = 0$)

rate. This result shows that the queuing model for load balancing in the PCSS performs well. Fig. 3.8 shows that the busy channel probability increases with an increase in the λ_{cu}. When $\lambda_{cu} = 0$, channel 4 has the smallest busy probability, but for $\lambda_{cu} \geq 0.06$, channel 4 has the maximum busy probability. The reason behind this is; all CUs wish to select channel 4. Table 3.3 shows various values of busy channel probability at different channels for multiple values of CU's average traffic arrival rate.

Table 3.2: Optimum probability distribution vector for different channels in scenario 1

	Optimum probability distribution vector			
λ_{cu}	**Channel 1**	**Channel 2**	**Channel 3**	**Channel 4**
0.01	0	0	0.030	0.970
0.02	0	0	0.059	0.941
0.03	0	0.029	0.242	0.728
0.04	0.003	0.067	0.299	0.631
0.05	0.010	0.094	0.384	0.512
0.06	0.028	0.190	0.340	0.442
0.07	0.017	0.141	0.412	0.430
0.08	0.033	0.209	0.309	0.449
0.09	0.044	0.238	0.278	0.440
0.10	0.070	0.204	0.299	0.427

Table 3.3: Busy channel probability at different channels for scenario 1

	Busy channel probability			
λ_{cu}	**Channel 1**	**Channel 2**	**Channel 3**	**Channel 4**
0	0.470	0.39	0.320	0.200
0.01	0.495	0.41	0.300	0.320
0.02	0.524	0.512	0.458	0.410
0.03	0.535	0.530	0.485	0.450
0.04	0.543	0.539	0.536	0.490
0.05	0.548	0.539	0.535	0.527
0.06	0.564	0.540	0.539	0.566
0.07	0.566	0.524	0.531	0.601
0.08	0.583	0.560	0.540	0.634
0.09	0.625	0.642	0.590	0.658
0.10	0.650	0.693	0.660	0.723

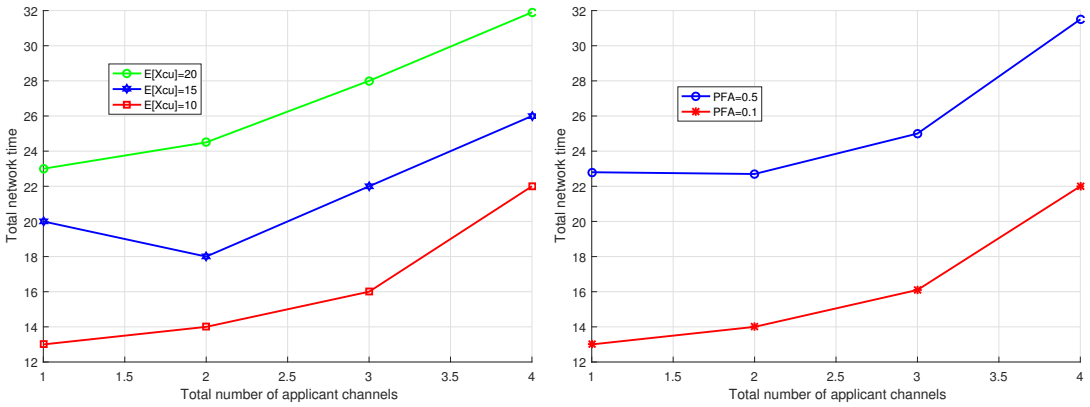

(a) With variation in E(Xcu) **(b)** With variation in (P_{FA})

Figure 3.10: Total network time in SCSS

3.3.1.2 Scenario 2

In this scenario, the following traffic parameters are considered: ${\lambda_{pu}}^{(1)} = 0.06$, ${\lambda_{pu}}^{(2)} = 0.04$, ${\lambda_{pu}}^{(3)} = 0.02$, ${\lambda_{pu}}^{(4)} = 0.01$ and $E[{X_{pu}}^{(1)}] = 5$, $E[{X_{pu}}^{(2)}] = 15$, $E[{X_{pu}}^{(3)}] = 20$, $E[{X_{pu}}^{(4)}] = 30$ as well as $P_{FA} = 0$ and $P_{MD} = 0$. Fig. 3.9 indicates that most of the CUs approach a channel which has the highest arrival rate and smallest PU's service time. By (3.10) and (3.11), it is clear that due to the lowest value of $E[S^{(j)}]$, channel 1 has the smaller average request time. Therefore, channel 1 has the largest busy probability because most of the CUs select channel 1 when $\lambda_{cu} > 0$. Table 3.4 shows various values of busy channel probability at different channels for multiple values of CU's average traffic arrival rate in this scenario.

3.3.1.3 Scenario 3

In this scenario the following traffic parameters are considered: ${\lambda_{pu}}^{(1)} = 0.05$, ${\lambda_{pu}}^{(2)} = 0.03$, ${\lambda_{pu}}^{(3)} = 0.02$, ${\lambda_{pu}}^{(4)} = 0.01$ and $E[{X_{pu}}^{(1)}] = 10$, $E[{X_{pu}}^{(2)}] = 15$, $E[{X_{pu}}^{(3)}] = 20$, $E[{X_{pu}}^{(4)}] = 25$,$P_{MD} = 0.1$ and varying value of $P_{FA} = 0.05, 0.1, 0.15, 0.2, 0.25, 0.3, 0.35$. Fig. 3.11 illustrations the variation in optimum distribution probability vector and presents the comparison for different values of the false alarm probability. We can observe that there are only 3 applicant channels for $P_{FA} = 0.05$. But, when $P_{FA} \geq 0.1$, all the 4 channels are considered as the applicant channels. The reason for this phenomenon is as follows: for high value of P_{FA}, $E[\widehat{X_{cu}}]$ increases because of the higher false alarms. Therefore, the real traffic load $\varphi_{cu} = \lambda_{cu} E[\widehat{X_{cu}}]$ of the CUs become large. Then, CUs must allocate total traffic loads to more channels for avoiding channel contention. Table 3.5 shows the various values of optimum probability distribution vector at different channels for multiple values of false alarm probability.

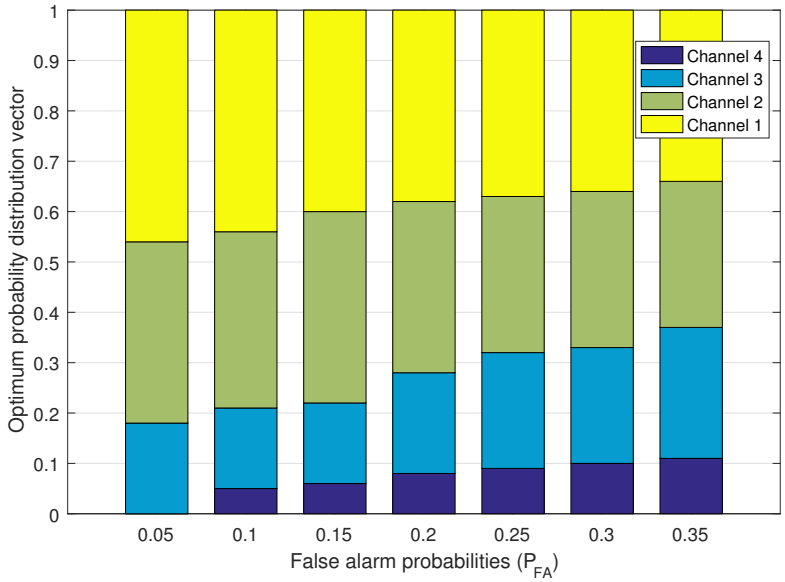

Figure 3.11: Optimum probability distribution vector in PCSS

3.3.2 Sensing-based Channel Selection Strategy

The impact of $E[X_{cu}]$ and P_{FA} on optimum number of applicants channels ($\hat{n}$) can be seen by Figs. 3.10a and 3.10b, respectively. A four channels system is considered with ($\widehat{\theta}_{scan} = 3$) and $\lambda_{cu} = 0.03$. The other parameters value shown in Table 5.1. Fig. 3.10a shows that for $P_{FA} = 0.1$, $\hat{n} = 1, 2, 1$ for $E[X_{cu}] = 10, 15, 20$, respectively. From Fig. 3.10b

Table 3.4: Busy channel probability at different channels for scenario 2

	Busy channel probability			
λ_{cu}	**Channel 1**	**Channel 2**	**Channel 3**	**Channel 4**
0	0.500	0.500	0.500	0.500
0.01	0.540	0.530	0.520	0.500
0.02	0.580	0.560	0.550	0.500
0.03	0.620	0.590	0.570	0.500
0.04	0.650	0.630	0.590	0.500
0.05	0.680	0.660	0.580	0.500
0.06	0.720	0.680	0.620	0.500

Table 3.5: Optimum probability distribution vector ($\hat{p}$) at different channels for scenario 3

	Optimum probability distribution vector			
P_{FA}	**Channel 1**	**Channel 2**	**Channel 3**	**Channel 4**
0.05	0.460	0.360	0.180	0
0.01	0.440	0.350	0.160	0.050
0.15	0.400	0.380	0.160	0.060
0.20	0.380	0.340	0.200	0.080
0.25	0.370	0.310	0.230	0.090
0.30	0.360	0.310	0.230	0.100
0.35	0.340	0.290	0.260	0.110

it is observed that for $E[X_{cu}] = 10$, $\hat{n} = 1, 2$ for $P_{FA} = 0.1, 0.5$, respectively. The optimum value of channels rises as $E[X_{cu}]$ or P_{FA} increases because according to (3.25), a higher value of $E[X_{cu}]$ or P_{FA} provides a high value of $E[\widehat{X_{cu}}^{(j)}]$.

3.3.3 Comparison among Various Channel Selection Strategies

Fig. 3.12 shows the performance comparison of three distinct channel selection strategies (1) non-load-balancing strategy; (2) probability-based strategy; (3) sensing-based strategy and presents the outcomes of λ_{cu} on the average total network time. A framework of three-channel system is considered with following arrival rates: ${\lambda_{pu}}^{(1)} = 0.01$, ${\lambda_{pu}}^{(2)} = 0.02$, ${\lambda_{pu}}^{(3)} = 0.03$, $E[{X_{pu}}^{(1)}] = 15$, $E[{X_{pu}}^{(2)}] = 20$, $E[{X_{pu}}^{(3)}] = 25$ and $E[X_{cu}] = 15$. It is observed that for a high value of λ_{cu}, both the channel selection strategies can decrease the average total network time as compared to the non-load balancing strategy.

In a non-load balancing strategy, all the CUs selects channel 4, due to smallest busy probability of this channel. By using (3.8) and (3.9), the total network time is calculated for PCSS and SCSS. For a small value ($\widehat{\theta}_{scan} = 6$), the SCSS results in the shortest total network time. But when ($\widehat{\theta}_{scan} = 14$) and $\lambda_{cu} < 0.03$, the PCSS performs better than the SCSS, because this strategy selects the channels which have low interrupted probability. In contrast, when $\lambda_{cu} > 0.03$, the SCSS results in shorter total network time because with the help of wideband sensing this strategy potentially minimizes the request time. Table 3.6 shows total network time in different channel selection strategies. The two channels selection strategies can reduce the total network time over 60% compared to the present non-load balancing strategy for $\lambda_{cu} = 0.05$.

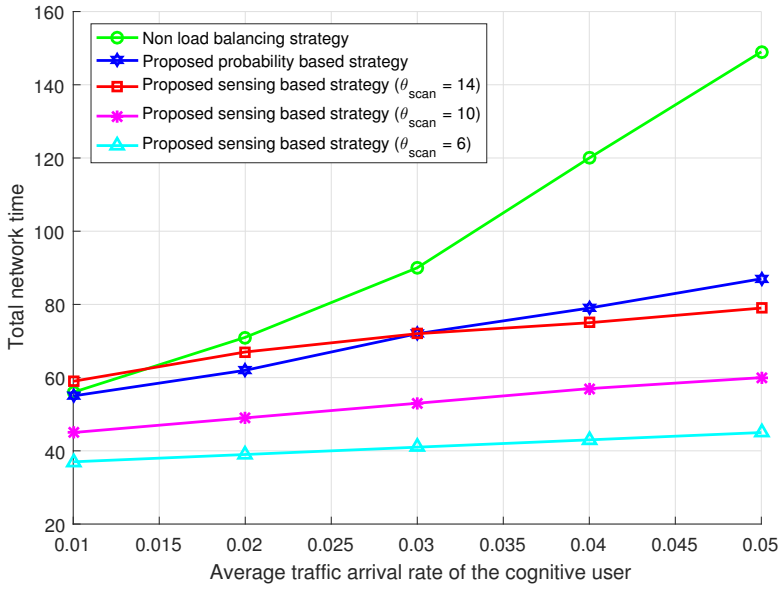

Figure 3.12: Comparison among channel selection strategies

Table 3.6: Total network time in different channel selection strategies

λ_{cu}	**Total network time**				
	Non load balancing	**PCSS**	**SCSS** ($\theta_{scan} = 14$)	**SCSS** ($\theta_{scan} = 10$)	**SCSS** ($\theta_{scan} = 6$)
0.01	56	55	59	45	37
0.02	71	62	67	49	39
0.03	90	72	72	53	41
0.04	120	79	75	57	43
0.05	146	90	79	60	45

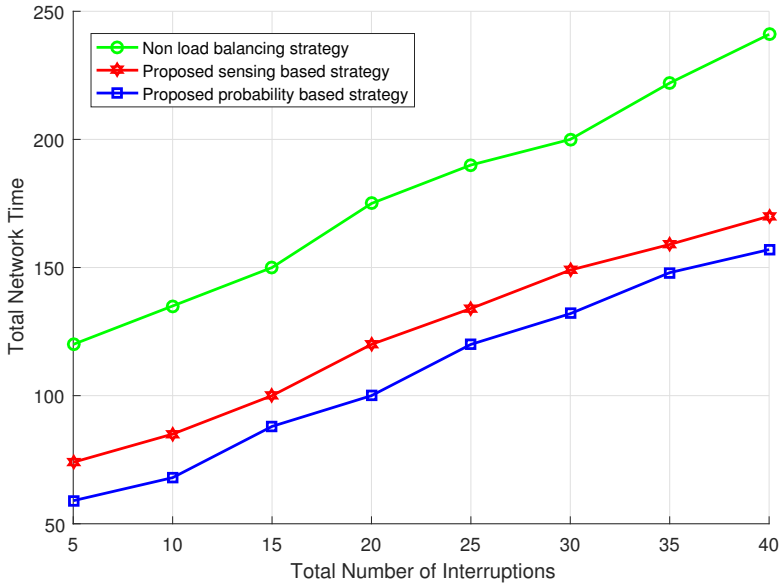

Figure 3.13: Total network time v/s Total number of interruptions

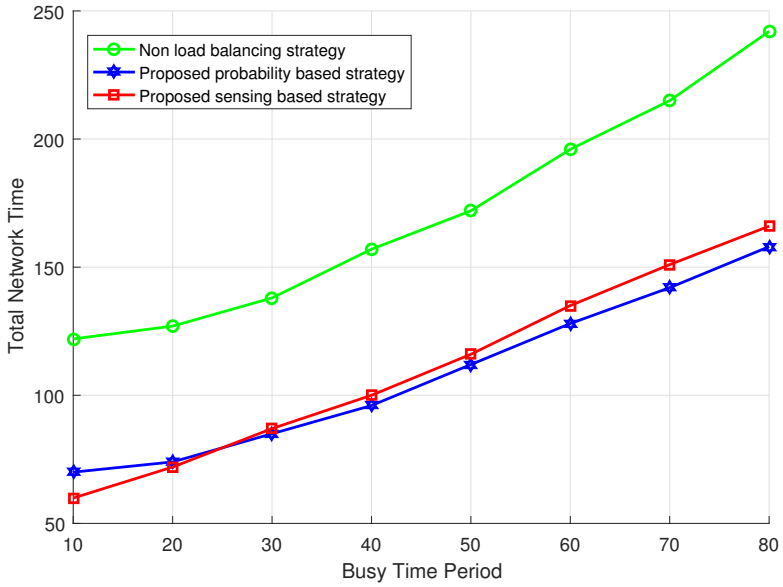

Figure 3.14: Total network time v/s Busy time period

Fig. 3.13 and Fig. 3.14 represent the performance comparison of three distinct channel selection strategies and show the effects of $N^{(j)}$ and ${Y_{pu}}^{(j)}$ on the average total network time, respectively. According to (3.17) the value of data transmission time depends on $N^{(j)}$ and ${Y_{pu}}^{(j)}$. High value of $N^{(j)}$ shows more PU's interruption during the CU's transmission, which leads the extended service time of CUs. Therefore, the total network time of CU have been increased in both the strategies. Fig 3.13 shows that the by varying the value $N^{(j)}$, the PCSS performs better as compared to SCSS, because this strategy selects the channels which have low interrupted probability. Fig 3.14 shows

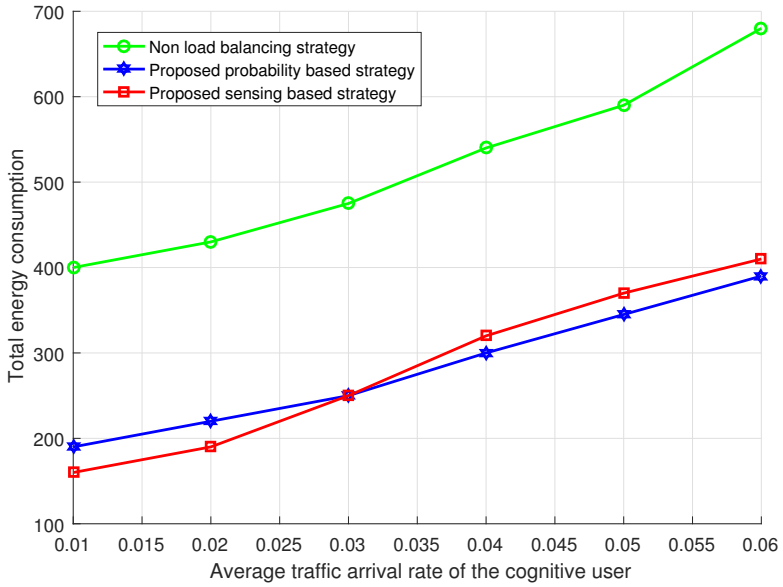

Figure 3.15: Energy consumption in channel selection strategies

Table 3.7: Energy consumption in channel selection strategies

	Total energy consumption		
λ_{cu}	**Non load balancing**	**PCSS**	**SCSS**
0.01	402	190	161
0.02	428	221	192
0.03	476	249	248
0.04	540	298	320
0.05	589	344	373
0.06	681	390	411

that by varying the value of ${Y_{pu}}^{(j)}$, SCSS gives better results as compared to the others till ${Y_{pu}}^{(j)} < 26$, because for high value of ${Y_{pu}}^{(j)}$, there is a high queue waiting time in this strategy. So, for ${Y_{pu}}^{(j)} > 26$, PCSS performs better than the others.

In a non-load balancing strategy, all the CUs try to approach the same channel which has the smallest busy probability. In this case, there is a large number of contending CUs for a channel, which increases the packet collisions and packet transmission time. According to (3.35) a large amount of energy is wasted due to collision. On the other hand with the help of traffic load balancing strategies, CU's traffic load is distributed among all the applicants channel, therefore packet collisions and transmission time are reduced, thus energy can be saved. By using (3.33) total energy consumption is calculated for various strategies. The following parameter values are considered for the calculation:

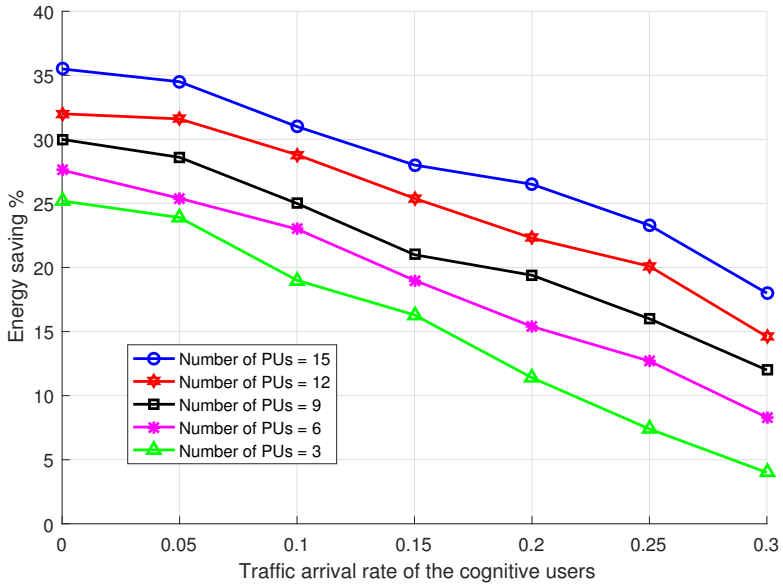

Figure 3.16: Impact of traffic arrival rate on energy consumption for different PUs

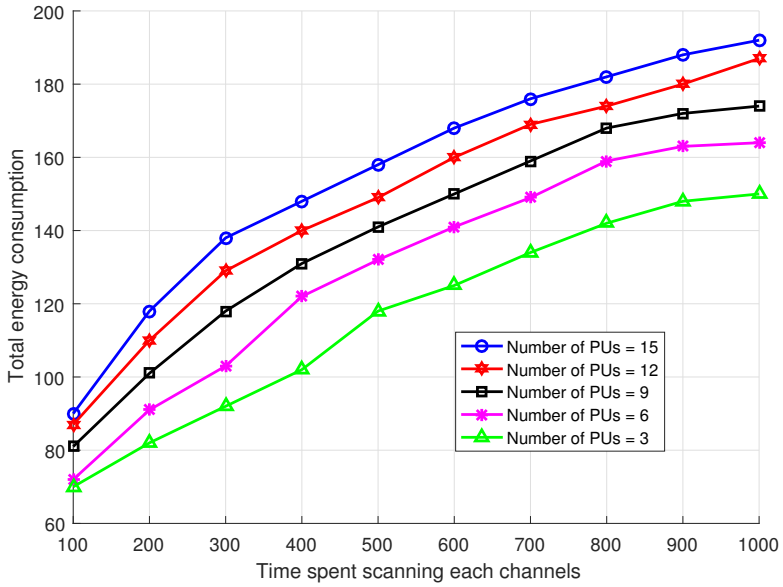

Figure 3.17: Impact of scanning time on energy consumption at various number of PUs

$\widehat{P}_{trx} = 800$, $\widehat{P}_{rcx} = 800$, $\widehat{P}_{idle} = 500$, $\widehat{P}_{sleep} = 20$, $\widehat{P}_{sw} = 700$, $\widehat{\theta}_{data} = 0.22$, $\widehat{\theta}_{ack} = 0.004$, $\widehat{\theta}_{difs} = 0.05$, $\widehat{\theta}_{pkt.hdr} = 0.003$, $\widehat{\theta}_{pkt.hdr} = 0.008$, $\widehat{\theta}_{sw} = 0.008$, $\widehat{\theta}_{slot} = 0.004$. Fig. 3.15 shows that for $\lambda_{cu} < 0.03$, SCSS performs better but for $\lambda_{cu} > 0.03$, PCSS gives improve result because when λ_{cu} increases, scanning energy is also increase for traffic balancing of CUs. Table 3.7 shows energy consumption in channel selection strategies. Fig 3.16, shows that the energy-saving percentage of CUs improve by increasing the number of PUs, but output performance is diminished when λ_{cu} increases. High traffic arrival rate makes more packets to be transferred of the CU, which appears in a high transmission

time for the CU. From Fig. 3.17, it is observed that the total energy consumption increases with an increase in $\widehat{\theta}_{scan}$. With the help of (3.43), energy consumption can be calculated for different values of J.

3.4 Conclusions

In this chapter, a multiuser channel decision framework is designed, which is incorporated with the preemptive resume priority (PRP) based M/G/1 queue model. The proposed model helps to calculate the various parameters in two proposed channel selection strategies: probability-based and sensing-based channel selection strategies. The proposed channel selection methods evenly allocate the CU's traffic load among various applicant channels. We have considered the PU's interruption effects and sensing errors in our calculation. Results of the work present that in the circumstances of huge traffic, SCSS reduces the total network time, while in the situation of low traffic, PCSS gives better results. These observations offer a vital perception in designing of traffic-adaptive channel selection strategy in the existence of PU's interruptions and sensing errors. The proposed strategies can minimize the total network time by 60% as compared to non-load balancing strategy for $\lambda_{cu} = 0.05$. Next, we calculate the total energy consumption at various operational modes in GCRN. The results indicate that the arrival rate of the CUs and the time spent on channel scanning affect the energy consumption of the network. The proposed channel selection strategies reduce energy consumption by 75% as compared to non-load balancing strategy.

Chapter 4

Cooperation and Energy Harvesting based Spectrum Sensing Schemes for Green Cognitive Radio Networks

TO fulfill the demand for the next-generation wireless system, the efficient utilization of the spectrum is essential. The principle of cognitive radio networks (CRNs) is to use the available spectrum band intelligently, and this approach can greatly diminish the spectrum scarcity problem. Proper spectrum sensing is crucial for observing the vacant spectrum, and SUs perform this continuously to preserve the PU's transmission. Cooperative communication can be categorized into two types i) cooperation among SUs, which supports the improvement in spectrum sensing and data transmission rate of SUs, and ii) cooperation between PU and SU, which supports enhancing the spectrum's opportunities for SU. In this chapter, the amplify-and-forward (AF) cooperation protocol effect and the network's inherent asymmetry property are considered between SUs to improve the sensing probability of the SUs. In GCRNs, most SUs are mobile devices, so they must be more energy efficient because they exploit extra battery power. Due to the longer sensing time, a huge amount of energy is wasted in the connection setup, and the time required for complete data transmission is also reduced. It indicates that an energy-efficient network should have a proper trade-off between sensing time and data delivery time. Therefore, in the proposed work, the total energy consumption in CRNs is examined and two different spectrum sensing schemes, preset spectrum sensing (PSS) and viscous spectrum sensing (VSS) are proposed, to consider

energy saving. For the SUs, the total energy consumption is the sum of the required energy for sensing a vacant spectrum and the energy spent to transmit a packet through an obtained spectrum.

In the present scenario, efficiently utilizing the available spectrum has become a critical challenge. In the practical scenario of GCRNs, both homogeneous and heterogeneous PUs are located, so the major concern of SUs is to sense the PU's vacant spectrum carefully. Therefore, in this chapter, the SUs explore the licensed spectrum collaboratively to find more spectrum opportunities. This chapter presents the analysis of many significant parameters of GCRNs, such as; spectrum sensing time, sensing probability, number of contending users on the medium, number of spectrum in the system, and energy consumption. In this chapter, these issues are addressed by examining the cooperative behavior of SUs and proposing a cooperation-based sensing scheme to improve the sensing probability and minimize the sensing time. Furthermore, two energy harvesting-based sensing schemes are also suggested with the aim of energy-saving. The significant contributions of this chapter are outlined as follows;

- The advantages of cooperative communication are discussed, and a joint cooperation spectrum sensing (JCSS) scheme is proposed for CRNs. We consider the amplitude-and-forward (AF) cooperative technique and the network's inherent asymmetry property, which results in faster spectrum sensing with cooperation.

- The total sensing time and rapidity gain under the proposed cooperation scheme is investigated. The results show a significant reduction in sensing time for PU's spectrum.

- Energy harvesting based two spectrum sensing schemes, preset spectrum sensing (PSS) and viscous spectrum sensing (VSS), are proposed. These schemes are based on different parameters (i.e., total energy consumption, sensing time, energy-saving percentage, and number of contending users in any spectrum).

4.1 A System Model

In this chapter, the JCSS scheme is proposed between two SUs and calculate the sensing probability for two different cases (cooperation and non-cooperation). After this, the

total sensing probability, total sensing time, and rapidity gain (rapidity gain is defined as the network's hardware and software capacity to automatically manage and configure other network resources among any number of connected devices) are analyzed. The sensing time is an important parameter in CRNs; therefore, we consider the inherent asymmetry (in the wireless network's user node mobility, various radio technology, variations in radio ranges, and data packet loss patterns all contribute to asymmetry and in these networks, heterogeneity is inherent; each user node contains distinct protocols, properties, and characteristics) of the system that encourages faster PU's detection. It is assumed that all the channels undergo Rayleigh fading, and the channels communicating with various SUs are independent. Let the input signal h is transmitted, then the received signal 'g' is,

$$g = f_c h + n^* \tag{4.1}$$

here n^* (additive noise) and f_c (fading coefficient) are designed as independent complex gaussian random variables. Apart from this, the other assumptions are: first, the noise has a unit variance and zero mean; second, there is a centralized controller (adequate to transmit and receive) with which all the SUs communicate. Each SU can access its channel state information (CSI).

The major necessity of a CRNs is to discover the idle PU's spectrum rapidly. Therefore, the SUs constantly sense the spectrum. The SUs must leave the band immediately when the PU returns to its frequency band. Hence, if the distance between PU and any SU (SU_2 in this work) is large, then the sensing of PU will be affected, and the sensing time taken by the SU_2 is having high value because the signal received by the PU is weak due to a significant distance. To solve this problem, cooperative communication is the most promising solution. Cooperation between the SUs improves the system's rapidity and minimizes the sensing time.

In this chapter, the secondary users, SU_1 and SU_2 cooperate, and SU_1 works as a relay for SU_2. Fig. 4.1 shows that there are two SUs, represented as SU_1 and SU_2 transmitting the data to a common receiver by using the TDMA mode operation. Based on the amplify-and-forward protocol, slotted communication is used where SU_1 and SU_2 communicate in consecutive slots represented in Fig. 4.2. In time slot TS_1, SU_2 transmits, and SU_1 listens, while in the next slot TS_2, SU_1 transmits the same data which it has been obtained in the previous slot. But the PU has the highest priority to

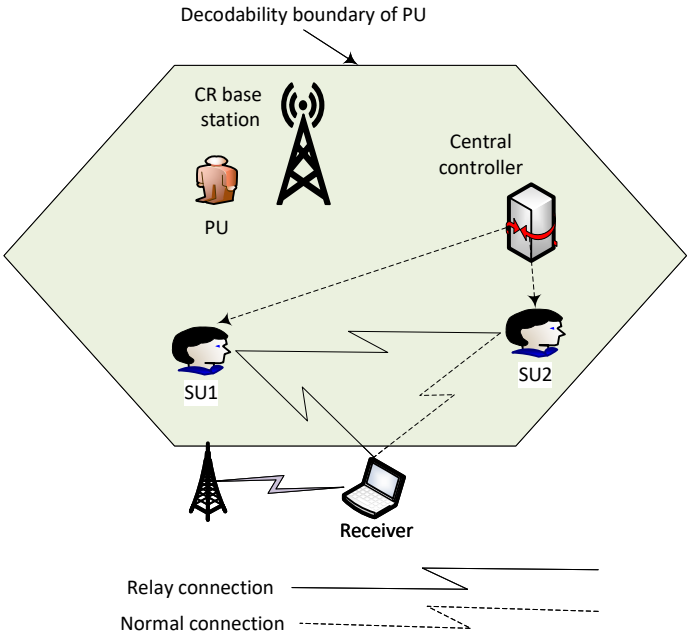

Figure 4.1: Scenario of cooperative CRNs

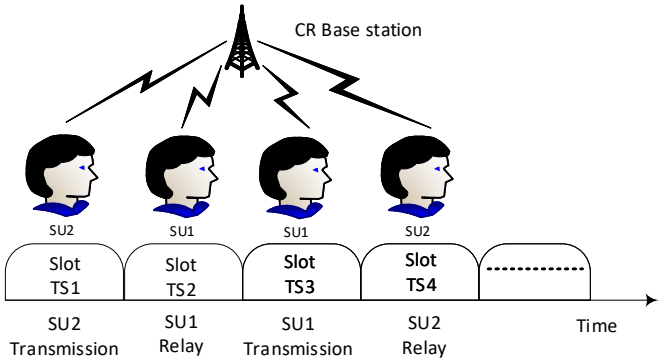

Figure 4.2: Relay protocol management

occupy the spectrum. In time slot TS_1, the signal transmitted by the SU_2 and received by the SU_1 is written as,

$$g_1 = \Delta q_{pu1} + a q_{21} + {n_1}^* \tag{4.2}$$

The instantaneous channel gain between PU and SU_i is q_{pui}, and between SU_2 and SU_1 is q_{21}. The additive Gaussian noise is represented by ${n_1}^*$. Some assumptions are considered here as the channel gain q_{pu1}, q_{21}, and noise ${n_1}^*$ are zero mean complex Gaussian random variables; it means that these are pairwise independent, and channels

are following reciprocal property, i.e., $q_{21} = q_{12}$. a is the signal sent from SU_2, and Δ denotes the presence and absence of PU.

If $\Delta = 0$, it shows the PU's absence, and if $\Delta = 1$, it shows the PU's presence. Let the transmitter power constraint of SU_2 is S then,

$$E\left\{|aq_{21}|^2\right\} = SM_{21} \tag{4.3}$$

where $M_{21} = E\left\{|q_{21}|^2\right\}$ shows the channel gain between SU_2 and SU_1 and q_{pu1}, q_{21}, ${n_1}^*$ are independent which has already mentioned, then from (4.2)

$$E\left\{|g_1|^2\right\} = \Delta^2 S_1 + SM_{21} + 1 \tag{4.4}$$

here $S_i = E\left\{\left|q_{pui}\right|^2\right\}$ shows the received signal power at SU_i due to the PU. In the duration of time slot, TS_2, SU_1 (which works as a relay user) relays the information from SU_2 to the common receiver. The maximum power constraint of the relay user is $\widetilde{S}$. SU_1 (relay user) calculates the average received power of the signal and estimates it properly for satisfying its power constraint $\widetilde{S}$. When user SU_1 relays the information of user SU_2 to the common receiver, at that time SU_2 also listens to its own information. This process takes place in slot TS_2. The signal transmitted by the SU_1 to SU_2 is,

$$g_2 = \sqrt{\Omega_2} g_1 q_{12} + \Delta q_{pu2} + {n_2}^* \tag{4.5}$$

put the value of g_1 from (6.32) to (4.5)

$$g_2 = \sqrt{\Omega_2}\left(\Delta q_{pu1} + aq_{21} + {n_1}^*\right) q_{12} + \Delta q_{pu2} + {n_2}^* \tag{4.6}$$

where ${n_2}^*$ represents the additive Gaussian noise [84] and the scaling factor is represented by Ω_2 which is used by the SU_1 for relaying the message signal to the receiver. Now Ω_2 can be written as [85].

$$\Omega_2 = \frac{\widetilde{S}}{E\{|g_1|^2\}} = \frac{\widetilde{S}}{\Delta^2 S_1 + SM_{21} + 1} \tag{4.7}$$

After the cancellation of the message signal component, SU_2 remains with the signal,

$$G = \Delta Q + N^* \tag{4.8}$$

where $Q = q_{pu2} + \sqrt{\Omega_2} q_{12} q_{pu1}$ and $N^* = {n_2}^* + \sqrt{\Omega_2} q_{12} {n_1}^*$. Now the detection problem is:

Given observations are

$$G = \Delta Q + N^*, \tag{4.9}$$

The detector decision is:

$$H_1 : \Delta = 1$$

$$H_0 : \Delta = 0$$

4.1.1 Energy Detector Method

The energy detection method is exploited to illustrate the proposed cooperation method's benefits and is an optimal method [86]. It is given that $q_{12} = q_{21}$ and from (4.9) the random variables Q and N^* are complex gaussian distributed and have zero-mean and variances.

$${\sigma^2}_Q = S_2 + \Omega S_1 q \tag{4.10}$$

$${\sigma^2}_{N^*} = 1 + \Omega q \tag{4.11}$$

where

$$q = \frac{|q_{12}|^2}{E\{|q_{12}|^2\}} = \frac{|q_{12}|^2}{M_{12}} \tag{4.12}$$

$$\Omega = \frac{\tilde{S} M_{12}}{\Delta^2 S_1 + S M_{21} + 1} \tag{4.13}$$

here, channel state q_{21} is accessed by SU_2, and this is possible because of the transmission of pilot symbols at regular intervals. Because q_{21} is a complex Gaussian function so, the probability density function of q can write as,

$$f(q) = \begin{cases} e^{-q} & q > 0 \\ 0 & q \leq 0 \end{cases} \tag{4.14}$$

The energy detection makes the statistics-

$$V(G) = |G|^2 \tag{4.15}$$

and this decision statistics are compared with a threshold (ζ, i.e., calculated by a pre-specified false alarm probability (P_{FA})):

$$\beta\,(v; a, c) = \int_0^\infty e^{-q-\frac{v}{a+cq}}\,dq \tag{4.16}$$

for the positive value of v, a and c. Let the cumulative density function of random variable $V(G)$ is written by $F_i(v)$ under the hypothesis $H_i, i = 0, 1$. Because q is the complex gaussian provided by the G, It is obvious that $V(G)$ given q is exponential, now from (4.11)

$$E\{V(G)\,|H_0\,, q\} = E\{|N^*|^2\,|q, \Delta = 0\} = 1 + \frac{\tilde{S}M_{21}}{SM_{21}+1}q \tag{4.17}$$

For $H_0(\Delta = 0)$

$$F_0(v) = S(V(G) > v\,|\eta_0\,) = \int_0^\infty S(V(G) > v\,|\eta_0, q) f(q) dq = \beta(v; 1, \frac{\tilde{S}M_{12}}{SM_{21}+1}) \tag{4.18}$$

In the same way,

$$F_1(v) = \beta\,(v; S_2 + 1, \Omega(S_1 + 1)) \tag{4.19}$$

where Ω has taken from (4.13). The calculation of threshold ζ, is required for the false alarm probability (P_{FA}), such that

$$\beta\left(\zeta; 1, \frac{\tilde{S}M_{21}}{SM_{21}+1}\right) = P_{FA} \tag{4.20}$$

ζ can be uniquely calculated since the value of β in (4.16) is strictly decline in v. Now, with the cooperation of SU_1, the sensing probability (p_{sc}) given by SU_2, is written as,

$${p_{sc}}^{(2)} = \beta\,(\zeta; S_2 + 1, \Omega(S_1 + 1)) \tag{4.21}$$

In the case of non-cooperation between SU_1 and SU_2, Ω_2 is zero in (4.6). Let ${p_{snc}}^{(1)}$ and

${p_{snc}}^{(2)}$ represent the sensing probability in the case of non-cooperation, and according to the system model these are written as,

$$ {p_{snc}}^{(1)} = {P_{FA}}^{\frac{1}{S_1+1}} \tag{4.22} $$

and

$$ {p_{snc}}^{(2)} = {P_{FA}}^{\frac{1}{S_2+1}} \tag{4.23} $$

Now, we discuss the total sensing probability (probability to sense the PU by the SU_1 and SU_2) in CRNs. The total sensing probability of two users (when they independently detect the PU) is given by,

$$ {p_{snc}}^{(1)} + {p_{snc}}^{(2)} - {p_{snc}}^{(1)}{p_{snc}}^{(2)} \tag{4.24} $$

The value of ${p_{snc}}^{(1)}$ and ${p_{snc}}^{(2)}$ can be obtained by equation (4.22) and (4.23), respectively. In the same way, the total sensing probability in the JCSS scheme is given by,

$$ {p_{sc}}^{(2)} + {p_{snc}}^{(1)} - {p_{sc}}^{(2)}{p_{snc}}^{(1)} \tag{4.25} $$

The value of ${p_{sc}}^{(2)}$ is given by (4.21).

4.1.2 Rapidity and Sensing Time for Two Secondary Users

In this subsection, the total sensing time is minimized with the help of the proposed JCSS scheme. Note that, in complex networks, the sensing probability and sensing time do not obey the strict inverse relationship. Two cases are considered to represent the cooperation effect in total sensing time, operating at distinct levels of cooperation. In addition, there is a central controller through which all the SUs are interconnected.

Non-Cooperation case: All the SUs independently detect the PU; when the first user detects the PU presence, it informs other users with the help of the central controller.

Cooperation case: This case is based on the JCSS scheme. In this, if two SUs function in the identical carrier and are situated sufficiently close to each other, they cooperate in searching for PU's presence. As soon as the first SU detects the PU, it informs other SUs with the help of the central controller.

In Fig. 4.1, there are two SUs, SU_1 and SU_2, cooperating in finding the PU presence,

and SU_1 works as a relay for SU_2. In the non-cooperation case, let the number of slots occupied by SU_2 to sense the PU's presence is τ_s. Then τ_s is

$$\Pr\{\tau_s = d\} = (1 - {p_{snc}}^{(2)})^{d-1} {p_{snc}}^{(2)} \tag{4.26}$$

where ${p_{snc}}^{(2)}$ indicates the sensing probability of SU_2 in one slot under the non-cooperative models and is given by (4.23). Let the sensing time involved in the cooperation and non-cooperation case mentioned above is T_{sc} and T_{snc}, respectively.

$$T_{sc} = \frac{2 - \frac{{p_{sc}}^{(2)} + {p_{snc}}^{(1)}}{2}}{{p_{sc}}^{(2)} + {p_{snc}}^{(1)} - {p_{sc}}^{(2)} {p_{snc}}^{(1)}} \tag{4.27}$$

$$T_{snc} = \frac{2 - \frac{{p_{snc}}^{(2)} + {p_{snc}}^{(1)}}{2}}{{p_{snc}}^{(1)} + {p_{snc}}^{(2)} - {p_{snc}}^{(1)} {p_{snc}}^{(2)}} \tag{4.28}$$

For the two users, the rapidity gain of the cooperation protocol over the non-cooperation protocol is written as

$$\Im_{\frac{nc}{c}}(1) \triangleq \frac{T_{snc}}{T_{sc}} \tag{4.29}$$

Rapidity gain is the function of S_1 and S_2.

4.2 Energy Consumption during Spectrum Sensing

After analyzing the sensing time and sensing probability, in this section, the total energy consumption is investigated. The energy consumption in the sensing process depends on the applied sensing scheme. In this chapter, two sensing schemes are proposed and examine the consumed energy when these schemes are used for sensing.

- Preset spectrum sensing scheme (PSS)- In the PSS scheme, a user senses each spectrum in a preset order and selects a spectrum that has less contention as compared to the pre-defined threshold (α) selected by the user.

  Let 'd' represent the probability that the next detected spectrum is better than the current spectrum by a threshold (α). The number of the spectrum that would require to be sensed is denoted by the $\mathbb{Q}$; here, $\mathbb{Q}$ contains the values from 1 to $J-1$. In this context, J shows the total number of available spectrum, including the current spectrum. For the first $J-2$ spectrum, the probability distribution of

$\mathbb{Q}$, which is based on the geometric distribution, is given as:

$$\Pr(\mathbb{Q} = b) = d(1-d)^{b-1}, \forall b \; = \; 1 \; to \; J-2 \tag{4.30}$$

Sensing probability of the last spectrum is,

$$\Pr(\mathbb{Q} = J-1) = 1 - \sum_{b=1}^{J-2} d(1-d)^{b-1} \tag{4.31}$$

Based on (4.30), the probability of the user switch from the current spectrum to others can be calculated as:

$$p_{sw} = \sum_{b=1}^{J-1} d(1-d)^{b-1}, \tag{4.32}$$

Hence, by (4.30) and (4.31), we estimate the expected value of sensed spectrums,

$$E_{\mathbb{Q}} = \frac{\left[1-(1-d)^{J-2}\right]^2}{d} + (J-1)(1-d)^{J-2} \tag{4.33}$$

Therefore, the sensing energy can be given as:

$$\tilde{E}_{sense} = E_{\mathbb{Q}}\left[\tilde{P}_{sw}\tilde{\theta}_{sw} + \tilde{E}^{ch}_{sense}\right] + p_{sw}\tilde{P}_{sw}\tilde{\theta}_{sw} \tag{4.34}$$

where $\tilde{E}^{ch}_{sense}$ is calculated by [87] and the value of d, can be determined as follows. Suppose K indicates a random variable denoting the number of users present in the sensed spectrum, and $F_K(.)$ represents the CDF of the number of users in each spectrum. Thus,

$$d = \Pr(K < r - r\alpha) = F_K(r - r\alpha) - \Pr(K = r - r\alpha) \tag{4.35}$$

- Viscous spectrum sensing scheme (VSS)- According to this scheme, a SU holds a spectrum till the expected energy consumption reaches more than a certain threshold. The consumption of energy depends on the number of contending users. Therefore, we can say that a user searches another spectrum when the contending users reach over a specified number, suppose i. But the user must periodically

sense its spectrum to get the information regarding the number of contending users, r, on the current spectrum.

Let m represent the probability for a user to stay on its current spectrum, and Z show the average number of spectrums that require to be sensed. In the context of the adhesive sensing scheme, Z has a value from 1 to J (where 1 shows the current spectrum). We have,

$$\Pr(Z = 1) = m \tag{4.36}$$

Let d represent the probability that on sensing, the next detected spectrum has contending nodes less than i. Thus based on (4.32) and (4.36) the probability to sense spectrums 2 to $J-1$ expressed as similarity to previous scheme:

$$\Pr(Z = b) = (1-m)\, d(1-d)^{b-2}, \forall b \;=\; 2\; to\; J-2 \tag{4.37}$$

Therefore, the probability to sensed J^{th} spectrum is,

$$\Pr(Z = J) = \left[1 - m - (1-m)\sum_{b=2}^{J-1} d(1-d)^{b-2}\right] \tag{4.38}$$

Hence, by (4.35), (4.36) and (4.37), we can estimate the expected average number of spectrums are sensed:

$$E_Z = m + (1-m)\left[1 + \frac{1-(1-d)^{J-2}}{d} + (3-J)\,(1-d)^{J-2}\right] \tag{4.39}$$

Suppose K indicates a random variable denoting the number of users present in the sensed spectrum, and $F_K(.)$ represents the CDF of the number of users in each spectrum. Thus,

$$m = \Pr(K \le i) = F_K(i) \tag{4.40}$$

In this sensing scheme, if $r \le i$, a user senses only its own spectrum. Otherwise, it starts sensing other spectrums until it finds $r \le i$; when it obtains such a spectrum, it consumes energy to switch to the new spectrum. Therefore, the sensing is:

$$\tilde{E}_{sense} = E_Z \tilde{E}^{ch}_{sense} + (E_Z - 1)\,\tilde{P}_{sw}\tilde{\theta}_{sw} + (1-m)\,\tilde{P}_{sw}\tilde{\theta}_{sw} \tag{4.41}$$

4.3 Performance Evaluation

4.3.1 Testbed Environment

A real-time hardware testbed is utilized to analyze the performance of the proposed schemes. A testbed consists of the two Universal Software Radio Peripherals (USRPs) that contain software and hardware composition provided by National Instruments (NI). The USRP-2922 of Ettus Research is equipped with filters, wide-band RF converters, a general-purpose processor to manage signal processing, Digital-to-Analog Converter (DAC), and an Analog-to-digital Converter (ADC) and Voltage Controlled Oscillator (VCO) to improve frequency accuracy and synchronization capabilities [88]. Each USRP consists of Rx/Tx ports that can be programmed with the help of LabVIEW Communication System Design Suite (CSDS) software. Table 4.1 shows the specifications and parameters of USRP-2922 used for implementing the testbed.

Table 4.1: Real time setup parameters

Real time setup parameters and values			
Parameter	Value	Parameter	Value
Gain step	0.5 dB	Frequency range	400 MHz-4.4 GHz
Peak I/Q sample rate	25MS/s	Noise figure	5 dB-7 dB
Frequency step	¡1 kHz	Gain range	0 dB-31 dB
DAC	16 bit	Power requirement	6 V

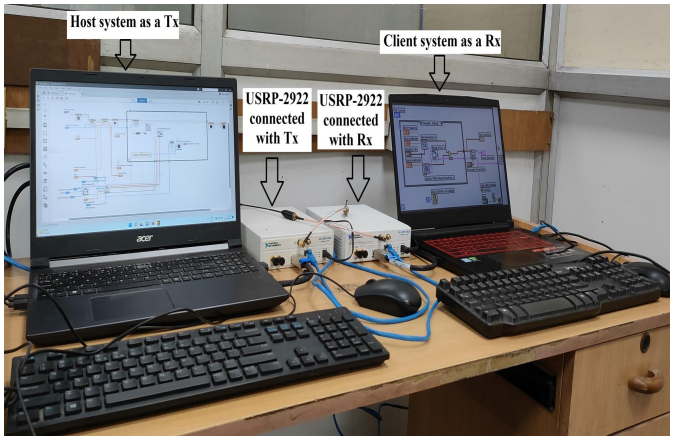

Figure 4.3: A testbed SDR platform for cognitive radio networks

4.3.2 Simulation Results

The proposed sensing schemes have been verified using MATLAB. The system metrics like sensing probabilities, sensing time, rapidity gain, energy consumption, and energy saving percentage are analyzed.

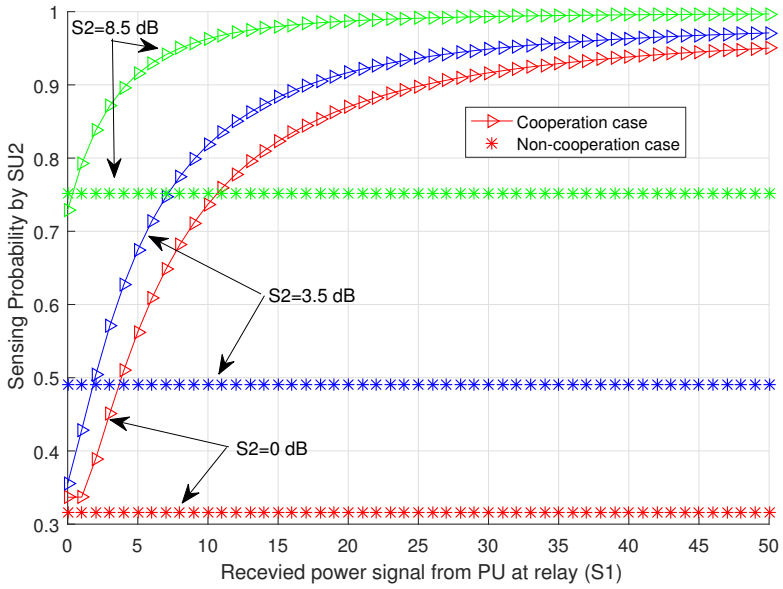

Figure 4.4: Improvement in sensing probability by cooperation technique.

Fig. 4.4, represents the plot of sensing probability in case of cooperation (${p_{sc}}^{(2)}$) and non-cooperation (${p_{snc}}^{(2)}$). ${p_{sc}}^{(2)}$ is determined by (4.21) and ${p_{snc}}^{(2)}$ is determined by (4.23) as a function of S_1, in the case for $\tilde{S} = S = 0$. We consider the value of P_{FA} is 0.1. In Fig. 4.4 the plot of ${p_{sc}}^{(2)}$ and ${p_{snc}}^{(2)}$ is plotted for three values of S_2 : S_2 = 8.5 dB, 3.5 dB and 0 dB. From Fig. 4.4, it is observed that the proposed JCSS scheme presents better outcomes in comparison to the non-cooperation scheme (${p_{sc}}^{(2)} > {p_{snc}}^{(2)}$) for each value of S_2 and for higher values of S_1.

The total sensing probability under the proposed JCSS scheme is indicated in Fig. 4.5. This probability is estimated and plotted the (4.25) by considering the network asymmetry function S_1 for $S_2 = 0$ dB and $P_{FA} = 0.1$. Fig. 4.5 shows that the cooperation between two SUs increases the total sensing probability.

For integrity's sake, the plot in Fig. 4.6 presents the actual sensing time in the number of slots required to detect the PU. This result indicates the reduction in sensing time in the process of PU's detections with the help of the proposed JCSS technique. For analyzing the exact savings, either in the form of sensing time or rapidity, the signal

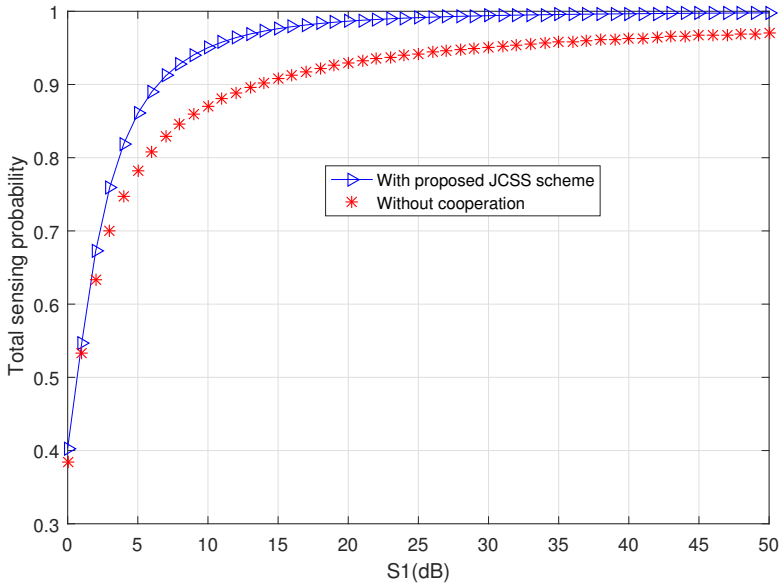

Figure 4.5: Total sensing probability under joint cooperation spectrum sensing scheme

power obtained from the PU at the SU is very significant.

In Fig. 4.7, the rapidity gain ($\Im_{\frac{nc}{c}}$) is plotted based on the JCSS scheme by considering the network asymmetry function S_1 for $S_2 = 0$ dB and $P_{FA} = 0.1$. The maximum rapidity gain for this scenario is 1.35. An increase in rapidity gain is advantageous for the long-term case since the SUs need to monitor the spectrum for the PU's existence.

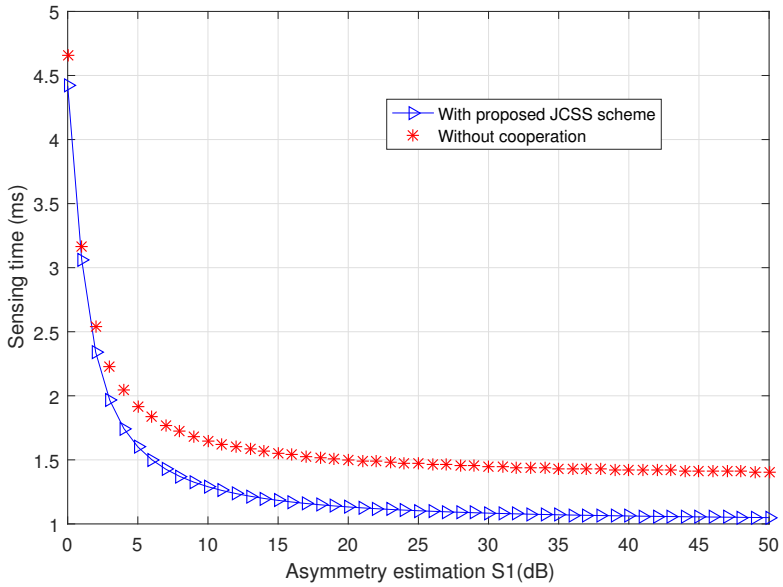

Figure 4.6: Sensing time under joint cooperation spectrum sensing scheme ($S_2 = 0dB$).

The following values are considered for the analysis of total energy consumption: $\tilde{P}_{trx} = 800$ mW, $\tilde{P}_{rcx} = 750$ mW, $\tilde{P}_{idl} = 500$ mW, $\tilde{P}_{slp} = 20$ mW, $\tilde{P}_{sw} = 700$ mW, $\tilde{\theta}_{data} =$

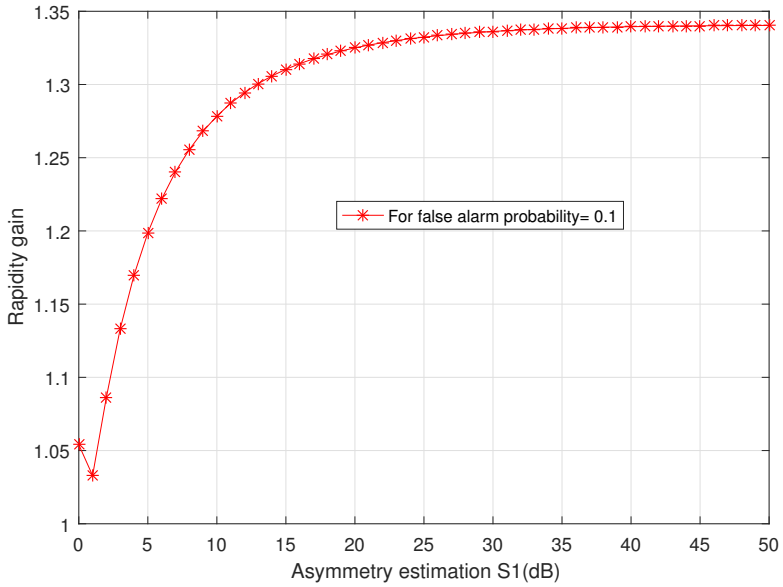

Figure 4.7: Rapidity gain under joint cooperation spectrum sensing scheme

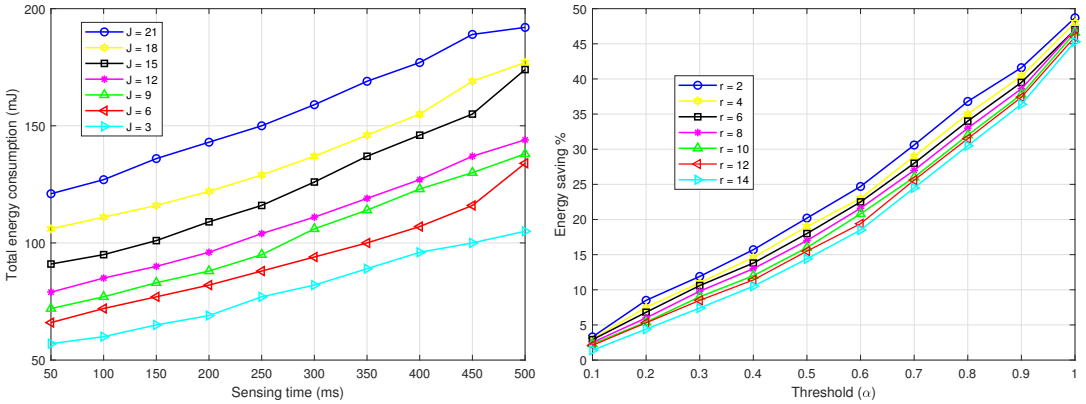

(a) Energy consumption for different values of sensing time

(b) Energy saving percentage for different values of α.

Figure 4.8: Preset spectrum sensing scheme: a) Total energy consumption, b) Energy saving percentage

0.22 ms, $\tilde{\theta}_{ack.pkt}$ = 0.004 ms, $\tilde{\theta}_{difs}$ = 0.05 ms, $\tilde{\theta}_{hdr.pkt}$ = 0.003 ms, $\tilde{\theta}_{pkt.hdr}$ = 0.008 ms, $\tilde{\theta}_{sw}$ = 0.007 ms, $\tilde{\theta}_{slot}$ = 0.004 ms.

Fig. 4.8a, shows the total energy consumption for different values of number of available spectrum (J). According to the result, the energy consumption of SU increases with an increase in sensing time, and it has a maximum value when the number of the available spectrum is high. The explanation is as follows when the number of the available spectrum is high; then the SU takes more time to sense each spectrum. It stops the sensing process when it gets a spectrum with fewer contending users compared to the pre-defined threshold value.

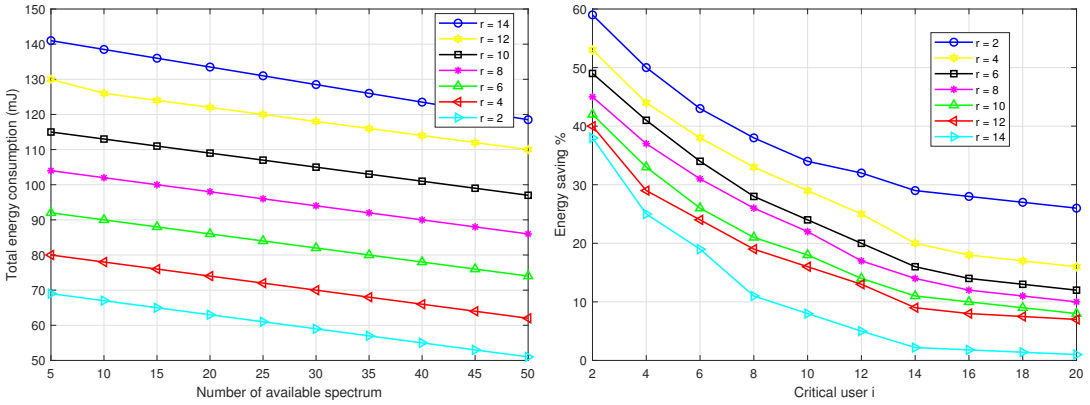

(a) Energy consumption for different values of available spectrum.

(b) Energy saving percentage for different values of i.

Figure 4.9: Viscous spectrum sensing scheme: a) Total energy consumption, b) Energy saving percentage.

Fig. 4.8b, shows that the energy-saving percentage increases with the threshold value increase. The reason is that by increasing the threshold value (α), more spectrum will come into the range of the qualified spectrum. Therefore, the SU can get a more appropriate spectrum in less time because the options have been increased. Hence, this scheme saves energy, and the energy-saving percentage is increased.

Fig. 4.9a, shows the total energy consumption of SU for different values of contending users (r) in the current spectrum. The result reveals that with an increase in the available spectrum (J), the SUs have more options to select an appropriate spectrum. According to the proposed scheme, a SU searches another spectrum when the contending users in the current spectrum are increased over a specified value. Due to more spectrum availability, the number of contending users in any spectrum will be below the specified value. So, each SUs can complete its transmission in a single spectrum, and there is no need to switch to another spectrum. Therefore the energy consumption in the scheme is decreased when the value of J increases.

The proposed VSS scheme is used to get an optimum value of i. According to the proposed scheme, the SU tries to obtain a spectrum with low contending users. A small value of i leads to a lower contention on the spectrum, but detecting a spectrum with a lower value of i might demand extra sensing. On the other hand, for the low value of r, the energy-saving percentage will be maximum. The reason is as follows when the value of r increases, then the SU has to spend energy not only to sense another low contending spectrum but also to switch on them. Hence, Fig. 4.9b shows that the

energy-saving percentage decreases with the increase in the value of r. It is observed from Fig. 4.9b that for the value $J = 10$ and $\tilde{\theta}_{sense} = 150$ ms, $i = 2$ is the smallest possible value for which the energy-saving percentage is highest due to less contention.

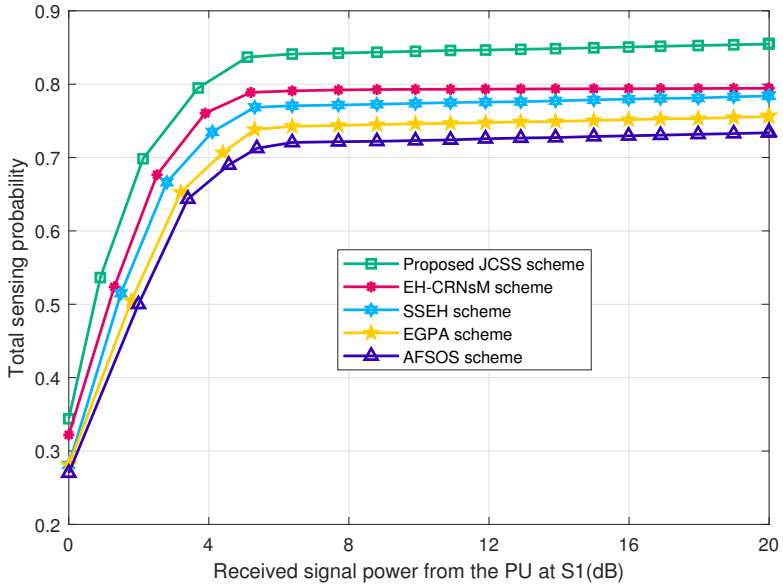

Figure 4.10: Sensing probability comparison of proposed JCSS scheme with other existing schemes

Fig. 4.10, demonstrates the variation in sensing probability w.r.t. the received signal power. It can be surveyed from the graph that the proposed JCSS scheme achieves maximum sensing probability as compared to the other existing sensing schemes.

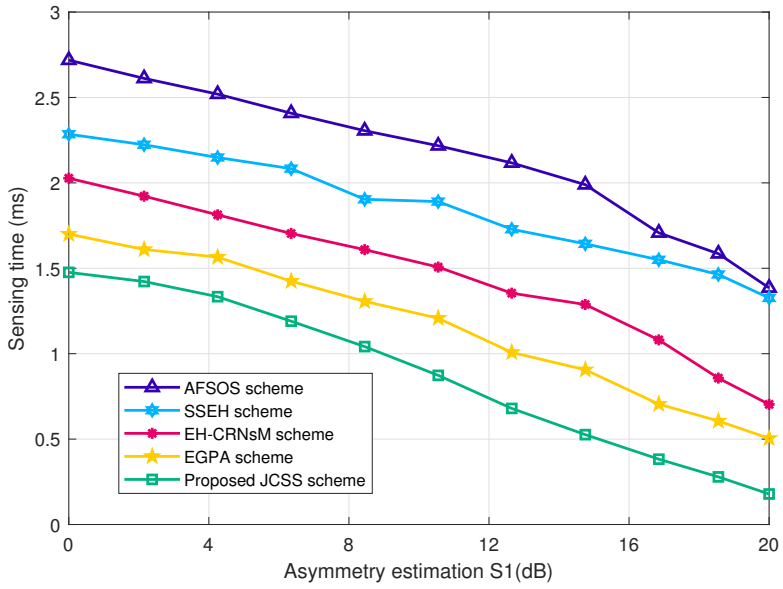

Figure 4.11: Sensing time comparison of proposed JCSS scheme with other schemes

Fig. 4.11, shows the comparison among various sensing schemes with the proposed

JCSS scheme regarding total sensing time. Fig. 4.11 shows that the proposed JCSS scheme requires minimum sensing time to sense a vacant spectrum.

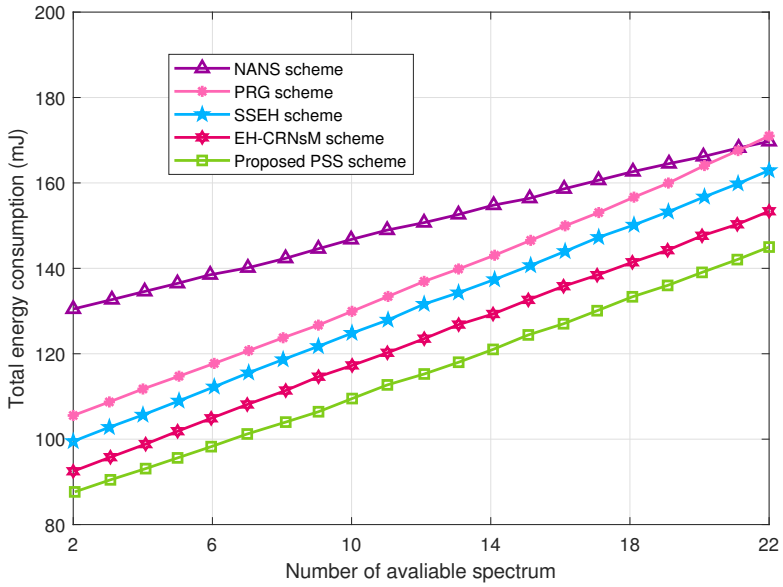

Figure 4.12: Energy consumption variation for different number of available spectrum

Variation in energy consumption for different schemes w.r.t. the available number of spectrum is presented in Fig. 4.12. From the result, we can conclude that with an increase in the number of available spectrum, the energy consumption increase, but the proposed PSS scheme presents the lowest energy consumption with the other scheme. The reason behind this is; in the proposed PSS scheme, the user selects a spectrum with less contention than the pre-defined threshold (α) selected by the user. This property of the proposed PSS scheme reduces energy consumption.

4.4 Conclusions

This chapter analyzes the benefits of cooperation between SUs for detecting the PU's spectrum, through which the rapidity of the network can be improved. Two cases (having a distinct level of cooperation) have been exploited to reduce the sensing time. The first one is non-cooperative, in which all SUs independently sense the PU, and the first user who senses first, informs the presence of the PU to the other SUs via a central controller. The second is cooperative, in which SUs follow the protocols of Amplify-and-Forward cooperation to minimize the sensing time. The results show that the proposed joint cooperation spectrum sensing (JCSS) scheme increases the sensing probability for

a vacant spectrum by as much as 34%. After this, we propose two distinct spectrum sensing schemes preset spectrum sensing (PSS) and viscous spectrum sensing (VSS) that presents the energy savings percentage in GCRNs under specific conditions. These conditions depend on various factors like total contending users in the current spectrum, the time required to sense a spectrum, and the total number of the considered spectrum. These results conclude that the energy consumed by the user's contention increases due to the increase in sensing time. The proposed schemes are better in terms of scalability.

Chapter 5

CEAR: A Cooperation based Energy Aware Reward Scheme for Next Generation Green Cognitive Radio Networks

IN recent years, energy-efficient green communications have been gaining much attention in the field of advanced wireless networks. The reason is that information and communication technologies (ICT) are responsible for 3% of greenhouse gas emissions and 4% to 8% of overall global energy consumption. This problem arises due to inappropriate spectrum management, improper traffic load balancing, and inefficient resource utilization. The major issue in existing wireless networking is that the data transmission of PU experiences attenuation and interference because of the multi-path fading in the practical scenario of the wireless system. The multi-path fading diminishes the network performance and disrupts the two different networks' coexistence. For solving this issue, cooperative communication (CopCom) is recognized as the most promising solution in which a direct path is divided into many shorter paths. The other advantage of the CopCom is that it works on the principle of antenna diversity, and a lower power signal is used for transmission between source and relays. In this chapter, the CopCom in green CRN is considered and categorized in two parts: the first is CopCom between CUs, and the second is CopCom between CUs and PUs. Initially, the CUs work as cooperative relays and finish the transmission of PUs, and then CUs get

the PU's spectrum as a reward for completing their data transmission. In this way, this proposed cooperation-based CEAR (Cooperation based Energy Aware Reward) scheme provides mutual benefit to both CUs as well as to the PUs, and also it helps to improve the EE and SE of CUs in the CRNs.

The rapid increment of new mobile subscribers having extra demand for bandwidth cannot be controlled. Thus, we have to focus on designing advanced energy-efficient wireless communication systems to handle this problem related to spectrum management. Therefore, in the context of CRNs, more analyses are required for investigating the EE and SE for efficient spectrum management. Nowadays, the number of cognitive wireless devices plays a significant role in the ICT industry, and the goal of these devices is to work at a low energy dissipation rate. Therefore, in this chapter, we focus on addressing this issue by examining the cooperative behavior of CUs and propose a CEAR scheme to improve EE and SE in GCRN. We considered a time-slotted framework where the CUs observe and sense the state of PN and perform the decision-making process to complete the data transmission. The key objective of this work is to design an analytical model for improving the SE and EE metrics. The significant contributions of this work are outlined as follows:

- A novel CEAR scheme has been proposed for CUs that takes antennae diversity and temporal diversity into account for improving the EE in CRNs.

- Two different cases have been considered for the analysis of proposed CEAR scheme. In the first case, the CUs contain a fixed amount of packets to transmit. In second, the CUs contain continuously new incoming packets throughout the data transmission and decision process. The data transmission time limit is considered dynamic in nature and depends on the CUs' buffer overflow probability.

- For both cases, the optimal stopping protocol is implemented for decision problem analysis, and the backward induction method is exploited for determining the optimal solution.

- We investigate an optimal cooperative solution for CUs in both the diversity (antennae and temporal). In antenna diversity, the PU that one has the least traffic load is selected by the CU. In temporal diversity, the CUs select a specific time slot when an immediate incentive is higher than anticipated in terms of EE.

5.1 A System Model

The CUs with delay-tolerant packets and light data traffic load does not involve in cooperation until CUs get rewards. This approach allows directly utilizing the PU's vacant spectrum. We consider an example in Fig. 5.1 to explain the cooperation approach between CUs in CRNs. There is N PUs that utilize various spectrum bands in CRNs. The CUs make a decision about the selection of cooperation and when and with which PU they will cooperate. This decision depends upon the time-varying attributes of PUs' traffic load and spectrum availability. For example, at time t_1, a CU may select PU_1 for CopCom and can receive PU_1's spectrum for its transmissions as a reward for cooperation. Additionally, a CU can wait till t_2 to immediately utilize the PU_2's spectrum band. These different selections of PU's unused channel result in different data rates, delays, energy consumption, and throughput.

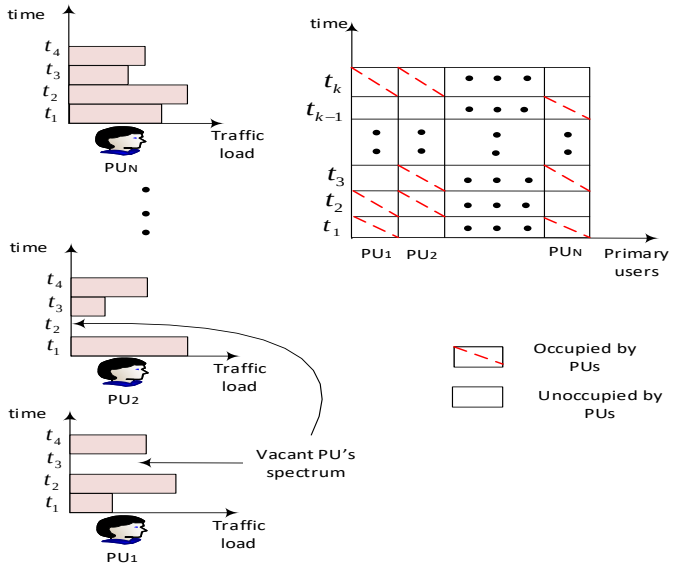

Figure 5.1: PU's time-varying properties for different traffic load

Fig. 5.2 represents the proposed framework, where a centralized control cognitive router (CCCR), a PN, a SN, a group of CUs, and PUs are present in the heterogeneous network area. The users associated with PN and SN are PUs and CUs, respectively. The CCCR collects the traffic load situation, CSI, and spectrum availability of PUs. It is assumed that the PUs occupy the orthogonal primary channels of the same bandwidth B. The cooperation among these components is illustrated as follows:

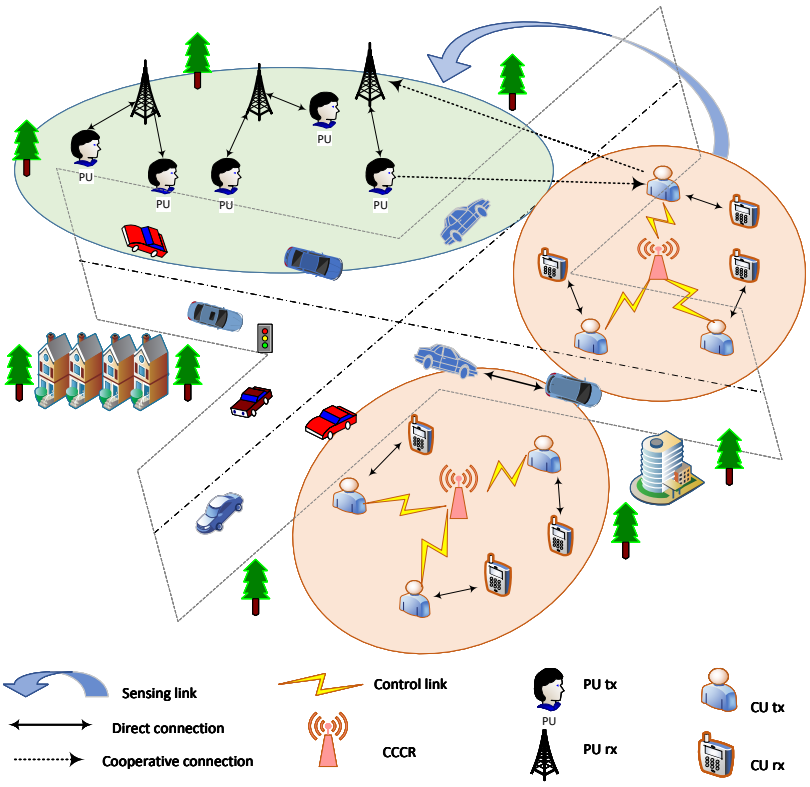

Figure 5.2: A system model of cooperative cognitive radio networks.

- Step 1: Initially, the PUs with data for transmission; convey their data traffic information to CCCR and try to find the possible CU for cooperation. On the other hand, PUs with no data for transmission lives in silent mode.
- Step 2: After getting the request from PUs, the CCCR estimates the CSI and then transmits the PU's request to all available CUs existing within the coverage range.
- Step 3: Based on the request from CCCR and the awareness about its power budget and traffic data, CUs (that require access to primary channel) evaluate the EE and send back the decision (cooperate/ non-cooperate) to CCCR.
- Step 4: The CCCR receives the decisions from CUs obtained after step 3 and informs a particular PU for creating a radio link with CUs.

In this chapter, a time-slotted structure has been considered for CUs and PUs. In each time slot k for $k \in \{1,2,...M\}$, it is assumed that every PUs has distinct traffic load and channel state availability as shown in Fig. 5.1. The cooperative decisions are executed

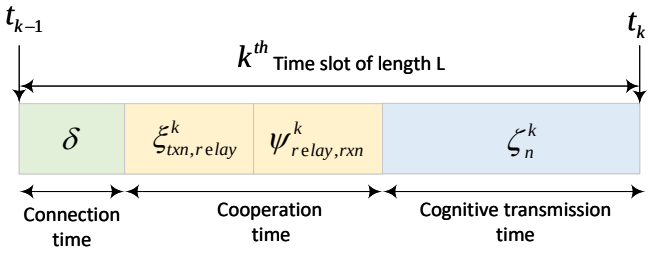

Figure 5.3: Cognitive user's multi-phase time slot.

in each time slot with a proper synchronization between PU and CUs. The media access control (MAC) layer coordination is provided by the CCCR between PU and CUs.

Fig. 5.3 represents the time slot for CUs with length L and is divided into four stages as follows:

Connection time (δ)- It is the time taken for wireless link setup to be established between CU and PU.

First section of cooperation time ($\xi^k_{txn,relay}$)- It is the time taken by PU to deliver its data traffic to the CU.

Second section of cooperation time ($\psi^k_{relay,rxn}$)- It is the time taken for CU to receive data traffic from the PU's transmitter and transfer it either by the DF/AF method to PU's receiver.

Cognitive transmission time (ζ^k_n)- It is the time taken for CU sends its data traffic by utilizing the associated PUs channel as a reward.

In some environments, these stages can be changed. These environments are (i) there is no cooperation time stage when a CU finds a vacant channel and decides not to cooperate, so the entire time slot is used for cognitive activities. (ii) If there is no vacant channel and the CU decides on no cooperation, then the CU stays in the silent state throughout the cooperation time and cognitive transmission time and waits for the next time slot. Moreover, there is an assumption that a PU can only be connected with a single CU during the cooperation. The CCCR performs the coordination within the connection time to avoid interference among CUs.

5.1.1 Power control mechanism

The signal propagation model $\hat{P}_{rx} = \theta \cdot d^{-\sigma} \cdot \hat{P}_{tx}$ is considered in the proposed framework, where θ is a constant associated with various parameters (i.e., gain, frequency, and radiation pattern) of antenna. Using Shannon's theorem, the capacity of the transmitter-receiver link can be estimated as:

$$C_{tx,rx} = B\log_2\left(1 + \frac{\theta \cdot d_{tx,rx}^{-\sigma} \cdot \hat{P}_{tx}}{B \cdot N_0}\right) \tag{5.1}$$

here $B \cdot N_0$ is received noise power, and N_0 represents power spectrum density. The PU's transmitting power ($\hat{P}_{ptx}$) and various states of CU's power are assumed constant. The various states of CU's power are as follows: $\hat{P}_{empty}$ in empty state, $\hat{P}_{crx}$ in receiving state, $\hat{P}_{cop}$ in cooperation state, and $\hat{P}_{ctx}$ in cognitive transmission state.

5.1.2 Traffic Load of Primary User

It is assumed that the PUs have delay-sensitive data traffic, i.e., the data traffic should be sent in the same time slot at which it reaches. β indicates the number of arriving packets in every time interval. The packet arrival supports probability distribution with PMF $f_\beta(\phi)$. It is assumed that the PU's packet arrival is independent of PU's arrival process and follows an identically distributed random sequence. There are two possibilities for channel availability; first, when $\phi = 0$ (i.e., PU has zero traffic load and is considered in an empty state), at this time slot, the CU can obtain the empty channel of PU immediately. On the other hand, when $\phi \neq 0$ (i.e., PU has a non-zero traffic load and its channel is in an occupied state), at this time slot, CU can cooperate with PU and receive an opportunity to access the channel as a reward. Furthermore, the probability of the empty channel and the occupied channel is represented as,

$$p_{empty} = f_\beta(\phi = 0) \tag{5.2}$$

$$p_{occupied} = \sum_{\phi>0}^{\infty} f_\beta(\phi \neq 0) \tag{5.3}$$

5.1.3 Traffic Load of Cognitive Users

In this subsection, the two cases are elaborated for CU's cooperative strategy. In the first case, it is assumed that CU has h packets for transmission, and the data size of these packets is $A = h \cdot m$, where m represents per-packet data size. In the second case, packets frequently arrive at the CU when CU performs the decision-making process. In the second case, j^k denotes the CU's queued packets at k^{th} time slot. The data size of packets is $R^k = j^k \cdot m$, and a finite-size buffer is considered for CU. The proposed cooperation strategy is designed for a single CU, and the data packets of the CU are delay tolerant. Moreover, It is assumed that at the start of the time slot, packets arrive. It is expressed by a vector $\gamma = [\gamma_0, \gamma_1, ..., \gamma_S]$, where γ_α shows α packets arriving probability here $\alpha \in \{0, 1, 2....., S\}$. Therefore, the average arrival rate is represented as,

$$\lambda^{CU} = \sum_{\alpha=0}^{S} \alpha \gamma_\alpha \tag{5.4}$$

5.2 Problem Formulation for Proposed CEAR Scheme

The objective is to optimize the energy efficiency (EE) and spectral efficiency (SE) of the CRNs, which operate in limited power conditions while maintaining the interference of PU not exceeding their specified thresholds. To attain the maximum EE, the CU decides with which PU and at what time slot it will cooperate because the CU can obtain only present knowledge, not future knowledge of the PU's network. The CU sequentially examines the PN in the proposed time-slotted framework. Therefore, optimal stopping theory is considered, which helps the CU to get the optimal stopping time for maximizing its EE. In this chapter, initially, the cooperation scheme is developed for the temporal diversity, and after that implemented, the optimal stopping rule for the decision problem. In the proposed scheme, at a particular time slot, an adequate PU channel with a lower traffic load is selected by CU. This analysis is stopped when the value of the instantaneous utility function is higher than the expected one; otherwise, this process is repeated by CU. The maximum EE obtained by the CU when it observes the k^{th} time slot is denoted V_k and it is calculated as:

$$V_k = \max\{G_k, E[V_{k+1}]\} \tag{5.5}$$

s.t.

$$C.1 : \log_2(1 + SNR_{txn,rxn}) \leq \min\left\{\begin{array}{l} \dfrac{\xi^k_{txn,relay}}{L} \cdot \log_2\left(1 + SNR_{txn,relay}\right), \\ \dfrac{\psi^k_{relay,rxn}}{L} \cdot \log_2\left(1 + SNR_{relay,rxn}\right) \end{array}\right\} \tag{5.6}$$

$$C.2 : \xi^k_{txn,relay} \cdot B\log_2\left(1 + \frac{\theta \cdot d^{-\sigma}_{txn,relay} \cdot \hat{P}_{ptx}}{B \cdot N_0}\right) = \psi^k_{relay,rxn} \cdot B\log_2\left(1 + \frac{\theta \cdot d^{-\sigma}_{relay,rxn} \cdot \hat{P}_{cop}}{B \cdot N_0}\right) \tag{5.7}$$

$$C.3 : \delta + \xi^k_{txn,relay} + \psi^k_{relay,rxn} + \zeta^k_n \leq L \tag{5.8}$$

$$C.4 : p\left(R^k > R_{\max}\right) < r \tag{5.9}$$

$$C.5 : N > 0 \tag{5.10}$$

In (5.5), G_k indicates the value of instantaneous utility function at time k^{th}, and V_{k+1} shows the expected value of EE observe in next time slot. According to CEAR scheme, if $V_k = G_k$ at the k^{th} time slot, then the CU stops and if $G_k = E[V_{k+1}]$ then CU skips the present time slot. To obtain an optimal solution of proposed CEAR scheme for CRNs, the following practical conditions are considered as constraints expressed as.

- *C.1*: Cooperation Reward Constraint- The CEAR scheme is very beneficial for the networks because it improves the EE and SE of CU for a large number of PUs. The PUs can achieve a more reliable data transmission rate by leveraging CUs, and in return, CUs can get access to PU's channels. A situation is considered when the channel of CU is congested and it has data packets to send. The cooperation reward for CU to obtain the PUs channel has been satisfied. Therefore, the inequality described in (5.6) represents the incentive for the PUs. The RHS of inequality expresses the rate of cooperative transmission per unit bandwidth. A direct connection is not considered by the cooperation rate and we can write $SNR_{txn,rxn} = \frac{\theta \cdot d^{-\sigma}_{txn,rxn} \cdot \hat{P}_{ptx}}{B \cdot N_0}$, $SNR_{txn,relay} = \frac{\theta \cdot d^{-\sigma}_{txn,relay} \cdot \hat{P}_{ptx}}{B \cdot N_0}$ and $SNR_{relay,rxn} = \frac{\theta \cdot d^{-\sigma}_{relay,rxn} \cdot \hat{P}_{cop}}{B \cdot N_0}$. The constraint mentioned above ensures that the transmission rate of PU is not less in the case of cooperation as compared to non-cooperation.

- *C.2* : Packet relay constraint- Packet relay: For efficient cooperation, it is required that the entire data packets obtained by the CU from the n^{th} PU in the second stage must be forwarded to the n^{th} PU's address by the CU in the third stage. Hence, the packet relay constraint is represented by (5.7). If (5.7) exists, then the cooperation reward inequality can be represented as, $\log_2\left(1+SNR_{txn,rxn}\right) \leq \frac{\xi^k_{txn,relay}}{L} \cdot \log_2\left(1+SNR_{txn,relay}\right)$.

- *C.3* : Time slot constraint- Based on the time slot frame structure represented in Fig. 5.3, the other conditions represented in (5.8) should also be satisfied as well, where, $\xi^k_{txn,relay}$ and $\psi^k_{relay,rxn}$ can be estimated as:

$$\xi^k_{txn,relay} = \frac{\phi}{B\log_2\left(1+\frac{\theta \cdot d^{-\sigma}_{txn,relay} \cdot \hat{P}_{ptx}}{B \cdot N_0}\right)} \tag{5.11}$$

$$\psi^k_{relay,rxn} = \frac{\phi}{B\log_2\left(1+\frac{\theta \cdot d^{-\sigma}_{relay,rxn} \cdot \hat{P}_{cop}}{B \cdot N_0}\right)} \tag{5.12}$$

  There is an assumption that the time slot has a fixed length L and constant connection time δ. The parameter ζ^k_n will be discussed later for the two different situations, and it depends upon the channel capacity.

- *C.4* : The proposed CEAR scheme depends on the principle that the probability of packet loss should be under a definite limit during the sensing and decision-making operation. Let $R_{\max}$ and r represent maximum data size (manageable by buffer) and pre-defined threshold packet loss probability, respectively.

- *C.5* : The available resources must be greater than zero, i.e., for taking the CU's cooperative decision, the network's available PUs must be greater than zero.

Spectral efficiency is defined as the network throughput per unit of bandwidth. It is denoted as $\mathbb{Q}_{SE}$.

$$\underset{P_N, \mathfrak{R}_N}{max} \{\mathbb{Q}_{SE}\} \tag{5.13}$$

s.t.

$$C.1 : P_N \geq 0 \tag{5.14}$$

$$C.2 : \mathfrak{R}_N \in \{0,1\}, \forall N \tag{5.15}$$

- *C.1*: P_N is the transmission power of CU on the N^{th} PU.
- *C.2*: $\mathfrak{R}_N$ can be valued as 0 and 1. If it is 0 means the N^{th} PU is not used by the CU and If it is 1 means the PU is used by the CU.

5.3 CEAR Scheme under Antenna Diversity

In this section, initially, we propose CU's antenna cooperation scheme to pick the PU with a low traffic load. This traffic load lies under a specified threshold considered by CU's data transmission fulfillment at each time slot. After this, we describe the utility function at the present slot as an immediate reward (i.e., EE).

Based on the obtained CSI from CCCR and according to their own data traffic load information, the CU determines a threshold value to decide on an adequate PU. Therefore, the CEAR scheme facilitates the CU to select adequate PU, which has lower metric value traffic load. It has been discussed above that the packet arrivals of PUs are independent of other PUs' packet arrivals and follow a random process. First, the random variables are arranged in ascending manner of magnitude, i.e., $\beta_{(1)} \leq \beta_{(2)} \leq \ldots\ldots\ldots \leq \beta_{(N)}$ where $\beta_{(i)}$ is the i^{th} smallest number among the N PUs. Now, by using the concept of order statistics [89], we can calculate the probability mass function of the smallest traffic load as follows:

We assumed that the traffic load of a^{th} PU is a random variable β_a and for a given time slot it is i.i.d. from other PUs that follows probability mass function $f_\beta(\phi)$ here $\phi \geq 0$. At a given time slot, we will calculate the probability distribution of the minimum β_a. Initially, we arrange these N random variables in ascending manner of magnitude, i.e. $\beta_{(1)} \leq \beta_{(2)} \leq \ldots\ldots \leq \beta_{(i)} \leq \ldots. \leq \beta_{(N)}$, where $\beta_{(i)}$ is the i^{th} order least number in collection. The probability mass function of $\beta_{(i)}$ is estimated as:

$$f_{\beta_{(i)}}(\phi) = p(\beta_{(i)} = \phi) = p\begin{pmatrix} \text{z } of\ the\ \beta < \phi,\ b\ of\ the\ \beta > \phi, \\ (N-z-b)\ of\ the\ \beta = \phi \end{pmatrix} \tag{5.16}$$

$$= \sum_{z=0}^{i-1}\sum_{b=0}^{N-i}\binom{N}{z}\binom{N-z}{b} p(\beta < \phi)^z p(\beta > \phi)^b p(\beta = \phi)^{N-z-b} \tag{5.17}$$

$$= \sum_{z=0}^{i-1} \sum_{b=0}^{N-i} \binom{N}{z} \binom{N-z}{b} [F(\phi)]^z [1-F(\phi)]^b f(\phi)^{N-z-b} \tag{5.18}$$

Basically, it is required the probability mass function of 1^{st} order statistic, i.e., $\beta_{(1)} = \min(\beta_1, \beta_2, ...\beta_N)$. Next, we set $i = 1$ and let $z = 0$; then, the probability mass function can be written as,

$$f_{\beta_{(1)}}(\phi) = p(\beta_{(1)} = \phi) = \sum_{b=0}^{N-1} \binom{N}{b} [1-F(\phi)]^b \cdot f(\phi)^{N-b} \tag{5.19}$$

$$f_{\beta_{(1)}}(\phi) = \sum_{h=1}^{N} \frac{N!}{h!(N-h)!} \left[f_\beta(\phi)\right]^h \cdot \left[1-F_\beta(\phi)\right]^{N-h} \tag{5.20}$$

where the CDF of the random variable β is $F_\beta(\phi)$.

5.3.1 Threshold Selection for Two Cases

5.3.1.1 Case 1: Without newly incoming packets at CU

For such a case, the CU has data packets to send, and in the duration of the sensing and decision-making process, no new packets arrived. Now, substituting the value of $\xi^k_{txn,relay}$ from (5.11) and $\psi^k_{relay,rxn}$ from (5.12) in (5.8),

$$\delta + \frac{\phi}{B\log_2\left(1+\frac{\theta \cdot d^{-\sigma}_{txn,relay} \cdot \hat{P}_{ptx}}{B \cdot N_0}\right)} + \frac{\phi}{B\log_2\left(1+\frac{\theta \cdot d^{-\sigma}_{relay,rxn} \cdot \hat{P}_{cop}}{B \cdot N_0}\right)} + \zeta^k_n = L \tag{5.21}$$

Here $\zeta^k_n = \frac{A}{B\log_2\left(1+\frac{\theta \cdot d^{-\sigma}_{relay,relay} \cdot \hat{P}_{ctx}}{B \cdot N_0}\right)}$ shows the cognitive transmission time.

Let $C_{relay,relay} = B\log_2\left(1+\frac{\theta \cdot d^{-\sigma}_{relay,relay} \cdot \hat{P}_{ctx}}{B \cdot N_0}\right)$, $C_{txn,relay} = B\log_2\left(1+\frac{\theta \cdot d^{-\sigma}_{txn,relay} \cdot \hat{P}_{ptx}}{B \cdot N_0}\right)$ and $C_{relay,rxn} = B\log_2\left(1+\frac{\theta \cdot d^{-\sigma}_{relay,rxn} \cdot \hat{P}_{cop}}{B \cdot N_0}\right)$.

$$\delta + \frac{\phi \cdot m}{C_{txn,relay}} + \frac{\phi \cdot m}{C_{relay,rxn}} + \frac{A}{C_{relay,relay}} = L \tag{5.22}$$

$$\phi\left(\frac{1}{C_{txn,relay}} + \frac{1}{C_{relay,rxn}}\right) + \delta + \frac{A}{C_{relay,relay}} = L \tag{5.23}$$

$$\phi\left(\frac{1}{C_{txn,relay}}+\frac{1}{C_{relay,rxn}}\right)=L-\delta-\frac{A}{C_{relay,relay}} \tag{5.24}$$

$$\phi=\frac{L-\delta-\frac{A}{C_{relay,relay}}}{\left(\frac{1}{C_{txn,relay}}+\frac{1}{C_{relay,rxn}}\right)} \tag{5.25}$$

Now the final traffic threshold can be written as:

$$\phi_{th}^{n}=\left(L-\delta-\frac{A}{C_{relay,relay}}\right)\cdot\left(\frac{1}{C_{txn,relay}}+\frac{1}{C_{relay,rxn}}\right)^{-1} \tag{5.26}$$

It is observed that each PU has a separate traffic threshold limit for a certain time slot due to the diverse channel situations of PU. Hence, using (5.26), a specific traffic threshold can be determined for every PU. The traffic threshold provides the CSI of CU's different connections and traffic information.

According to the proposed antenna cooperative scheme, cooperation exists till the lowest traffic load is less than the threshold value. The smallest threshold between all the PUs is utilized for comparing the lowest traffic load. The operative traffic threshold is described as $\phi_{th}=\min\left\{\phi_{th}^{1},\phi_{th}^{2},.....\phi_{th}^{N}\right\}$. In this way, we can estimate the probability that a selected PU is suitable for establishing a cooperative connection with CU. In a special case, when PU has no traffic load, the CU directly exploits PU's channel without cooperation. The probability is calculated as:

$$p_{k}^{*}=p\left(0<\beta_{(1)}\leq\phi_{th}\right)+p\left(\beta_{(1)}=0\right)=\sum_{\phi=0}^{\phi_{th}}f_{\beta_{(1)}}\left(\phi\right) \tag{5.27}$$

here p_{k}^{*} shows the overall probability that a CU can communicate either by CopCom or by direct access.

5.3.1.2 Case 2: Continuously incoming packets at CU

The number of CU's data packets keeps growing continuously in the buffer if the CU has incoming data packets at the starting of every time period slot. Hence, substituting the value of $\xi_{txn,relay}^{k}$ from (5.11) and $\psi_{relay,rxn}^{k}$ from (5.12) in (5.8), and considers the solving steps as mentioned in previous case, the traffic load threshold is represented by:

$$\phi_{th}^{n,k}=\left(L-\delta-\frac{R^{k}}{C_{relay,relay}}\right)\left(\frac{1}{C_{txn,relay}}+\frac{1}{C_{relay,rxn}}\right)^{-1} \tag{5.28}$$

where R^k is the queued packets data size at k^{th} time slot. Since the threshold represented in (5.28) is considered as the selection criterion. At k^{th} time slot, the value of threshold and R^k can be evaluated similarly as, $\phi_{th}^k = \min\left\{\phi_{th}^{1,k}, \phi_{th}^{2,k}, ...\phi_{th}^{N,k}\right\}$. This metric value is compared with the minimum value of PU's traffic load at time k^{th}.

The number of incoming packets is described as a random variable and follow the probability vector $\gamma = [\gamma_0, \gamma_1, ..., \gamma_S]$ at each time slot. Therefore, the queued packets j^k can obtain the value $w \in \{h, h+1, ...h+Sk\}$, at the k^{th} time slot. This indicates the cardinality of j^k is $Sk+1$, where $k = 1, 2, ...M$. Hence, the random variable R^k and ϕ_{th}^k have cardinality same as $Sk+1$. The ϕ_{th}^k is determined by (5.28). Now, to find out the PMF of ϕ_{th}^k, first, the PMF of R^k is calculated as follows:

- **Lemma 1**. *For evaluating the probability mass function of a R^k, we consider $(k-1)^{th}$ order convolution of probability vector γ's, and it is represented as:*

In every time slot, the incoming packets are considered as the random variable that supports the vector $\gamma = [\gamma_0, \gamma_1, ...\gamma_S]$. Suppose $\alpha_k \in \{0, 1, ..., S\}$ represents the incoming packets in k^{th} time slot. Hence, the queued packets are represented as $w = h + \alpha_1 + \alpha_2 + ... + \alpha_k$, till the k^{th} time slot. Then, the PMF is given as,

$$f_{R^k}(w) = p(h + \alpha_1 + \alpha_2 + ... + \alpha_k = w) \tag{5.29}$$

$$= \sum_{\alpha_1=0}^{S} p(\alpha_2 + ... + \alpha_k = w - h - \alpha_1) \cdot \gamma_{\alpha_1} \tag{5.30}$$

$$= \sum_{\alpha_{k-1}=0}^{S} .... \sum_{\alpha_1=0}^{S} p(\alpha_k = w - ... - \alpha_{k-1}) \cdot \gamma_{\alpha_1} .... \gamma_{\alpha_{k-1}} \tag{5.31}$$

$$= \sum_{\alpha_{k-1}=0}^{S} .... \sum_{\alpha_1=0}^{S} \gamma_{w-...-\alpha_{k-1}} \cdot \gamma_{\alpha_1} ... \gamma_{\alpha_{k-1}} \tag{5.32}$$

$$= \sum_{\alpha_{k-1}=0}^{S} \gamma_{\alpha_{k-1}} .... \sum_{\alpha_1=0}^{S} \gamma_{\alpha_1} \cdot \gamma_{w-...-\alpha_{k-1}} \tag{5.33}$$

$$f_{R^k}(w) = \sum_{\alpha_{k-1}=0}^{S} \gamma_{\alpha_{k-1}} ... \sum_{\alpha_2=0}^{S} \gamma_{\alpha_2} \sum_{\alpha_1=0}^{S} \gamma_{\alpha_1} \cdot \gamma_{w-h-\alpha_1-....-\alpha_{k-1}} \tag{5.34}$$

The PMF of ϕ_{th}^k can be calculated according to the $f_{R^k}(w)$. Thus, in the case of continuously incoming packets, the probability of effectively selecting an adequate PU for

cooperation is calculated by same as (5.27), the probability is,

$$\begin{aligned} p_k^{**} &= p\left(0 \le \beta_{(1)} \le \phi_{th}^k\right) \\ &= p\left(0 \le \beta_{(1)} \le d | \phi_{th}^k = d\right) p\left(\phi_{th}^k = d\right) \\ &= \sum_{d=0}^{\infty} \sum_{\phi=0}^{d} f_{\beta_{(1)}}(\phi) \cdot p\left(\phi_{th}^k = d\right) \end{aligned} \tag{5.35}$$

If CU holds the data transmission, the buffer will fill after a fixed time slot due to the continuous incoming data packets. In this situation, the newly incoming packets are lost. The proposed CEAR scheme depends on the principle that the probability of packet loss should be under a definite limit during the sensing and decision-making operation. The inequality mentioned in (5.9) must be fulfilled. With an increase in the time slots, if inequality (5.9) is satisfied at time k^{th} then R^k is non-decreasing. While it is not satisfied at time $(k+1)^{th}$, the sequential time slots up to M contain greater packet loss probabilities than the threshold. Hence, the novel decision and observation limit is up to k and expressed by $\tilde{M}$.

5.3.2 Utility Function

In this subsection, the energy-efficiency function (EEF) is calculated at every time slot. The proposed CEAR scheme analyzes the CU's SE, throughput as well as overall energy cost. If a CU selects a vacant channel, the cooperation phase consumes zero energy, and the connection phase shares the only energy cost according to Fig. 5.3. Hence, if the PU's channel is accessed by CU at k^{th} time slot, then the overall consumed energy (CE) can be represented as,

$$CE^k = (k-1)(L-\delta) \cdot \hat{P}_{empty} + k\delta \cdot \hat{P}_{crx} + \xi_{txn,relay}^k \cdot \hat{P}_{crx} + \psi_{relay,rxn}^k \cdot \hat{P}_{cop} + \zeta_n^k \cdot \hat{P}_{ctx} \tag{5.36}$$

In the RHS of (5.36), the first term shows the consumed energy for being silent in $(k-1)^{th}$ (i.e., previous) time slot. The next term represents connection phase energy cost up to the k^{th} time slot. The third and fourth terms indicate the energy cost in the cooperation phase, and the last term provides the energy cost in CU's transmission. Here, $\zeta_n^{k,*} = \frac{A}{C_{relay,relay}}$ and $\zeta_n^{k,**} = \frac{R^k}{C_{relay,relay}}$ indicate the CU's transmission time for both the cases, without new incoming packets and for continuously incoming packets,

respectively. Then for the CU, throughput is calculated as:

$$T_{CU}^{k,*} = \frac{A}{kL}$$
$$T_{CU}^{k,**} = \frac{R^k}{kL} \tag{5.37}$$

where $T_{CU}^{k,*}$ and $T_{CU}^{k,**}$ indicate the throughput of both the cases, respectively. The ratio of the CU's data traffic during the k^{th} time slot to the overall time is expressed as a throughput. By using this throughput function, the EEF can be derived:

$$G_k = \frac{T_{CU}^k}{CE^k} \tag{5.38}$$

where G_k represents the EEF for both cases. To save energy in the cooperation phase, the CU may wait for a vacant primary channel for direct access, but this waiting time for the vacant channel may be large. Therefore, according to (5.37), the throughput of CU will decrease for a large value of k. Thus, to attain maximum EE, the CEAR scheme carefully maintains the balance between consumed energy and high throughput, represented in (5.38).

5.4 Backward Induction Method for Solving the Optimal Stopping Problem

In this section, the backward induction method is utilized for solving the CU's cooperation scheme for both the cases.

5.4.1 Case 1: Usage of Backward Induction Method for without Newly Incoming Packets at CU

The delay-tolerant packets of the CU have a strict time limit to be sent before M^{th} time slot in this case. Therefore, the expected value of maximum EE is determined at the beginning of the procedure at time slot $(M-1)^{th}$. For explaining backward induction method we consider U_{M-k}^*, which shows the expected value of $E[V_{k+1}]$. There is an assumption that the comparison is stopped by CU at time slot M^{th} for $U_0^* = 0$ and expected EE at time slot $(M+1)^{th}$ for $E[V_{M+1}] = 0$. When CU observes at k^{th} time slot, U_{M-k}^*

can be determined as,

$$U^*_{M-k} = E\left[V_{k+1}\right] = E\left[\max\left\{G_{k+1}, U^*_{M-k-1}\right\}\right] \tag{5.39}$$

$$= \sum_{z} G_{k+1} \cdot f_{\beta_{(1)}}(\phi) + \sum_{b} U^*_{M-k-1} \cdot f_{\beta_{(1)}}(\phi) + \sum_{\phi=\phi_{th}}^{\infty} U^*_{M-k-1} \cdot f_{\beta_{(1)}}(\phi) \tag{5.40}$$

where $z \in \left\{\phi \middle| V_{k+1} \geq U^*_{M-k-1}, \phi = 0, 1, ..., \phi_{th}\right\}$, $b \in \left\{\phi \middle| V_{k+1} < U^*_{M-k-1}, \phi = 0, 1, ..., \phi_{th}\right\}$, $k \in \{1, 2, ..., M\}$ and probability is estimated by substituting the value of $f_{\beta_{(1)}}(\phi)$ from (5.20) in (5.27).

5.4.2 Case 2: Usage of Backward Induction Method for Continuously Incoming Packets at CU

In this case, there is no strict time limit. Therefore, after a particular stage like $\hat{M}^{th}$ time slot, where $\hat{M} < M$, the buffer will be filled because of the continuously incoming packets. Hence, the CU will dynamically decide the desired time duration so that the buffer overflow probability is maintained below a specified level, as written in (5.9). This desired time duration decision depends on the packet arrival rates λ^{CU} to fully transfer each queued packet before the buffer is filled. If the buffer size of CU is $R_{\max}$ and the pre-defined overflow probability threshold is r, then the equation for packet delivery time limit can be based on (5.34) and (5.9).

$$\sum_{R_{\max}/m}^{h+Sk} f_{R^k}(w) < r \tag{5.41}$$

where, $f_{R^k}(w)$ depends on the packet arrival rate $\lambda^{CU} = \sum_{\alpha=0}^{S} \alpha\gamma_\alpha$. Then, $\hat{M}$ can be estimated inversely from (5.41).

After finding the desired time duration, the backward induction method is implemented for the optimal stopping problem. Here, we consider (5.5) as the stopping rule of CU and put $E\left[V_{\hat{M}+1}\right] = 0$. The reason for this is the buffer overflow. Initially, the expected EE at $\left(\hat{M}-1\right)^{th}$ time slot is calculated and next, at $\left(\hat{M}-2\right)^{th}$, till the 1^{st} time slot. For simplicity, the identical symbol $U^{**}_{\hat{M}-k}$ is employed to express $E\left[V_{k+1}\right]$. When

the CU performs the analysis at k^{th} time slot, then $U^{**}_{\hat{M}-k}$ can be estimated as,

$$U^{**}_{\hat{M}-k} = E\left[V_{k+1}\right] = E\left[\max\left\{V_{k+1}, U^{**}_{\hat{M}-k-1}\right\}\right] \tag{5.42}$$

$$= \sum_{d=0}^{\infty}\sum_{z} V_{k+1}.f_{\beta_{(1)}}(\phi)\, p\left(\phi^{k}_{th} = d\right) + \sum_{d=0}^{\infty}\sum_{b} U^{**}_{\hat{M}-k-1}.f_{\beta_{(1)}}(\phi)\, p\left(\phi^{k}_{th} = d\right) + \sum_{d=0}^{\infty}\sum_{\phi=d}^{\infty} U^{**}_{\hat{M}-k-1}.f_{\beta_{(1)}}(\phi)\, p\left(\phi^{k}_{th} = d\right) \tag{5.43}$$

where, $z \in \left\{\phi \middle| V_{k+1} \geq U^{**}_{\hat{M}-k-1}, \phi = 0, 1, ..., d\right\}$, $b \in \left\{\phi \middle| V_{k+1} < U^{**}_{\hat{M}-k-1}, \phi = 0, 1, ..., d\right\}$, $k \in \left\{1, 2, ..., \hat{M}\right\}$ and by using (5.34)-(5.35) the probability will be evaluated.

5.5 Performance Evaluation

The proposed CEAR scheme is verified using MATLAB software. This software analyzes system metrics like EE, SE, packet loss probability, throughput, and consumed energy. In this work, a cooperative CRN has been considered. Several CUs and PUs are spread in the same region, and the total number of PU indicates the PN's density. There is an assumption that both the PN and SN use fixed power. In the PN, the traffic arrival of PUs follows the Poisson process with an average arrival rate λ^{PU} and PUs obtain various primary channels of the same bandwidth $B = 180\ KHz$. In the SN, we assume that each CU has an initial packet size $A = 80\ Kb$, which is terminated after $M = 18$ time slot. It is assumed that the unit of average arrival rate λ^{CU} is bits/second. Table 5.1 represents the list of simulation parameters. The simulation results are presented for both considered cases. To indicate an extensive insight into the proposed CEAR scheme for CUs, we analyze the effects of PU's traffic load, packet arrival rate of CUs, and number of PU, on the EE, SE, and the performance of CUs. The performance of the proposed CEAR scheme is compared with the greedy and sub-greedy schemes.

Table 5.1: Simulation Parameters

Name of Parameter	Parameters value
Distance between PU's sender and receiver pairs ($d_{tx,rx}$)	2500 m
Distance between CU's transceiver pairs ($d_{relay,relay}$)	150 m
$d_{tx,relay}$	1250 m
Path loss exponent (σ)	4
$\hat{P}_{ptx}$	4 W
$\hat{P}_{empty}$	0 W
$\hat{P}_{crx}$	0.2 W
$\hat{P}_{cop}$	2 W
$\hat{P}_{ctx}$	0.4 W
N_0	6.85×10^{-16} W/H_Z
Time slot length (L)	1 s
Connection phase time (δ)	1 ms
Buffer size of each CU ($R_{\max}$)	0.8 Mb
Packet loss probability (r)	0.01
Per packet data size (m)	40 Kb

5.5.1 Case 1: Without newly incoming packets at CU

For this case, the decision span and analysis are up to the M^{th} time slot, and it is considered that M = 18. We analyze the optimal stopping protocol's impact on CU's SE for various numbers of PUs. According to (5.37), the A is constant; therefore, the SE of CU is decided by factor kL. Fig. 5.4 presents the impact of PN's density (the number of PUs) on the SE of CU. After analyzing Fig. 5.4, we can see that with an increase in the number of PUs, CU's SE is improved while; it reduces when the average traffic load on PU becomes higher. The reason is that when the density of PNs is high, then at each time slot, the CU can observe more PUs and has a higher possibility of getting an adequate PU to cooperate with and can identify the unoccupied channel for communication. Furthermore, if the average traffic load of PU is high, the CU takes more time to detect a vacant PU for CopCom. Therefore, the SE of CU is decreased.

The impact of the PN's density (the number of PUs) on the EE of the CU is examined in Fig. 5.5. From the figure, it can be observed that the CU gets higher EE if there is more PUs in the PN because CU has more options to pick a PU's channel with a smaller traffic load or directly select a vacant PU's channel for cooperation. It represents that the antenna diversity of PN improves when the number of PUs increases. It assists CU in selecting a better PU for cooperation or provides a direct communication opportunity.

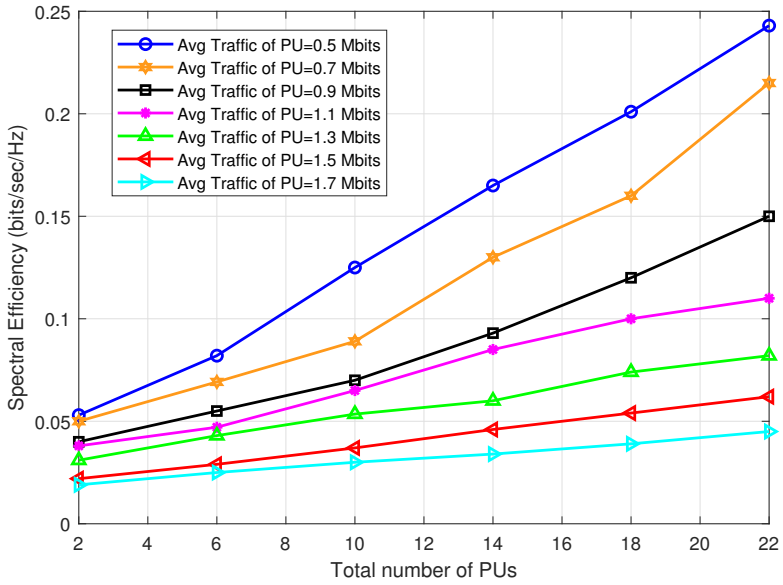

Figure 5.4: CU's spectral efficiency for various average traffic load of PUs

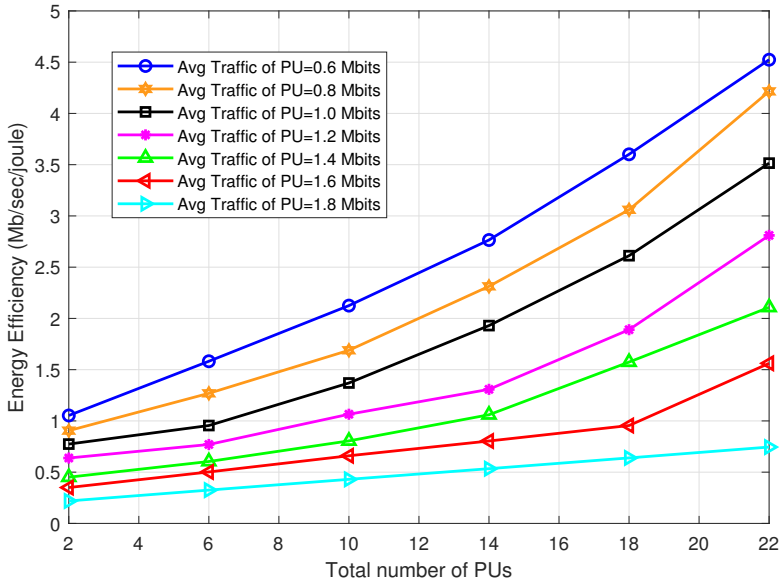

Figure 5.5: CU's energy efficiency for various average traffic load of PUs

The figure indicates that with an increase in the number of PU in the PN, the EE of CU also increases for a low value of PU's traffic load. Because of low PU traffic loads, the CU spends a low amount of energy on cooperation and can detect an appropriate PU after a few time slots. It results in a larger EE for the CU. It can be observed from Fig. 5.6 that, with the increase in the number of CU, the EE of network degrades. Fig. 5.6 that the network's EE increases with the number of PU. The explanation is that when more PUs are in the network, the CUs have more options to select an appropriate PU. In this case, the CU can directly exploit the PU's channel without cooperation.

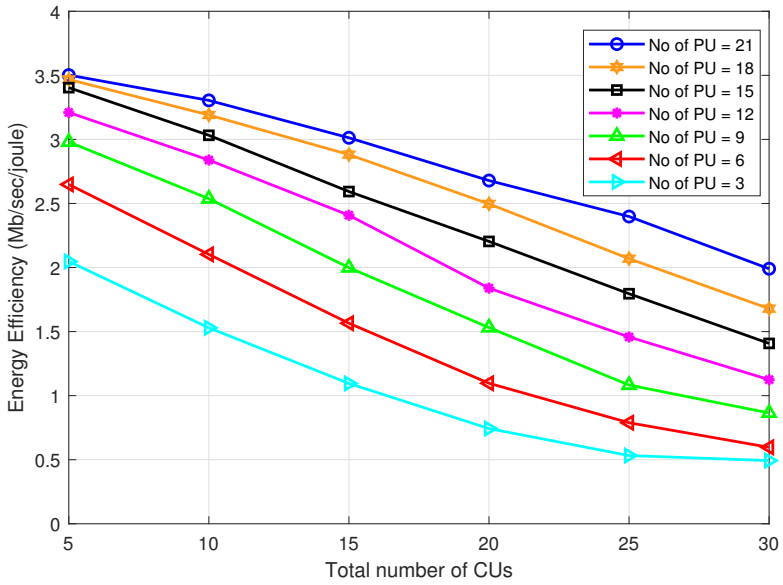

Figure 5.6: Network's energy efficiency for variable number of CUs

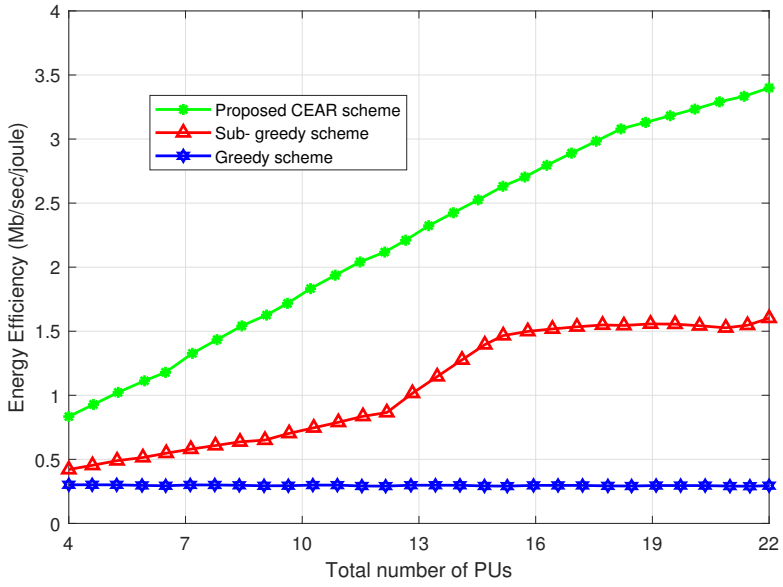

Figure 5.7: CU's energy efficiency comparison for various cooperative schemes

The performance of the proposed CEAR scheme is compared with the sub-greedy and greedy scheme, and we demonstrate the benefits of the CEAR scheme for enhancing the EE of the CU. In various existing works, the authors have considered the greedy scheme. According to this scheme, the CUs (cooperative relays) are expected to follow the PU's decision for cooperation, and in this, the value of consumed energy and throughput is assured for CUs. The sub-greedy scheme utilizes antenna diversity of PN in which CU prefers that PU for cooperation, which one has the smallest traffic load instead of obeying PU's decision. Fig. 5.7 reveals that with an increase in the number

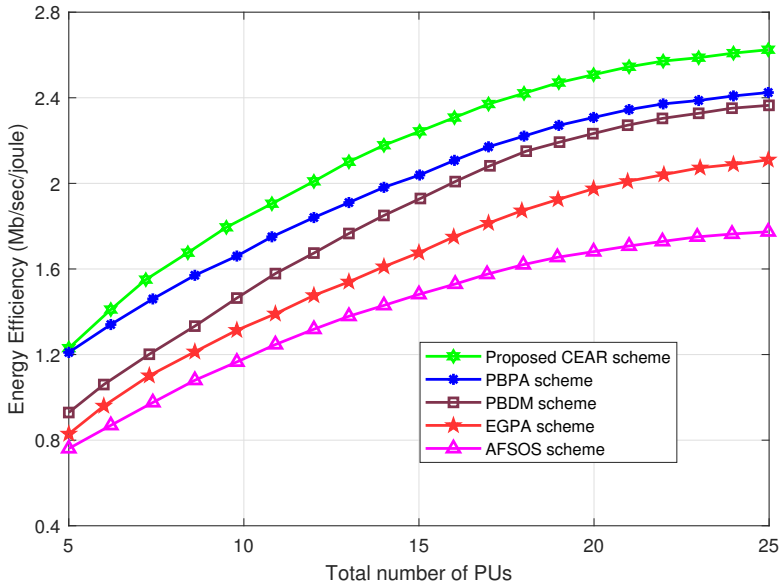

Figure 5.8: CU's energy efficiency for variable number of PUs

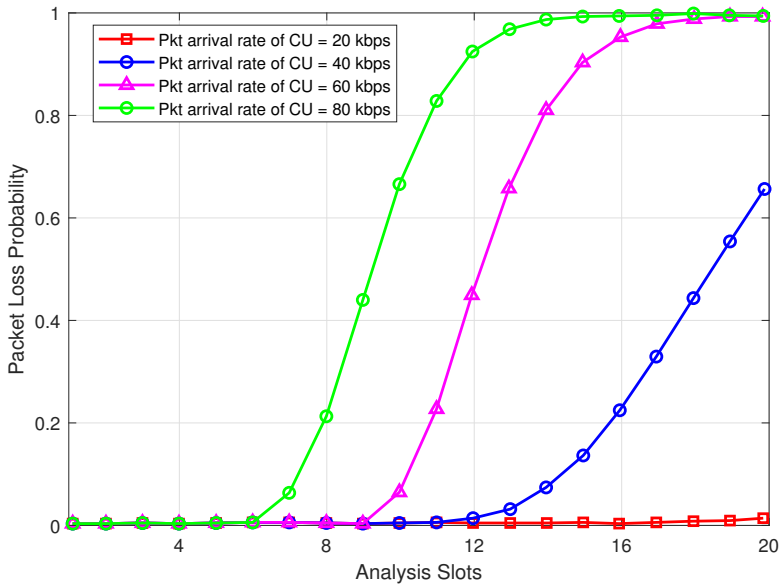

Figure 5.9: Packet loss probability versus analysis slots

of PUs, the CEAR scheme presents improved results against the other two in terms of CU's EE. The reason is that the greedy scheme does not employ the temporal and antenna diversity of PN and blindly considers the decision of PU, while the sub-greedy scheme uses the antenna diversity but not the temporal diversity of PN. However, the proposed CEAR scheme exploits the benefits of both antenna and temporal diversity of PN. It improves the EE of CU and significantly achieves the objective of energy-efficient green communications.

The performance of the proposed CEAR scheme is compared with other existing

schemes, like the PBPA scheme, PBDM scheme, EGPA scheme, and AFSOS scheme in Fig. 5.8. It is observed in Fig. 5.8 that the proposed scheme outperforms other benchmark schemes. For more PUs in the PN, the CU gets higher EE because CU has more options to pick a PU's channel with a smaller traffic load or directly select a vacant PU's channel for cooperation.

5.5.2 Case 2: Continuously incoming packets at CU

In this subsection, the SE and EE of CU are discussed when the CU has continuously incoming packets. In this case, we set a novel time limit for analysis due to the possible buffer overflow after a specific time. The CU can find a unique data delivery time limit according to pre-defined parameters and (5.41). Within this time limit, the transmission of queued data traffic must be completed. On the other hand, the packet loss probability exceeds the threshold value after some time. Fig. 5.9 shows that the packet loss probability rises with the rise in the analysis slots and increases rapidly when the packet arrival rate of CU grows. According to the figure, the CU can dynamically schedule an analysis slot based on the parameters like buffer size, threshold, packet arrival rates, pre-defined overflow probability, etc.

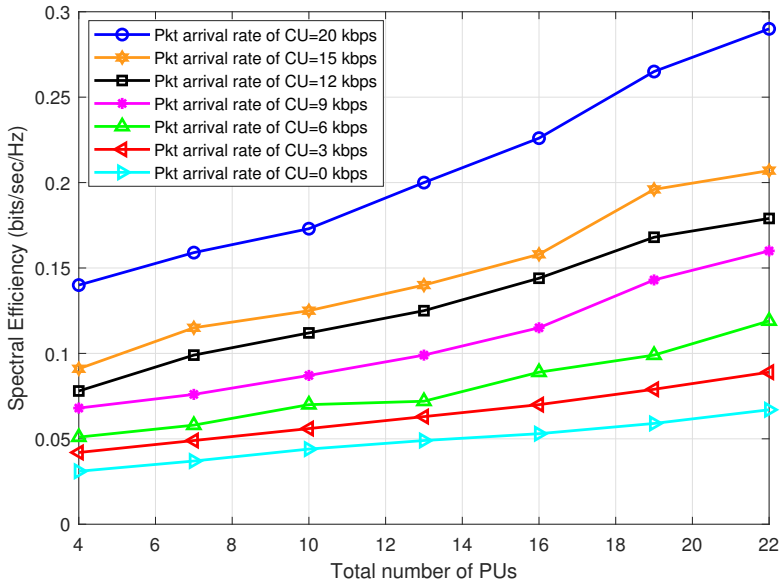

Figure 5.10: CU's spectral efficiency versus the total number of PUs

Fig. 5.10 shows that with an increase in the number of the PUs, the SE of CU at different packet arrival rates also increases. The reasons are as follows, the decision and observation period are smaller to maintain the packet loss probability under the

threshold, so the CU selects the PU for cooperation purposes much before the previous case. Therefore, there is a large number of packets at CU to transmit. According to the (5.37), the SE of CU will surely increase. In addition, if there are more PUs in the PN, CU can directly get the vacant PU or has more options to choose a PU with a smaller traffic load, which leads to higher SE. The simulation result reveals that with an

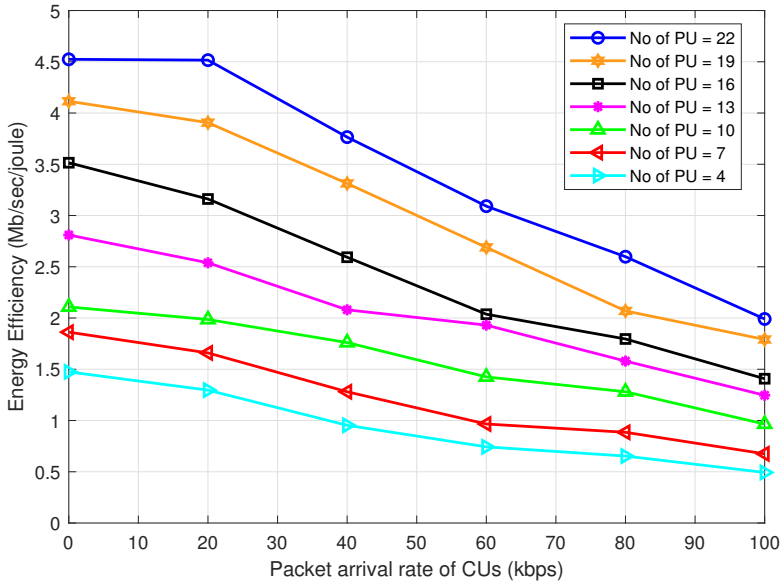

Figure 5.11: CU's energy efficiency versus packet arrival rate

increase in the CU's packet arrival rate, the EE of CU degrades, as shown in Fig. 5.11. It can be observed that the EE of CU is increased by increasing the PU's density in PN, but system performance is diminished by increasing the packet arrival rate of CU. The explanation is as follows when the packet arrival rate is high, then the CU has to send more packets, which produces a larger time for the cognitive transmission. Thus, the CU follows a more rigorous selection criterion on the traffic load of the PUs, which results in fewer qualified PUs, and because of the probability of buffer overflow, the CU selects the PU very soon and does not efficiently employ the temporal diversity of PN. It decreases the opportunity to choose an appropriate PU for cooperation and extends its energy expenditure.

The result of the proposed CEAR scheme is compared with the greedy and sub-greedy schemes in terms of EE performance. From Fig. 5.12, it can be concluded that the proposed CEAR scheme performs better than the other schemes in the case of continuously incoming packets. The result shows that the greedy scheme gives a constant EE curve. Because in this scheme, the antenna diversity is not employed by

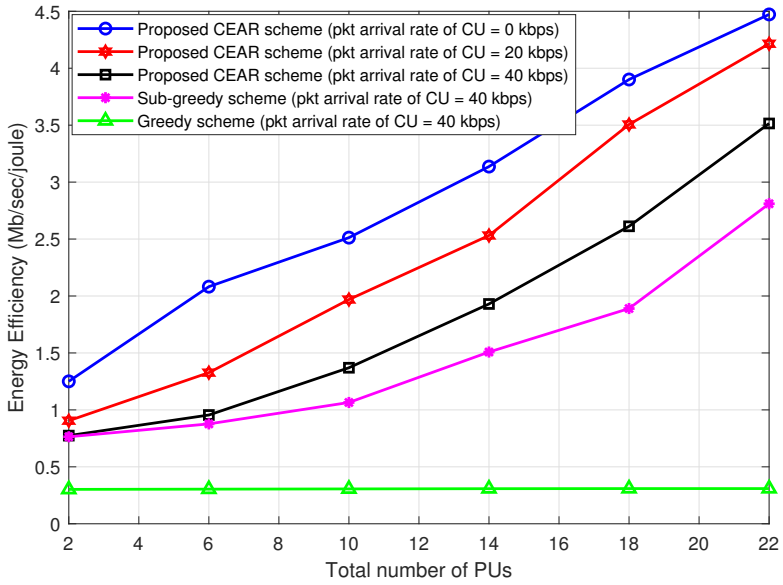

Figure 5.12: Comparison of CU's energy efficiency for various cooperative schemes

the CU. Although the sub-greedy scheme provides an improved EE for more PUs, it does not consider temporal diversity for cooperation. Thus, it gives a lower EE than the proposed CEAR scheme. The result shows that the EE grows up high for an increased number of PUs. It represents that the CEAR scheme is more energy-efficient for ultra-dense network deployment. Fig. 5.13 shows that the EE of CU in case 1 is higher than

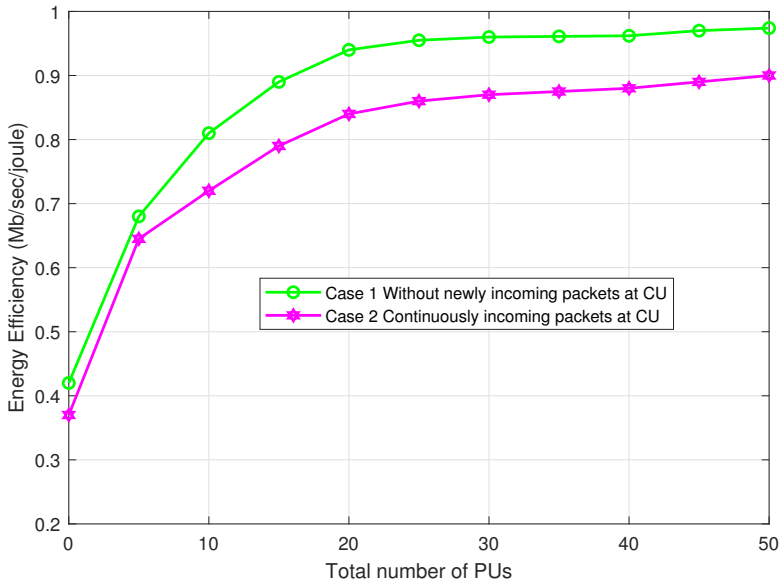

Figure 5.13: Comparison of CU's energy efficiency for two different cases.

in case 2. There are continuously incoming packets at CU in the case of 2. Therefore, the CU has to transmit more packets. It results in a longer cognitive transmission time. So, the CU becomes more careful in selecting the adequate PU, and it is also restricted

from making a decision rapidly. Therefore, the PN's temporal diversity is not employed efficiently, and it reduces the number of adequate PU for selection. Hence, the EE, in this case, is degraded.

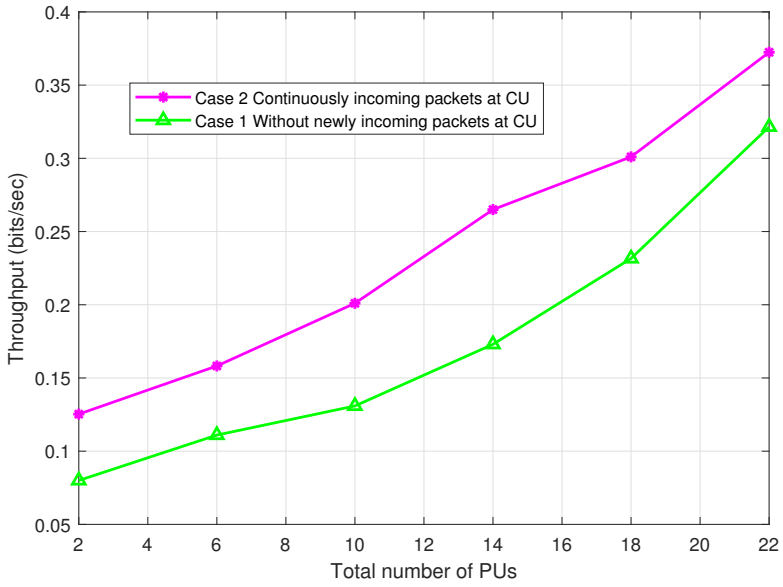

Figure 5.14: Comparison of CU's throughput for two different cases.

Fig. 5.14 represents that the higher throughput is obtained in case 2 than the case 1. Because of maintaining the packet loss probability below the threshold, the CU takes the decision regarding cooperation with PU much quicker than in the first case. Therefore, the CU can transmit more packets for a high packet arrival rate. Furthermore, the throughput of the CU improves when the number of PUs increases because a CU can select a vacant channel or a PU with the lowest traffic load. It offers higher throughput in the second case.

Fig. 5.15 illustrates the consumed energy w.r.t. the average traffic of PU for various schemes. As seen from the figure, the higher value of the average traffic load of PU, the lower the energy consumption in the proposed CEAR scheme. The reason behind this in the proposed scheme is based on the antenna and temporal diversity of PN; therefore, the CU can obtain a vacant PU's channel for direct transmission, or it can select an adequate PU which has a lower metric value traffic load after exploring more PUs.

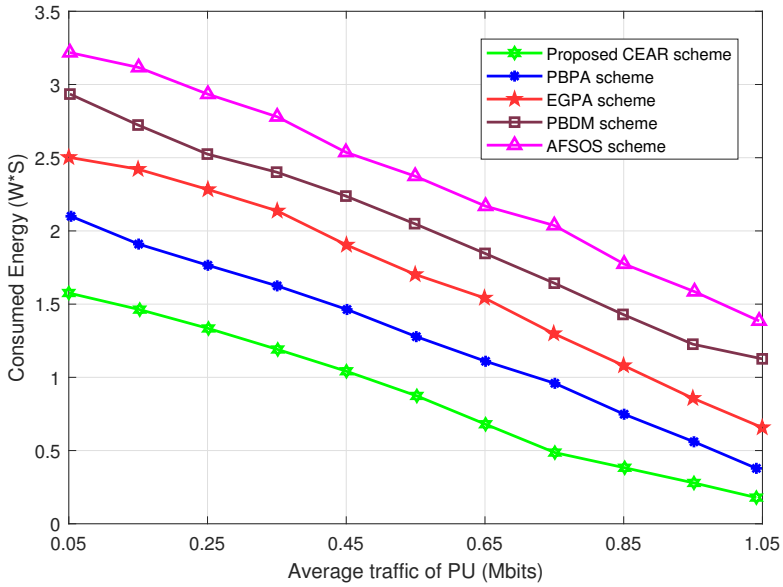

Figure 5.15: Variation in consumed energy for different values of average traffic of PU.

5.6 Conclusions

The wireless network infrastructure is extending day by day due to the addition of mobile subscribers, which degrades energy efficiency, spectral efficiency, and system performance. This chapter presents a cooperation-based energy-efficient scheme for cognitive users in CRNs to improve the energy efficiency of CU. The proposed CEAR scheme supports CUs to actively cooperate by utilizing temporal and antenna diversity to improve energy efficiency. The proposed CEAR scheme is compared with other existing schemes, and it is presented that the CEAR scheme provides up to 28% improvement in energy efficiency. In this work, the optimal stopping protocol is used for problem formulation, and the backward induction method is employed for solving the decision problem. This chapter has contributed significant insight in terms of energy efficiency, spectral efficiency, throughput, and consumed energy, which motivates the design of future green communications systems.

Chapter 6

Machine Learning based Optimal Power Control Scheme for Next Generation Multi-layer Green Cognitive Radio Networks

NOWADAYS, telecommunication systems provide various important services such as real-time data transmission, 360° video applications, web browsing, online gaming, etc., with a high number of mobile users. The upcoming applications will require more data, and it will be challenging for the existing communication systems to cope with this requirement. This requirement raises energy consumption challenges in wireless networks. The information and communication technologies (ICT) have accounted for 2% to 7% of world's total energy consumption. The vision of the next-generation networks (NGNs) is to develop a framework that allows existing networks to link seamlessly. The $5G$ architecture is the multilayer network having distinct cell sizes, variable data transmission rates, powers, and numerous heterogeneous wireless technologies. The interference in $5G$ networks is arisen due to the heterogeneous networking architecture, ultra-dense networks, and transmitters with different transmission powers, which leads to traffic imbalance problems, licensed and unlicensed network access regulations in distinct layers, and the effect of carrier aggregation and $M2M$ communications. Thus, it is required to investigate an intelligent power control schemes to improve the system performance and reduce signal interference for various layer users.

This chapter proposes a reinforcement learning-based optimal power control scheme (ROPC) that utilizes the non-cooperative communication method. According to the proposed scheme, each CT estimates the other CTs' power control policies based on interacting with the environment and exploiting previous experience. ROPC scheme minimizes the overhead of either information exchange among the CTs or establishing a central control unit for information broadcasting. It indicates that less size of information interchange between CTs and optimal power control is achieved which is necessary condition for green communication. In addition to this, the proposed framework ensures that all users in the network achieve high QoS, which is evaluated in the form of improved EE, SE, and signal-to-interference-plus-noise ratio (SINR). Reinforcement learning (RL) is a powerful approach for designing highly adaptable and energy efficient wireless networks. Combining RL into CRNs is being widely studied, and now it has become an important research area in both industry and academia. Therefore, in this chapter, the non-cooperative behavior of CTs is examined to address the power issue and propose an ROPC scheme for GCRNs from the perspective of EE and SE. This work distinguishes itself from available literature as follows:

- A reinforcement learning-based optimal power control (ROPC) scheme is proposed to address the complex power-related issues in multilayer CRNs.
- The real-time learning feature is exploited in the proposed ROPC scheme. Real-time learning requires complete knowledge about all the learning agents present in dynamic environment, and this process is challenging in the context of the heterogeneous environment.
- In a CRNs environment, each CT updates its learning information by interacting with the environment and exploiting its previous experience, without cooperating with other CTs. This feature of the proposed scheme minimizes the cooperation overhead and helps to design the energy-efficient green CRNs.
- A concise representation of the Q-values is considered to minimize the network's computational complexity because the network complexity increases with the extent of the state-action pair. This concise representation feature diminishes the state space and accelerates the convergence of the algorithm.

6.1 A System Model

The proposed system model contains two layers of the heterogeneous $5G$ network: the layer-1 (primary layer) includes a macro-cell with a primary base station (PBS) and PUs, and layer-2, contains two different size cells micro-cells and femtocells and M2M communication, as represented in Fig. 6.1. The suggested model considers bandwidth distribution for down-link transmission. All the layer-2 cells and M2M are uniformly distributed under the area of layer-1. The group of PUs is represented by $L = (1, 2, ..., L)$ and the group of cognitive base stations (CBSs) situated at layer-2 are indicated by $K = (1, 2, ..., K)$. Furthermore, the group of the CUs connected with CBSs is represented by $N = (1, 2, ..., N)$, and the pair of M2M is represented by $M = (1, 2, ..., M)$. The m^{th} pair of M2M ($m \in M$) contains M2M transmitter (m_{tx}) and receiver (m_{rx}), and in this context $m_{tx} \in M_{tx}$, $M_{tx} = (1, 2, ..., M_{tx})$ and $m_{rx} \in M_{rx}$, $M_{rx} = (1, 2, ..., M_{rx})$. The group of CUs connected with the k^{th} CBS is indicated as N^k with the assumption that each CU can be connected with a single CBS.

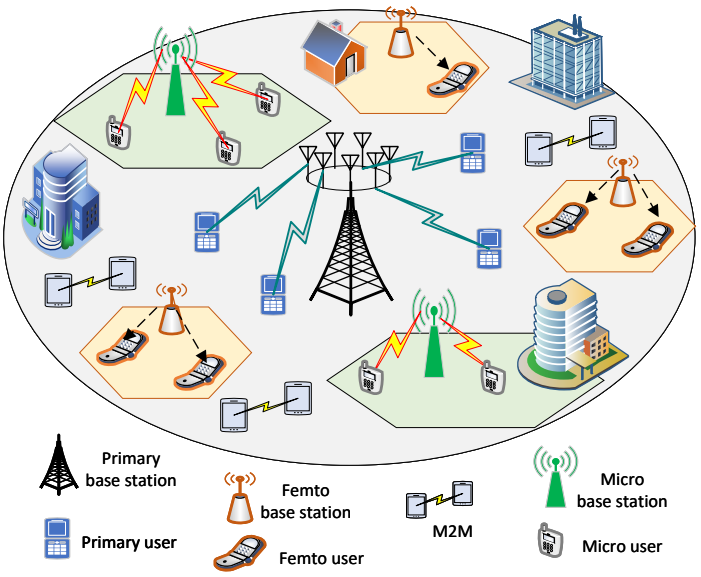

Figure 6.1: Proposed system model

A binary variable d_n^k is used to represent the connection between n^{th} CU with k^{th} CBS. The value $d_n^k = 1$ shows that the n^{th} CU ($n \in N$) is connected with k^{th} CBS, and $d_n^k = 0$, otherwise. The k^{th} CBS selects a random level of power denoted as p^v from the

group of discrete power levels to control the transmission power.

$$p^v = \begin{Bmatrix} \in [1, \tilde{p}^v], & if\ a\ CU\ get\ served\ by\ \ k^{th}CBS \\ 0 & otherwise \end{Bmatrix} \tag{6.1}$$

where $\tilde{p}^v$ is maximum required level of transmission power for CBS. The distributed power to the k^{th} cognitive base station is represented by p^k and it belongs to the group of $\left[0, \frac{1}{\tilde{p}^v}p^k_{\max}, \frac{2}{\tilde{p}^v}p^k_{\max}, .., \frac{p^v}{\tilde{p}^v}p^k_{\max}, .., p^k_{\max}\right]$, here $p^k_{\max}$ is the maximum transmission power for the k^{th} CBS. Furthermore, the m^{th} pair of M2M selects a power level $p^m \in (0, 1, 2, ..., \tilde{p}^v)$ that fulfill the requirements of minimum transmission power $p^m_{\min}$. It also assures that the receiver of M2M is situated within the M2M transmitter proximity (D^m), or it can be written as $D^m \leq D^m_{\max}$.

The SINR of m^{th} M2M pair is evaluated as follows

$$\beta^m = \frac{p^m G^{m_{tx},m_{rx}}}{X^{g,m} + X^{PBS,m} + X^{K,m} + \mathbb{N}_0} \tag{6.2}$$

where noise power is indicated by $\mathbb{N}_0$ and $G^{m_{tx},m_{rx}}$ is power gain between m^{th} M2M transmitter and receiver. The combined interference from all other M2M transmitters at ${m_{rx}}^{th}$ M2M can be represented as-

$$X^{g,m} = \sum_{g \in \frac{M_{tx}}{m_{tx}}} p^g G^{g,m_{rx}} \tag{6.3}$$

In (6.3) the transmission power of g^{th} M2M transmitter is p^g and power gain between g^{th} M2M transmitter and ${m_{rx}}^{th}$ M2M is $G^{g,m_{rx}}$.

The interference due to the PBS at ${m_{rx}}^{th}$ M2M can be written as,

$$X^{PBS,m} = p^{PBS} G^{PBS,m_{rx}} \tag{6.4}$$

where $G^{PBS,m_{rx}}$ is the power gain between the PBS and ${m_{rx}}^{th}$ M2M. Thus, the interference due to all CBSs (represented by K) at ${m_{rx}}^{th}$ M2M is,

$$X^{K,m} = \sum_{k \in K} p^k G^{k,m_{rx}} \tag{6.5}$$

where $G^{k,m_{rx}}$ is the power gain between CBSs and ${m_{rx}}^{th}$ M2M.

The SINR of the n^{th} CU connected with the k^{th} CBS is,

$$\beta^{k,n} = \frac{p^k G^{k,n}}{X^{M,n} + X^{y,n} + X^{PBS,n} + \mathbb{N}_0} \tag{6.6}$$

where $G^{k,n}$ is the power gain between k^{th} CBS and n^{th} CU. The combined interference due to all M2M transmitters at the n^{th} CU is-

$$X^{M,n} = \sum_{m_{tx} \in M_{tx}} p^m G^{m_{tx},n} \tag{6.7}$$

where $G^{m_{tx},n}$ is power gain between M2M transmitter and n^{th} CU. Furthermore, the interference due to the all other CBSs y at the n^{th} CU is,

$$X^{y,n} = \sum_{y \in \frac{K}{k}} p^y G^{y,n} \tag{6.8}$$

where $G^{y,n}$ and p^y show the power gain between the other CBSs y and n^{th} CU, and transmission power of CBS y, respectively. The interference due to the PBS at n^{th} CU can be written as,

$$X^{PBS,n} = p^{PBS} G^{PBS,n} \tag{6.9}$$

where term p^{PBS} and $G^{PBS,n}$ indicate the transmission power of PBS, and power gain between the PBS and n^{th} CU, respectively.

The SINR of l^{th} PU is defined as follows,

$$\beta^l = \frac{p^{PBS} G^{PBS,l}}{\sum_{k \in K} p^k G^{k,l} + \sum_{m_{tx} \in M_{tx}} p^m G^{m_{tx},l} + \mathbb{N}_0} \tag{6.10}$$

where $G^{PBS,l}$, $G^{k,l}$, $G^{m_{tx},l}$ shows the power gains of l^{th} PU with PBS, CBSs k, and M2M transmitters m_{tx}, respectively.

6.1.1 Problem Formulation with EE Perspective

In this chapter, energy efficiency (η) is considered for analyzing the power control mechanism and it can be written as the data transmission rate divided by the power consumed by the CT.

$$\eta^j = \frac{W \log_2 (1 + \beta)}{cp + p^j} \tag{6.11}$$

where W shows the bandwidth, and the power consumed by the CT device is represented by cp . The term j refers for CT device which includes both M2M transmitters and CBSs. β is the SINR at the cognitive receiver. Hence, the optimization of the power control mechanism in the heterogeneous CRNs is expressed as follows-

$$\underset{p^j}{max} \left\{\eta^j\right\} \tag{6.12}$$

Subjected to:

$$\mathbb{C}.1 : \sum_{k \in K} d_n^k = 1, \forall n \in N$$

$$\mathbb{C}.2 : \beta^l \geq \tilde{\beta}^l, \forall l \in L$$

$$\mathbb{C}.3 : \beta^{k,n} \geq \tilde{\beta}^{k,n}, \forall n \in N$$

$$\mathbb{C}.4 : \beta^m \geq \tilde{\beta}^m, \forall m_{rx} \in M_{rx}$$

$$\mathbb{C}.5 : \sum_{n \in N} d_n^k \leq \xi, \forall k \in K$$

Constraint $\mathbb{C}.1$ shows that each CU can be connected with a single CBS. The constraint $\mathbb{C}.2$ reveals that the SINR of PUs should be above the specified threshold $\tilde{\beta}^l$. The PBS exchanges the information of the PU's SINR with M2M transmitter and CBSs. $\mathbb{C}.3$ reveals that the SINR of n^{th} CU should be above the specified threshold $\tilde{\beta}^{k,n}$. The $\mathbb{C}.4$ illustrate that the SINR of m^{th} M2M should be above the specified threshold $\tilde{\beta}^m$. The constraint $\mathbb{C}.5$ express that each CBS can operate with maximum ξ CUs.

6.1.2 Power Control Learning Framework

The power management based on real time learning for CT devices is described in this section. This mechanism can be expressed as $\delta = \left(K, M_{tx}, p^j, \eta_j\right)$. The total available action space for all CT devices is represented as $p = \prod_{j \in K \cup M_{tx}} p^j$. For utilizing the available spectrum, both layers (layer-1 and layer-2) are considered time-slotted configuration for the long-term learning procedure. In this work, the continuous action format $p^j = \left[p^j_{\min}, p^j_{\max}\right]$ is discretized to be consistent with the real-time learning structure based on (6.1). It is specified that $a^j \in A^j$, here $A^j = \left\{0, \frac{1}{\tilde{p}^v} p^j_{\max}, \frac{2}{\tilde{p}^v} p^j_{\max}, .., \frac{p^v}{\tilde{p}^v} p^j_{\max}, .., p^j_{\max}\right\}$ as the action of CTs, and the action space $A = \prod_{j \in K \cup M_{tx}} A_j$ for all CTs. Hence, the term

in discrete format is $\delta' = \left(K, M_{tx}, \left\{p_j\right\}, \left\{\eta_j\right\}\right)$.

The parameters of real-time learning are illustrated as follows:

- Agent: In this work, each CT works as a learning agent, and its objective is to attain the optimal power control policy at different network states.

- State: The CT j follows the state,

$$s_t^j = \left(j, p^j\right) \tag{6.13}$$

  The CTs observe the local information to describe the state of the environment at a specific t time slot.

- Action: The transmission power of CT can be expressed as the action, $\left(a^j\right) = \left(p^j\right)$

- Reward: The reward in terms of state/action set $\mathbb{R}^j\left(s^j, a^j\right)$ can be estimated as,

$$\mathbb{R}^j\left(s^j, a^j\right) = \begin{cases} \mathbb{R}^j\left(a^j\right) = \eta^j, & If \;\; \mathbb{C}.1 - \mathbb{C}.5 \;\; satisfied \\ 0 & otherwise \end{cases} \tag{6.14}$$

  Note that the selection of a^j at state s^j ensures the achievement of the desired EE and maintains the required QoS transmission. As the constraints $\mathbb{C}.1$ to $\mathbb{C}.5$ are fulfilled, the proposed ROPC scheme achieves the reward by maintaining QoS.

- Transition function: The transition of state from s_t^j to s_{t+1}^j represents stochastic performance of CT. The CT independently performs the selection of policy $\pi^j\left[s^j\right]$, for maximizing its overall expected reward. The probability vector which describes the policy is, $\pi^j\left[s^j\right] = \left(\pi^j\left[s^j, 0\right], ..., \pi^j\left[s^j, p_{\max}^j\right]\right)$, where $\pi^j\left[s^j, a^j\right]$ shows the probability that at a particular state s^j, a CT j selects action a^j. The RL based power control process has been depicted in Fig. 6.2.

In the condition of possessing detailed information about all other CTs policies $\pi^{-j} = \left[\pi^1, ..., \pi^{j-1}, \pi^{j+1}, ..., \pi^K\right]$, the overall expected discount of CT j over an infinite time slot can be expressed as,

$$\upsilon^j\left(s^j, \pi^j, \pi^{-j}\right) = E\left[\sum_{t=0}^{\infty} \gamma^t \mathbb{R}^j\left\{s_t^j, \pi^j\left(s_t^j\right), \pi^{-j}\left(s_t^j\right)\right\}, s_0^j = s^j\right] \tag{6.15}$$

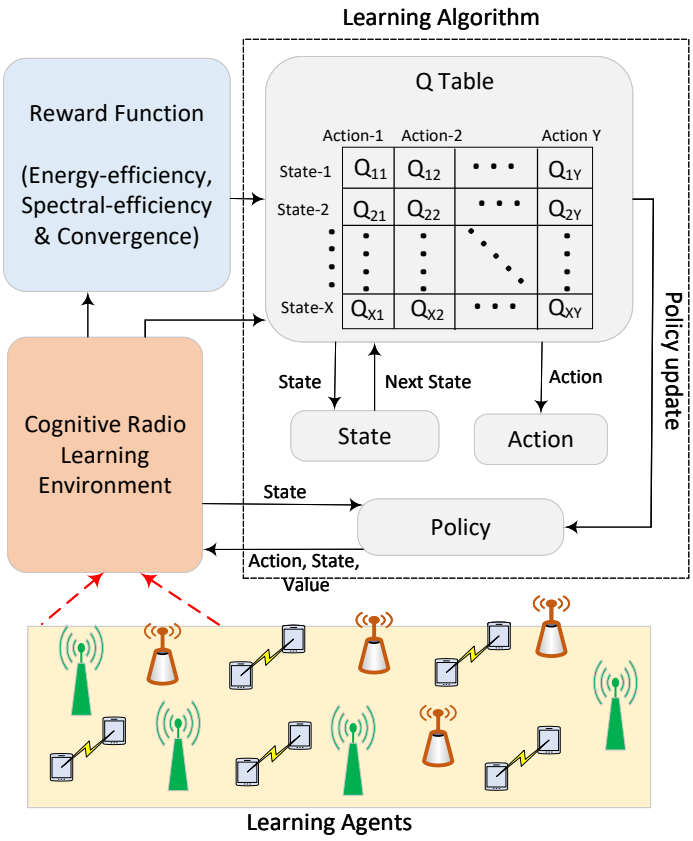

Figure 6.2: Reinforcement learning model for power control

$$= E\left[\mathbb{R}^j\left\{s^j, \pi^j\left(s^j\right), \pi^{-j}\left(s^j\right)\right\}\right] + \gamma \sum_{s_\Delta^j \in S^j} \rho_{s^j, s_\Delta^j}\left\{\pi^j\left(s^j\right), \pi^{-j}\left(s_t^j\right)\right\} \upsilon^j\left(s_\Delta^j, \pi^j, \pi^{-j}\right) \tag{6.16}$$

where γ is discount factor, $\rho_{s^j, s_\Delta^j}\{.\}$ indicates probability of state transition;

$$E\left[\mathbb{R}^j\left\{s^j, \pi^j\left(s^j\right), \pi^{-j}\left(s^j\right)\right\}\right] = \sum_{\left[a^j, a^{-j}\right] \in A}\left[\mathbb{R}^j\left(s^j, a^j, a^{-j}\right) \prod_{i \in K} \pi^i\left(s^j, a^j\right)\right] \tag{6.17}$$

where a^{-j} shows the action taken by the other CTs for state s^j. At each state s^j, a CT utilizes the stochastic learning theory for learning the policy associated with optimal power control π_*^j. To attain the optimal power control policy π_*^j, the following condition must be fulfilled for each CT j, $j \in K \cup M_{tx}$,

$$\upsilon^j\left(s^j, \pi_*^j, \pi_*^{-j}\right) \geq \upsilon^j\left(s^j, \pi^j, \pi_*^{-j}\right), \forall \pi^j \in \Pi^j \tag{6.18}$$

For CT j, the optimal power control policy must satisfied the Bellman's optimality equation [90], and it is show as,

$$\upsilon^j\left(s^j,\pi_*^j,\pi_*^{-j}\right)=\underset{a^j\in A^j}{max}\left[E\left\{\mathbb{R}^j\left(s^j,a^j,\pi_*^{-j}\left(s^j\right)\right)\right\}+\gamma\sum_{s_\Delta^j\in S^j}\rho_{s^j,s_\Delta^j}\left\{a^j,\pi_*^{-j}\left(s^j\right)\right\}\upsilon^j\left(s_\Delta^j,\pi_*^j,\pi_*^{-j}\right)\right] \tag{6.19}$$

here

$$E\left\{\mathbb{R}^j\left(s^j,a^j,\pi_*^{-j}\left(s^j\right)\right)\right\}=\sum_{a^{-j}\in A}\left[\mathbb{R}^j\left(s^j,a^j,a^{-j}\right)\prod_{i\in K/j}\pi_*^i\left(s^i,a^i\right)\right] \tag{6.20}$$

Hence, the optimal Q-value of CT j is the addition of present expected reward and future discount reward when other CTs follow the optimal policies,

$$\mathbb{Q}_*^j\left(s^j,a^j\right)=E\left\{\mathbb{R}^j\left(s^j,a^j,\pi_*^{-j}\left(s^j\right)\right)\right\}+\gamma\sum_{s_\Delta^j\in S^j}\rho_{s^j,s_\Delta^j}\left\{a^j,\pi_*^{-j}\left(s^j\right)\right\}\upsilon^j\left(s_\Delta^j,\pi_*^j,\pi_*^{-j}\right) \tag{6.21}$$

Now by considering (6.20) and (6.21) in a combined manner we can write,

$$\mathbb{Q}_*^j\left(s^j,a^j\right)=E\left\{\mathbb{R}^j\left(s^j,a^j,\pi_*^{-j}\left(s^j\right)\right)\right\}+\gamma\sum_{s_\Delta^j\in S^j}\rho_{s^j,s_\Delta^j}\left\{a^j,\pi_*^{-j}\left(s^j\right)\right\}\underset{q^j\in A^j}{max}\mathbb{Q}_*^j\left(s_\Delta^j,q^j\right) \tag{6.22}$$

The objective of the considered real-time learning technique is to achieve the optimal Q-value illustrated in (6.22) recursively. The information $\left(a^j,s^j,s_\Delta^j,\pi_t^i\right)$ is used at two different states, $s^j=s_t^j$ and $s_\Delta^j=s_{t+1}^j$, studied at t and $t+1$ time slots, respectively. Here π_t^j is the power control policy and a^j shows the action perform at t time slot. To achieve the optimal Q-value, the update rule for real time learning and it can be written by (6.23), where the learning rate $\alpha\in[0,1)$. Revised the Q-value by adding the latest

$$\mathbb{Q}_{t+1}^j\left(s^j,a^j\right)=\left(1-\alpha^t\right)\mathbb{Q}_t^j\left(s^j,a^j\right)+\alpha^t\left[\sum_{a^{-j}\in A^{-j}}\left\{\mathbb{R}^j\left(s^j,a^j,a^{-j}\right)\times\prod_{i\in K/j}\pi_j^i\left(s^i,a^i\right)\right\}+\gamma\underset{q^j\in A^j}{max}\mathbb{Q}_t^j\left(s_\Delta^j,q^j\right)\right] \tag{6.23}$$

expected reward with the previous price as soon as the transmission power action (a^j) is selected and CT j gets the expected reward.

6.2 Proposed Reinforcement Learning based Optimal Power Control Scheme (ROPC)

In this section, the power control issue for multilayer CRNs is addressed without the information of other CTs' power control policies. In Q-values, the problem of slow convergence is raised due to the large size; therefore, a novel concise representation-based approach is considered that permits each CT to infer the power control policies of other CTs without information exchange. Furthermore, it employs a brief representation of the Q-values in the form of a smaller group of variables. This technique improves convergence speed and decreases the computation steps of the algorithm.

6.2.1 ROPC based Power Control

Initially, it is assumed that a similar power control policy is followed by the various CTs at the same network state. To estimate the other CTs power control policies $\pi_t^{-j}\left(s^j\right) = \left\{\pi_t^1\left(s^1\right), \ldots\ldots\ldots, \pi_t^{j-1}\left(s^{j-1}\right), \pi_t^{j+1}\left(s^{j+1}\right), \ldots\ldots, \pi_t^{K+M}\left(s^{K+M}\right)\right\}$ without exchanging the information, we express the learning factor for CT j at t time slot is,

$$\psi_t^j\left(s^j, a^{-j}\right) = \prod_{i \in K \cup M/j} \pi_t^i\left(s^i, a^i\right) \tag{6.24}$$

Learning factor is used to estimate the transition in Q-value, such as $\mathbb{Q}_{t+1}^j\left(s^j, a^j\right)$ for $t+1$ time slot, when specific policies are followed by the other CTs. There is an assumption that the learning agent has the only information regarding the $\psi_t^j\left(s^j, a^{-j}\right)$ of the other CTs. The probability of receiving a reward $\mathbb{R}^j\left(s^j, a^j, a^{-j}\right)$ by CT j is similar to the probability of CT j experiences environment state s_{t+1}, and it can be written as,

$$\chi^j = \pi_t^j\left(s^j, a^j\right)\psi_t^j\left(s^j, a^{-j}\right) \tag{6.25}$$

The probability mentioned in the above equation is similar to the probability that CT j receives the reward expressed in (6.14). It is assumed that the CT j receives the same reward in θ consecutive time slots. Therefore, θ has i.i.d. with probability $\chi^j = \frac{1}{1+\theta'}$, here term θ' shows the mean of θ, and it is calculated by CT j after analyzing the history of its reward. Consequently, by using (6.25), the learning factor can be calculated as

$\psi_t^j\left(s^j, a^{-j}\right) = \frac{1}{(1+\theta')\pi_t^j\left(s^j, a^j\right)}$ as CT j knows its power control policy $\pi_t^j\left(s^j, a^j\right)$. Now the learning factor in terms of the power control policy of CT j is,

$$\psi_t^j\left(s^j, a^{-j}\right) = \psi_\Delta^j\left(s^j, a^{-j}\right) + \sigma^j\left\{\pi_t^j\left(s^j, a^j\right) - \pi_\Delta^j\left(s^j, a^j\right)\right\} \tag{6.26}$$

where σ is a positive scalar for linearization, and terms $\pi_\Delta^j\left(s^j, a^j\right)$ and $\psi_\Delta^j\left(s^j, a^{-j}\right)$ are reference points for the probability to select a specific action and for specific learning. For deciding the points of reference, it is assumed that the other CTs can identify the divergence of CT j from its reference points $\psi_\Delta^j\left(s^j, a^{-j}\right)$ and $\pi_\Delta^j\left(s^j, a^j\right)$ by an amount equal to $\left\{\pi_t^j\left(s^j, a^j\right) - \pi_\Delta^j\left(s^j, a^j\right)\right\}$. If the points of reference are $\psi_\Delta^j\left(s^j, a^{-j}\right) = \prod_{i \in K \cup M/j} \pi_*^i\left(s^i, a^i\right)$ and $\pi_\Delta^j\left(s^j, a^j\right) = \pi_*^j\left(s^j, a^j\right)$ then optimal learning factor is $\psi_*^j\left(s^j, a^{-j}\right) = \prod_{i \in K \cup M/j} \pi_*^i\left(s^i, a^i\right)$, which presents an optimal transmission. The CT's reference points are continuously updated according to their previous transmission information. For the improvement of reference points in the t time slot, the following rule is considered for the learning factor.

$$\psi_t^j\left(s^j, a^{-j}\right) = \psi_{t-1}^j\left(s^j, a^{-j}\right) + \sigma^j\left\{\pi_t^j\left(s^j, a^j\right) - \pi_{t-1}^j\left(s^j, a^j\right)\right\} \tag{6.27}$$

where $\psi_\Delta^j\left(s^j, a^{-j}\right)$ and $\pi_\Delta^j\left(s^j, a^j\right)$ are fixed to $\psi_{t-1}^j\left(s^j, a^{-j}\right)$ and $\pi_{t-1}^j\left(s^j, a^j\right)$ respectively. This shows that any changes in the current policy of any CT will be responsible for the modifications of other CTs in the next time slot. To observe the other CT's deviation policies; the considered framework is based on the variation of CT j from its reference points.

$$\psi_t^j\left(s^j, a^{-j}\right) - \psi_{t-1}^j\left(s^j, a^{-j}\right) = \sigma^j\left\{\pi_t^j\left(s^j, a^j\right) - \pi_{t-1}^j\left(s^j, a^j\right)\right\} \tag{6.28}$$

The updated rule mentioned in (6.23) can be revised by replacing the power control policies of other CTs with the learning of CT j.

In the proposed ROPC scheme, the most suitable power value contains the highest selection probability; on the other hand, other power values are organized on the basis of their Q-values. The Boltzmann distribution is utilized by the proposed learning algorithm for finding the power control action probability. This satisfies the constraints $\mathbb{C}.1$ to $\mathbb{C}.5$ to maximize the EE. Thus, the probability mentioned in (6.29) shows that at a

particular time slot t, the action a^j is selected by the ST j in the state s^j,

$$\pi_t^j\left(s^j, a^j\right) = \frac{e^{\mathbb{Q}_t^j\left(s^j, a^j\right)/\Gamma}}{\sum_{q \in A^j} e^{\mathbb{Q}_t^j\left(s^j, q^j\right)/\Gamma}} \tag{6.29}$$

here, for controlling the selection probability a positive integer Γ is considered. The low value of Γ indicates a major difference in action probability for various Q-values while the high value of Γ shows almost equal action probabilities.

6.2.2 Upgraded ROPC based Power Control

In this chapter, a concise description of the Q-values is considered for minimizing the computational complexity. The reason behind this is the system complexity increases with the extent of states/action pairs. The Q-values are estimated in terms of the smaller set of variables and a vector. The concise description of the Q-values using a function estimator $\tilde{\mathbb{Q}} = \tilde{S} \times A$, is attained by considering a vector $\Psi = [\Psi_h]_h^H$. This helps to minimize the difference between estimated Q-value $\tilde{\mathbb{Q}}_t^j\left(s^j, a^j, \Psi\right)$ and the optimal Q-value $\mathbb{Q}_*\left(s^j, a^j\right)$. The estimated Q-value can be represented as

$$\tilde{\mathbb{Q}}_t^j\left(s^j, a^j, \Psi\right) = \sum_{h=1}^{H} \Psi_h \Omega_h\left(s^j, a^j\right) = \Psi \Omega^T\left(s^j, a^j\right) \tag{6.30}$$

where scalar $\Omega_h\left(s^j, a^j\right)$ is a basis function over $\tilde{\mathbb{Q}} = \tilde{S} \times A$ and the related weights are Ψ_h. The gradient function $\Omega\left(s^j, a^j\right)$ is employed to integrate the real-time learning framework with a concise description.

Then the concise Q value,

$$\pi_t^j\left(s^j, a^j\right) = \frac{e^{\Psi_t^j \Omega^\tau\left(s^j, a^j\right)/\Gamma}}{\sum_{q \in A^j} e^{\Psi_t^j \Omega^\tau\left(s^j, q^j\right)/\Gamma}} \tag{6.31}$$

6.2.3 Convergence of Proposed Scheme

The convergence of the proposed ROPC scheme has been discussed in this subsection. The ordinary differential equations are considered to formulate the essential requirements for convergence. There are some assumptions have been followed for the analysis.

- **Definition**: Let $\zeta = E\left\{\Omega^T\left(s^j, a^j\right)\Omega\left(s^j, a^j\right)\right\}$. A vector $\Omega\left(s^j, \Psi\right) = \left\{\Omega_h\left(s^j, a^j\right)\right\}$ for $h = 1 \rightarrow H$ is considered for the specific state $s^j = S_\Delta$ and for vector Ψ. Here, $a^j \in \left[a^j = \arg\max_{q^j \in A^j} \Psi_j \Omega^T\left(s^j, q^j\right)\right]$ represents a set of actions for s^j associated optimal power control. The value of ζ is depend on Ψ and can be expressed as a function,

$$\tilde{\zeta} = E\left\{\Omega^T\left(s^j, \Psi\right)\Omega\left(s^j, \Psi\right)\right\} \tag{6.32}$$

- **Assumption** 1: The following conditions $\sum_{t=1}^{\infty} \alpha^t = \infty$ and $\sum_{t=1}^{\infty} \left(\alpha^t\right)^2 < \infty$ are satisfied by the learning rate.

- **Assumption** 2: The functions $\Omega_h\left(s^j, a^j\right)$ are linearly independent for each value of $\left(s^j, a^j\right)$.

- **Assumption** 3: All attributes of $\mathbb{Q}_t^j\left(s^j, a^j\right)$ can be applied to the dot product for the vectors $\Psi_t^j \Omega^T\left(s^j, a^j\right)$.

- **Assumption** 4: For all values of $h = (1, 2, ...H)$, $\Omega_h\left(s^j, a^j\right)$ is bounded, it shows that $E\left[\Omega_h^2\left(s^j, a^j\right)\right] < \infty$ and $E\left[\mathbb{R}^{j^2}\left(s^j, a^j, a^{-j}\right)\right] < \infty$.

- **Proposition**: According to the Definition 1 and assumptions $1-4$, the proposed algorithm converges at probability 1, if

$$\tilde{\zeta} < \zeta, \forall \Psi \tag{6.33}$$

Proof: The convergence proof is based on the calculating the stable fixed points of the ordinary differential equation (ODE).

According to the learning factor as discussed in (6.27), It can be written as,

$$\sum_{a^{-j} \in A^{-j}} \left[\left\{\psi_t^j\left(s^j, a^j\right) - \psi_{t-1}^j\left(s^j, a^j\right)\right\}\mathbb{R}^j\left(s^j, a^j, a^{-j}\right)\right] = \sum_{a^{-j} \in A^{-j}} \left[\sigma^j\left\{\pi^j\left(s^j, a^j\right) - \pi_\Delta^j\left(s^j, a^j\right)\right\}\mathbb{R}^j\left(s^j, a^j, a^{-j}\right)\right] \tag{6.34}$$

Replacing the $\pi^j\left(s^j, a^j\right)$ from (6.31) and for large value of Γ, the term will be

$$e^{\Psi_t^j \Omega^T\left(s^j, a^j\right)/\Gamma} = 1 + \frac{\Psi^j \Omega^T\left(s^j, a^j\right)}{\Gamma} + \mathrm{O}\left[\left\{\frac{\Psi^j \Omega^T\left(s^j, a^j\right)}{\Gamma}\right\}^2\right] \tag{6.35}$$

In (6.35), $\wp\left\{\frac{\Psi^j\Omega^T\left(s^j,a^j\right)}{\Gamma}\right\}$ shows the polynomial of order $\mathrm{O}\left[\left\{\frac{\Psi^j\Omega^T\left(s^j,a^j\right)}{\Gamma}\right\}^2\right]$ term. We can calculate,

$$\sum_{q\in A^j} e^{\Psi_t^j\Omega^T\left(s^j,q^j\right)/\Gamma} = z^j + 1 + \left(\frac{\Psi^j\Omega^T\left(s^j,q^j\right)}{\Gamma} + \wp\left\{\frac{\Psi^j\Omega^T\left(s^j,b^j\right)}{\Gamma}\right\}\right) \tag{6.36}$$

here, z^j shows power levels. Hence, we obtain,

$$\pi^j\left(s^j,a^j\right) = \frac{1}{z^j+1} + \frac{1}{z^j+1}\cdot\frac{\Psi^j\Omega^T\left(s^j,a^j\right)}{\Gamma} + \wp\left\{\frac{\Psi^j\Omega^T\left(s^j,q^j\right)}{\Gamma}\right\} \tag{6.37}$$

where $\wp\left\{\frac{\Psi^j\Omega^T\left(s^j,q^j\right)}{\Gamma}\right\}$ is the smaller order polynomial than $\mathrm{O}\left[\frac{\Psi^j\Omega^T\left(s^j,a^j\right)}{\Gamma}\right]$. By exploiting the optimal historic actions, the reference approach can be estimated as follows,

$$\pi_\Delta^j\left(s^j,a^j\right) = \frac{1}{z^j+1} + \frac{1}{z^j+1}\cdot\frac{\Psi^j\Omega^T\left(s^j,\Psi\right)}{\Gamma} + \wp\left\{\frac{\Psi^j\Omega^T\left(s^j,q^j\right)}{\Gamma}\right\} \tag{6.38}$$

By substituting (6.37) and (6.38) in (6.36), we obtain,

$$\sum_{a^{-j}\in A^{-j}}\left[\left\{\psi_t^j\left(s^j,a^j\right)-\psi_{t-1}^j\left(s^j,a^j\right)\right\}\mathbb{R}^j\left(s^j,a^j,a^{-j}\right)\right] = \sum_{a^{-j}\in A^{-j}}\frac{\sigma^j\mathbb{R}^j\left(s^j,a^j,a^{-j}\right)}{\Gamma}\cdot\frac{1}{z^j+1}\left[\Psi^j\Omega^T\left(s^j,a^j\right)-\Psi^j\Omega^\tau\left(s^j,\Psi\right)\right] \tag{6.39}$$

For large value of Γ, we formulate (6.40),

$$\sum_{a^{-j}\in A^{-j}}\left[\left\{\psi_t^j\left(s^j,a^j\right)-\psi_{t-1}^j\left(s^j,a^j\right)\right\}\mathbb{R}^j\left(s^j,a^j,a^{-j}\right)\right] \le \frac{1-\gamma}{z^j+1}\left[\Psi^j\Omega^T\left(s^j,a^j\right)-\Psi^j\Omega^T\left(s^j,\Psi\right)\right] \tag{6.40}$$

Replace $\frac{1-\gamma}{z^j+1} = \Im$ for notation simplification.

$$\Psi_t^j = E\left[\left(\Im\left[\Psi^j\Omega^T\left(s^j,a^j\right)-\Psi^j\Omega^T\left(s^j,\Psi\right)\right]+\gamma\Psi_t\Omega^T\left(s_\Delta^j,\Psi_t\right)-\Psi_t\Omega^T\left(s^j,a^j\right)\right)\Omega\left(s^j,a^j\right)\right] \tag{6.41}$$

${}^1\Psi_t$ and ${}^2\Psi_t$ are two trajectories of the ODE and it follows ${}^0\Psi_t = {}^1\Psi_t - {}^2\Psi_t$. These trajectories have distinct initial conditions. Then (6.42) shows that,

$$\frac{\partial\left\|{}^{0}\Psi_t\right\|^2}{\partial t} = 2\left({}^{1}\Psi_t - {}^{2}\Psi_t\right)\left({}^{0}\Psi_t\right)^{\tau} =$$
$$E\left[\begin{array}{l}\left(-2\Im\,{}^{1}\Psi_t\Omega^T\left(s^j,{}^{1}\Psi_t\right)+2\gamma\,{}^{1}\Psi_t\Omega^T\left(s^j_{\Delta},{}^{1}\Psi_t\right)\right)\Omega\left(s^j,a^j\right)\left({}^{0}\Psi_t\right)^{\tau}\\ -\left(-2\Im^2\Psi_t\Omega^T\left(s^j,{}^{2}\Psi_t\right)+2\gamma^2\Psi_t\Omega^T\left(s^j_{\Delta},{}^{2}\Psi_t\right)\right)\Omega\left(s^j,a^j\right)\left({}^{0}\Psi_t\right)^{\tau}\end{array}\right]+(2\Im-2)\,{}^{0}\Psi_t\zeta\left({}^{0}\Psi_t\right)^{T} \tag{6.42}$$

The following equalities can be solved according to the Definition 1.

$${}^{1}\Psi_t\Omega^T\left(s^j_{\Delta},{}^{1}\Psi_t\right) \le {}^{1}\Psi_t\Omega^T\left(s^j_{\Delta},{}^{2}\Psi_t\right) \tag{6.43}$$

$${}^{2}\Psi_t\Omega^T\left(s^j_{\Delta},{}^{2}\Psi_t\right) \le {}^{2}\Psi_t\Omega^T\left(s^j_{\Delta},{}^{1}\Psi_t\right) \tag{6.44}$$

In (6.42) the expectation function is obtained over various states and various actions; hence the two different groups are, $\Phi^+ = \left[\left(s^j,a^j\right)\in S^j\times A^j|{}^{0}\Psi_t\Omega^T\left(s^j,a^j\right)>0\right]$ and $\Phi^-\in S^j\times A^j-\Phi^+$. After combining the (6.43) and (6.42) in (6.42), we obtain (6.45),

$$\begin{aligned}\frac{\partial\left\|{}^{0}\Psi_t\right\|^2}{\partial t} &\le E\left[\left(-2\Im\,{}^{0}\Psi_t\Omega^T\left(s^j,{}^{2}\Psi_t\right)+2\gamma\,{}^{0}\Psi_t\Omega^T\left(s^j_{\Delta},{}^{2}\Psi_t\right)\right)\Omega\left(s^j,a^j\right)\left({}^{0}\Psi_t\right)^{\tau}|\Phi^+\right]\\ &+E\left[\left(-2\Im\,{}^{0}\Psi_t\Omega^T\left(s^j,{}^{1}\Psi_t\right)+2\gamma\,{}^{0}\Psi_t\Omega^T\left(s^j_{\Delta},{}^{1}\Psi_t\right)\right)\Omega\left(s^j,a^j\right)\left({}^{0}\Psi_t\right)^{\tau}|\Phi^-\right]\end{aligned} \tag{6.45}$$

After applying the Holder inequality [91] in (6.45),

$$\frac{\partial\left\|{}^{0}\Psi_t\right\|^2}{\partial t} \le \tau \le \varepsilon \tag{6.46}$$

As stated in (6.33), the following can be said that,

$$\frac{\partial\left\|{}^{0}\Psi_t\right\|^2}{\partial t} < (-2\Im+2\gamma)\,{}^{0}\Psi_t\zeta\left({}^{0}\Psi_t\right)^{T}+(2\Im-2)\,{}^{0}\Psi_t\zeta\left({}^{0}\Psi_t\right)^{T} = (2\gamma-2)\,{}^{0}\Psi_t\zeta\left({}^{0}\Psi_t\right)^{T} < 0 \tag{6.47}$$

It shows that ${}^{*}\Psi$ converges to the origin and confirms the existence of a stable point of the ODE in (6.34). As a result, the proposed scheme converges with probability 1. The ${}^{*}\Psi$ can be calculated as (6.48),

$$^{*}\Psi = E\left[\left\{\sum_{a^{-j}\in A^{-j}}\left[\psi_t^j\left(s^j,a^j\right)-\psi_{t-1}^j\left(s^j,a^j\right)\right]\mathbb{R}^j\left(s^j,a^j,a^{-j}\right)+\gamma\,{}^{*}\Psi\Omega^T\left(s_\Delta^j,{}^{*}\Psi\right)\right\}\Omega\left(s^j,a^j\right)\right]\zeta^{-1} \tag{6.48}$$

Therefore, the optimal learning based concise Q-function is expressed as,

$$\tilde{\mathbb{Q}}\left(s^j,a^j,{}^{*}\Psi\right) = {}^{*}\Psi\Omega\left(s^j,a^j\right) \tag{6.49}$$

6.3 Performance Evaluation

The convergence speed, EE, and SE metrics are considered to analyze the performance of the proposed ROPC scheme.

6.3.1 Experimental Results

As shown in Fig. 6.3, the convergence nature of the proposed scheme is evaluated for varied values of the learning rate (α). Note that, the α denotes an amount to which novel Q-values override the present Q-values. However, Fig. 6.3 indicates that the highest α value decreases the reward. The reason behind this is the local optimization causes to stuck the algorithm; thus, the reward goes down. Hence, the optimal value of α is considered to be 0.7.

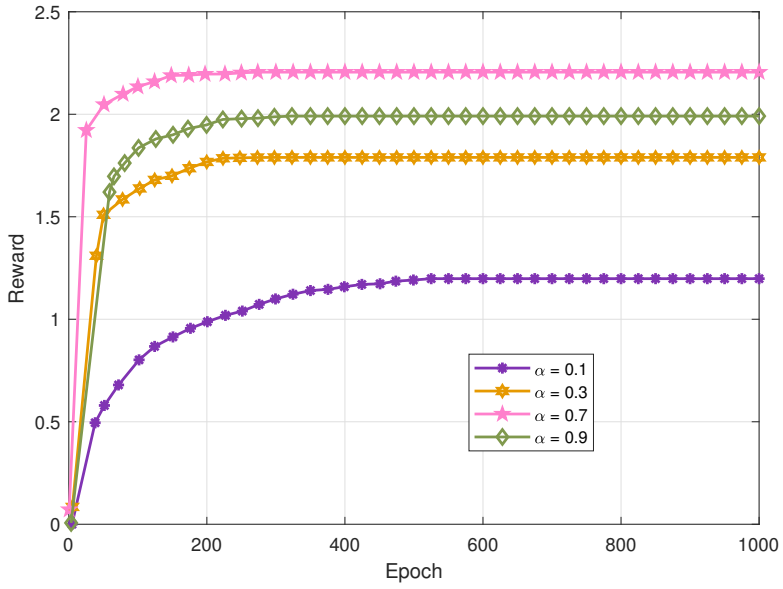

Figure 6.3: Convergence and reward for various learning rates α

Fig. 6.4 illustrates the convergence nature of the ROPC scheme for the distinct values of the discount factor. It has been observed that the value of the reward increases with the discount factor. The proposed scheme becomes improvident for $\gamma = 0.1$; hence, the immediate reward is considered for selecting the action. Instead of maximizing immediate rewards, each CT prefers to maximize future rewards for the high value of γ. Therefore, we consider the value of discount factor is 0.9. As the discount factor increases, the future reward become more significant compared to present rewards.

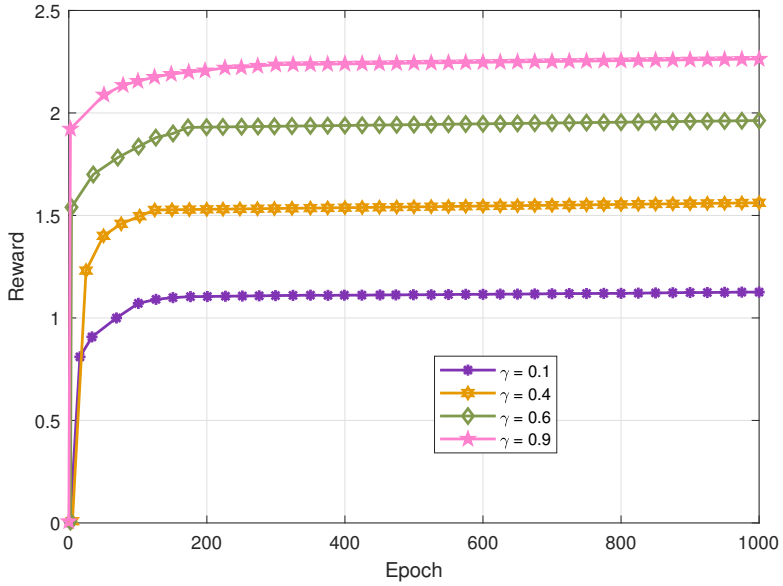

Figure 6.4: Convergence and reward for various values of discount factor γ

6.3.2 Simulation Results

The simulation results in terms of the EE, SINR, and SE have been presented in this subsection. The simulation environment contains multilayer heterogeneous CRNs. At each time t, the service request arrival follows the Poisson distribution having arrival rate 4λ here $\lambda = 0.2$. Next, the comparison of the proposed ROPC scheme with the non-learning (NL) scheme and other existing schemes has been illustrated. Table 6.1 represents the simulation parameters used for evaluation process.

6.3.2.1 EE Analysis

The network's EE in terms of reward is analyzed in Fig. 6.5. The convergence of proposed and various schemes is estimated in terms of the different number of epochs. The proposed scheme converges fast as; compared to the other schemes due to the real-time

Table 6.1: Simulation Parameters

Evaluation parameters and values			
Parameter	Value	Parameter	Value
Bandwidth	20 Mhz	No of macro cell	1
No of micro cell	5	No of femto cell	7
No of PUs	9	M2M connection	8
No of micro BS	5	No of femto BS	7
Radius of macro cell	300 m	Radius of micro cell	100 m
Radius of femto cell	15 m	Macro BS transmission power	45 dBm
Micro BS transmission power	15 dBm-40 dBm	Femto BS transmission power	12-20 dBm
cp of macro, micro, femto and M2M transmitter	120W, 20W, 6W, 0.1W	Thermal noise power	-120 dBm/Hz
Learning rate	0.7	Discount factor	0.9

analysis feature of the scheme. The other significant feature of the ROPC scheme is that this scheme can conjecture the policies of other agents. This feature minimizes the overhead of information exchange between CTs.

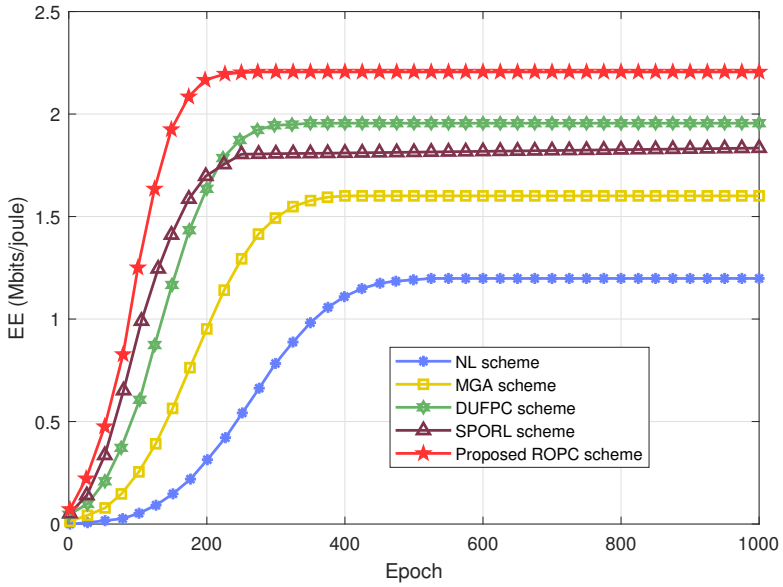

Figure 6.5: Comparison of network's EE for various schemes.

Fig. 6.6 shows the variation in network EE w.r.t. the number of CTs for the scenario of 7 Femto BSs, 5 micro-BSs, and 8 M2M connections. It is observed from Fig. 6.6 that initially, the EE rises with an rise in the number of CTs and then reduces with an rise in the number of CTs. The rationale behind this is that for a few numbers of CTs, there is

comparably low inter-cell interference and adequate signal strength to offset its effect. On the other hand, an inter-cell interference generated by the PBS and CTs increases with the number of CTs increases in the network. Therefore, more power level is needed to fulfill the QoS requirement of network, it results in lower EE.

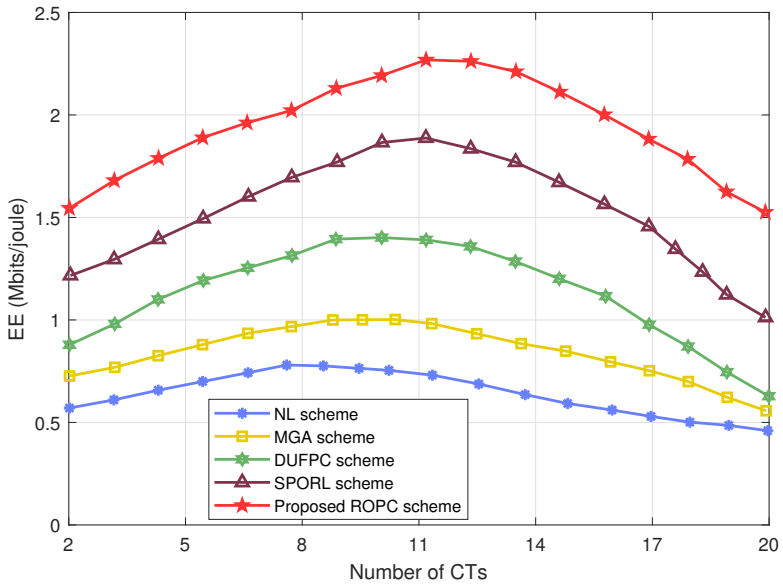

Figure 6.6: Network's EE for variable number of CT's

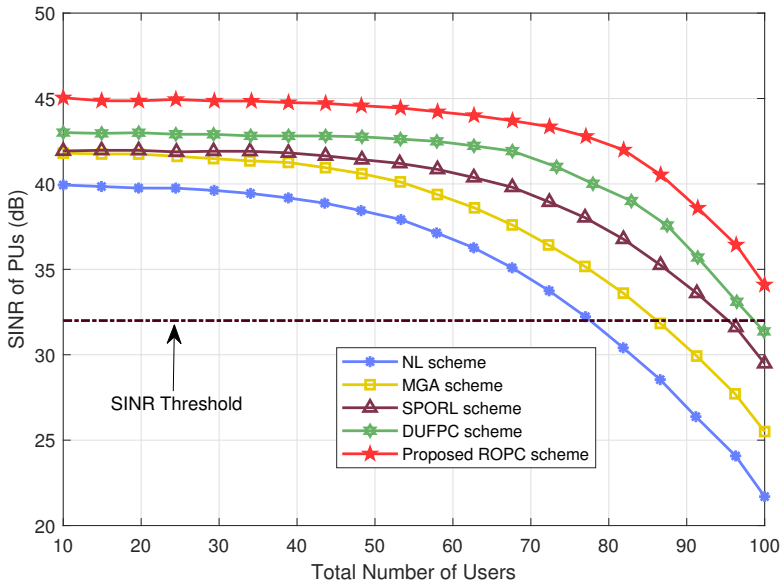

Figure 6.7: SINR for each PU vs total number of users

6.3.2.2 SINR Analysis

The achieved SINR of each PUs, femto users, and M2M receiver concerning the total number of users are indicated by the Fig. 6.7, Fig. 6.8, and Fig. 6.9, respectively. These

results conclude that the proposed scheme achieves the highest SINR as compared to the other schemes. Furthermore, despite a large number of users, the ROPC scheme maintains the minimal SINR needed by each layer. These results also indicate that implementing reinforcement learning in the suggested scheme sustains the QoS constraints throughout the learning approach. In addition to it, the constraints $\mathbb{C}.2$, $\mathbb{C}.3$, and $\mathbb{C}.4$ are satisfied by the ROPC scheme for both PUs and CUs.

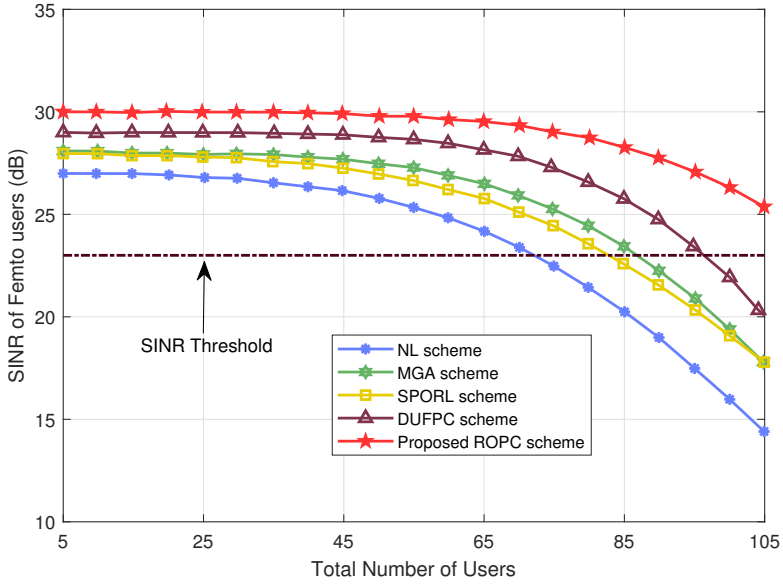

Figure 6.8: SINR for each FU vs total number of users

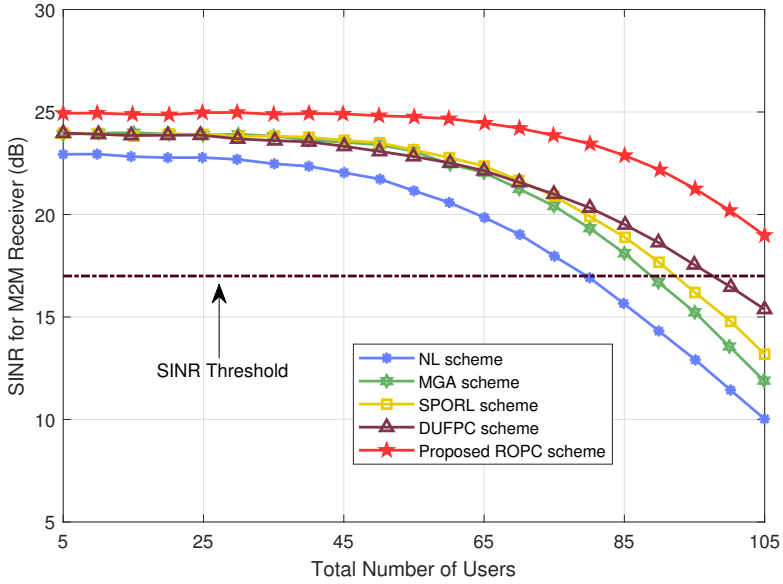

Figure 6.9: SINR for each M2M receiver vs total number of users

6.3.2.3 SE Analysis

These results indicate the performance of the proposed scheme in terms of SE metrics. This simulation part estimates the convergence speed and demonstrates the SE of the network. Fig. 6.10 shows that the proposed scheme achieves maximum SE in contrast to other conventional schemes and improve network performance.

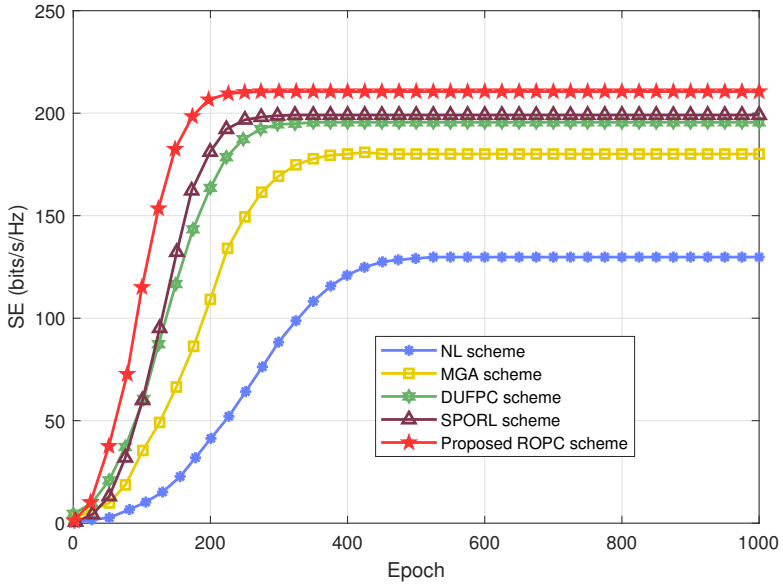

Figure 6.10: Network's SE for various schemes

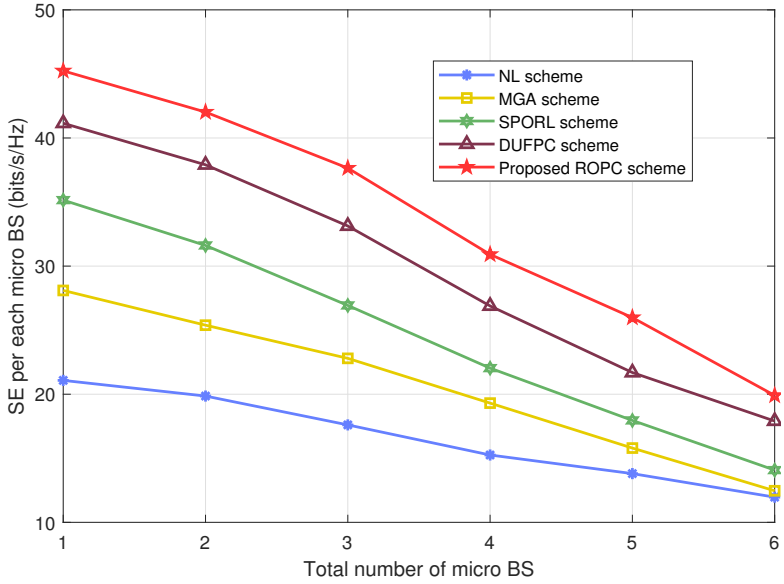

Figure 6.11: SE per each micro BS as a function of total number of micro BS

Additionally, an impact of the total number of specific kinds of CT on the attained SE per each CT of that kind is presented in Fig. 6.11. The SE per each microcell BS to

the total number of microcell BSs is plotted for various schemes. It can be observed that the proposed ROPC scheme achieves maximum SE and decreases with an increment in microcell BSs.

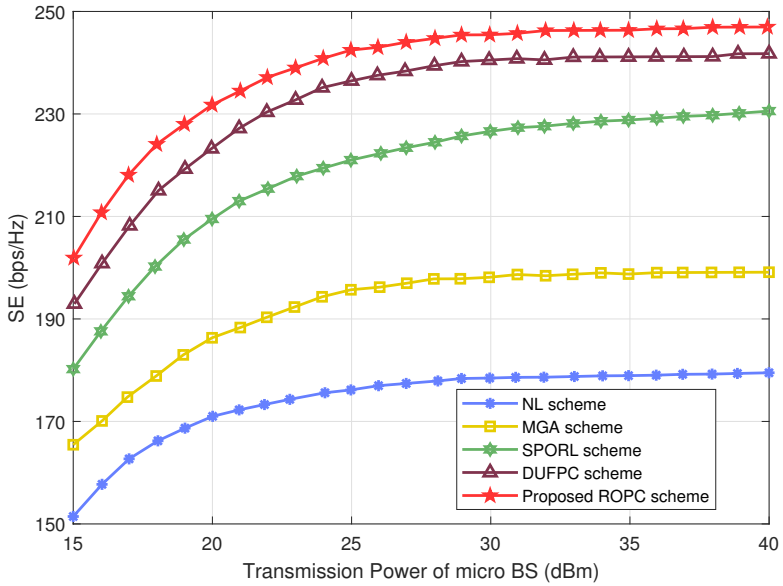

Figure 6.12: Network's SE for variable transmission power of micro BS

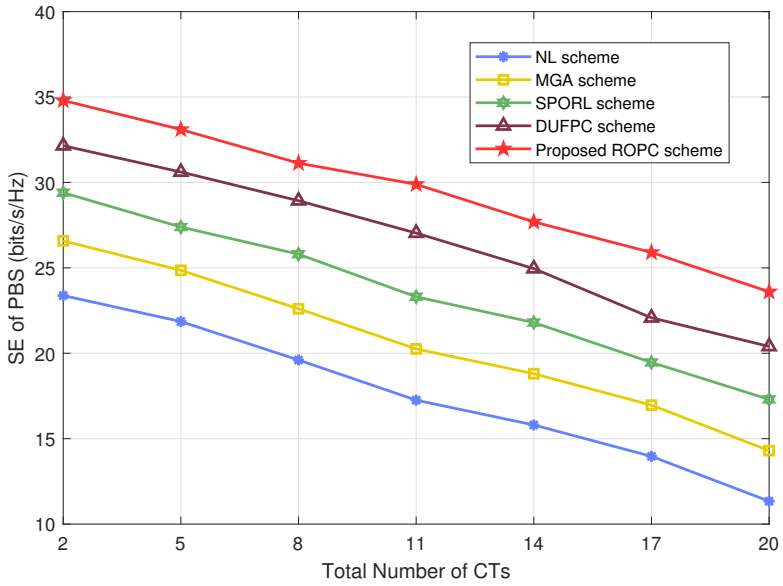

Figure 6.13: SE of PBS as a function of number of CTs

Fig. 6.12 illustrates the achieved network's SE for various schemes. Microcell BS is considered to analyze the impact of the transmission power on the netwok's SE. The result revels that the proposed ROPC scheme has highest SE with the fastest convergence. Fig. 6.13 indicates the SE of PBS as a function of the number of CTs. The SE

of PBS reduces with an increase in the number of CTs, because an increase in the number of CTs; the interference caused by the CTs is also increases in the network, which degrades the performance of PBS.

6.4 Conclusions

Energy saving is the key challenging issue in multilayer heterogeneous GCRNs architecture. This chapter addresses the power control issue for the downlink transmission in multilayer architecture, where microcells, femtocells, and M2M connections are inside the macro cell. A real-time learning-based scheme has been proposed to control transmission power and decrease the overall network power consumption while supporting QoS for multilayers. The reinforcement learning method takes into account the influence of cognitive transmitters' actions on the transmission power policy that has been chosen. In addition to this, the proposed ROPC scheme is based on the upgradation method for the Q-value. This feature of scheme helps to decrease the state/action pair and improves convergence speed. The suggested scheme's performance is proved by simulation, which shows that it achieves faster convergence and higher EE, SNIR, and SE than existing schemes.

Chapter 7

Conclusions and Future Directions

THIS chapter highlights the important conclusions drawn from these research objectives and gives the details of future scope of work in the field of next generation networks designing.

7.1 Conclusions

In first objective, various next generation green wireless communication networking techniques are investigated with consideration of energy-efficient transmission. The futuristic technologies like cognitive radio, carrier aggregation, Terahertz communication, Internet of Things (IoT), massive MIMO (multiple-input multiple-output) and mm wavelength are briefly reviewed to prepare for advancing recent research contributions. Further, the challenges related to green CRN and spectrum management are also reviewed.

The second objective examines two proposed channel selection strategies: probability-based and sensing-based channel selection strategies. The proposed channel selection methods evenly allocate the CU's traffic load among various applicant channels. Results of the work present that in the circumstances of huge traffic, SCSS reduces the total network time, while in the situation of low traffic, PCSS gives better results. These observations offer a vital perception in designing of traffic-adaptive channel selection strategy in the existence of PU's interruptions and sensing errors. The proposed strategies can minimize the total network time by 60% as compared to non-load balancing strategy for $\lambda_{cu} = 0.05$. Next, we calculate the total energy consumption at various op-

erational modes in GCRN. The results indicate that the arrival rate of the CUs and the time spent on channel scanning affect the energy consumption of the network. The proposed channel selection strategies reduce energy consumption by 75% as compared to non-load balancing strategy.

The third objective analyzes the benefits of cooperation between SUs for detecting the PU's spectrum, through which the rapidity of the network can be improved. Two cases (having a distinct level of cooperation) have been exploited to reduce the sensing time. The first one is non-cooperative, in which all SUs independently sense the PU, and the first user who senses first, informs the presence of the PU to the other SUs via a central controller. The second is cooperative, in which SUs follow the protocols of Amplify-and-Forward cooperation to minimize the sensing time. The results show that the proposed joint cooperation spectrum sensing (JCSS) scheme increases the sensing probability for a vacant spectrum by as much as 34%. After this, we propose two distinct spectrum sensing schemes preset spectrum sensing (PSS) and viscous spectrum sensing (VSS) that presents the energy savings percentage in GCRNs under specific conditions. These results conclude that the energy consumed by the user's contention increases due to the increase in sensing time. The proposed schemes are better in terms of scalability because it is not essential to sense all spectrums in these schemes.

The fourth objective has analysed a cooperation-based energy-efficient scheme for cognitive users in GCRN to improve the energy efficiency of CU. The proposed CEAR (cooperation-based energy-aware reward scheme) scheme supports CUs to actively cooperate by utilizing temporal and antenna diversity to improve energy efficiency. The proposed CEAR scheme is compared with other existing schemes, and it is presented that the CEAR scheme provides up to 28% improvement in energy efficiency. In this work, the optimal stopping protocol is used for problem formulation, and the backward induction method is employed for solving the decision problem. This chapter has contributed significant insight in terms of energy efficiency, spectral efficiency, throughput, and consumed energy, which motivates the design of future green communications systems.

In the final objective,a real-time learning-based scheme has been proposed to control transmission power and decrease the overall network power consumption while supporting QoS for multilayers. The reinforcement learning method takes into account

the influence of cognitive transmitters' actions on the transmission power policy that has been chosen. In addition to this, the proposed ROPC scheme is based on the upgradation method for the Q-value. This feature of scheme helps to decrease the state/action pair and improves convergence speed. The suggested scheme's performance is proved by simulation, which shows that it achieves faster convergence and higher EE, SNIR, and SE than existing schemes.

7.2 Future Directions

There are still new research areas for more effort to be achieved in this field. This part of the section delivers future research directions that entail the consideration of the research community. These new directions are discussed as:

7.2.0.1 Cooperative Heterogeneous Network (HetNet) Architecture

The upcoming generation of networks is likely to provision incorporation of various networks having diverse services and protocols. So, vertical handover, management of interference, enhancement in network capacity with the attention of energy efficient communication system is an important research topic. The tradeoff between spectral and energy efficiency and a tradeoff between network coverage and QoS in HetNet network also requires more investigation.

7.2.0.2 Green Networks

Energy-efficient approaches are the main prerequisite for the designing of GCRN. Thus, a new research area to minimize the EMR effect by the green networks is desired to be investigated. Two key research issues associated with GCRN are (1) decrease in consumption of power and energy overhead instigated by communication among mobile nodes and (2) optimization of dynamic spectrum allocation techniques to improve EE without distressing QoE of mobile subscribers.

7.2.0.3 Experimental Testbeds for Green Networks

For analyzing an impact of suggested energy-efficient approach for green networks, it is vital to test these approaches on realistic testbeds. In this way, the hardware realization

issues can be identified and would be able to check the viability of these proposed approaches. The absence of mature green networks modules in prevailing simulators offer new research direction to enterprise an experimental testbed to provision green networks.

7.2.0.4 Security

Auspicious of protected communication in green networks is a significant design objective for consistent advance next-generation wireless networks. It is a challenge to design an energy efficient approach for green communication to handle the EMR and GHG effect jointly with the utilization of RER for saving energy. In the available literature, energy-efficient approaches are focusing on the security of either network or mobile nodes. Secured green communication for both networks and mobile nodes, along with energy-efficient encrypted technique is required in future wireless communication systems.

7.2.0.5 Green networks Model for LTE/Wi-Fi coexistence

LTE network supports the modern wireless networks like carrier aggregation, massive MIMO, HetNet, D2D network with multiple cells of small size. The adaptive energy-efficient approach designed for green networks would be a promising technology in such advanced wireless networks. For example, HetNet comprises multiple cells of different sizes (termed as femto, pico, and microcells). So, the management of interference causes more complexity in networks. The coexistence of two different networks with combining their capabilities and energy- saving proposals would help in the formation of green networks, which is still an energetic research direction and will receive further attention.

References

[1] (01-11-2018) Internet user population will be increased. [Online]. Available: https://www.cisco.com

[2] (01-02-2019) Growth rate of different technologies. [Online]. Available: https://www.gsma.com/r/mobileeconomy/

[3] (11-11-2018) Growth rate of base station. [Online]. Available: https://www.telecomlead.com

[4] (01-06-2008) gas emmission. [Online]. Available: https://www.theclimategroup.org

[5] S. Lambert, W. Van Heddeghem, W. Vereecken, B. Lannoo, D. Colle, and M. Pickavet, "Worldwide electricity consumption of communication networks," *Optics express*, vol. 20, no. 26, pp. B513–B524, 2012.

[6] (01-02-2019) Population of mobile subscriber. [Online]. Available: https://www.gsma.com/r/mobileeconomy/asiapacific/

[7] (01-02-2019) Population of mobile subscriber in china. [Online]. Available: https://www.gsma.com/r/mobileeconomy/china/

[8] (01-02-2019) Population of mobile subscriber global. [Online]. Available: https://www.gsma.com

[9] (01-06-2019) addition of mobile users globally. [Online]. Available: https://www.ericsson.com

[10] (11-04-2019) 100s of birds drop from the sky at the hague in netherlands. [Online]. Available: http://www.radiationdangers.com

[11] (03-11-2018) Negetive impact on body organs. [Online]. Available: https://gizadeathstar.com

[12] S. S. Sandhu, A. Rawal, P. Kaur, and N. Gupta, "Major components associated with green networking in information communication technology systems," in *2012 International Conference on Computing, Communication and Applications*. IEEE, 2012, pp. 1–6.

[13] Y. Kremenetskaya, S. Markov, and S. Morozova, "Application of hybrid millimetre wave technology for green wireless communications," in *2018 IEEE 9th International Conference on Dependable Systems, Services and Technologies (DESSERT)*. IEEE, 2018, pp. 649–652.

[14] R. Mahapatra, Y. Nijsure, G. Kaddoum, N. U. Hassan, and C. Yuen, "Energy efficiency tradeoff mechanism towards wireless green communication: A survey," *IEEE Communications Surveys & Tutorials*, vol. 18, no. 1, pp. 686–705, 2016.

[15] D. Feng, C. Jiang, G. Lim, L. J. Cimini, G. Feng, and G. Y. Li, "A survey of energy-efficient wireless communications," *IEEE Communications Surveys & Tutorials*, vol. 15, no. 1, pp. 167–178, 2013.

[16] P. Gandotra and R. K. Jha, "A survey on green communication and security challenges in 5g wireless communication networks," *Journal of Network and Computer Applications*, vol. 96, pp. 39–61, 2017.

[17] T. Chen, H. Kim, and Y. Yang, "Energy efficiency metrics for green wireless communications," in *2010 International Conference on Wireless Communications & Signal Processing (WCSP)*. IEEE, 2010, pp. 1–6.

[18] L. Suarez, L. Nuaymi, and J.-M. Bonnin, "An overview and classification of research approaches in green wireless networks," *Eurasip journal on wireless communications and networking*, vol. 2012, no. 1, p. 142, 2012.

[19] T. A. Khan, A. Yazdan, and R. W. Heath, "Optimization of power transfer efficiency and energy efficiency for wireless-powered systems with massive mimo," *IEEE Transactions on Wireless Communications*, vol. 17, no. 11, pp. 7159–7172, 2018.

[20] M. R. Mili, L. Musavian, K. A. Hamdi, and F. Marvasti, "How to increase energy efficiency in cognitive radio networks," *IEEE Transactions on Communications*, vol. 64, no. 5, pp. 1829–1843, 2016.

[21] Y. Jiang, Y. Zou, J. Ouyang, and J. Zhu, "Secrecy energy efficiency optimization for artificial noise aided physical-layer security in ofdm-based cognitive radio networks," *IEEE Transactions on Vehicular Technology*, vol. 67, no. 12, pp. 11 858–11 872, 2018.

[22] J. Ouyang, M. Lin, Y. Zou, W.-P. Zhu, and D. Massicotte, "Secrecy energy efficiency maximization in cognitive radio networks," *IEEE Access*, vol. 5, pp. 2641–2650, 2017.

[23] C. Belady, A. Rawson, J. Pfleuger, and T. Cader, "Green grid data center power efficiency metrics: Pue and dcie," Technical report, Green Grid, Tech. Rep., 2008.

[24] R. C. Zoie, R. D. Mihaela, and S. Alexandru, "An analysis of the power usage effectiveness metric in data centers," in *2017 5th International Symposium on Electrical and Electronics Engineering (ISEEE)*. IEEE, 2017, pp. 1–6.

[25] A. A. Ibrahim, K. P. Kpochi, and E. J. Smith, "Energy consumption assessment of mobile cellular networks."

[26] P. Gandotra, R. K. Jha, and S. Jain, "Green communication in next generation cellular networks: A survey," *IEEE Access*, vol. 5, pp. 11 727–11 758, 2017.

[27] Y. Wu, Y. Chen, J. Tang, D. K. So, Z. Xu, I. Chih-Lin, P. Ferrand, J.-M. Gorce, C.-H. Tang, P.-R. Li *et al.*, "Green transmission technologies for balancing the energy efficiency and spectrum efficiency trade-off," *IEEE Communications Magazine*, vol. 52, no. 11, pp. 112–120, 2014.

[28] M. Parker and S. Walker, "Roadmapping ict: An absolute energy efficiency metric," *IEEE/OSA Journal of Optical communications and Networking*, vol. 3, no. 8, pp. A49–A58, 2011.

[29] Y. Zhang, Y. Xu, Y. Sun, Q. Wu, and K. Yao, "Energy efficiency of small cell networks: metrics, methods and market," *IEEE Access*, vol. 5, pp. 5965–5971, 2017.

[30] J. Wu, Y. Zhang, M. Zukerman, and E. K.-N. Yung, "Energy-efficient base-stations sleep-mode techniques in green cellular networks: A survey," *IEEE communications surveys & tutorials*, vol. 17, no. 2, pp. 803–826, 2015.

[31] M. Awasthi, M. Nigam, and V. Kumar, "Optimal sensing and transmission of energy efficient cognitive radio networks," *Wireless Personal Communications*, pp. 1–12, 2019.

[32] R. Saifan, I. Jafar, and G. Al Sukkar, "Optimized cooperative spectrum sensing algorithms in cognitive radio networks," 2017.

[33] I. S. Abdelfattah, S. I. Rabia, and A. M. Abdelrazek, "Optimal sensing energy and sensing interval in cognitive radio networks with energy harvesting," *International Journal of Communication Systems*, vol. 34, no. 7, p. e4742, 2021.

[34] X. Liu and M. Jia, "Intelligent spectrum resource allocation based joint optimization in heterogeneous cognitive radio," *IEEE Transactions on Emerging Topics in Computational Intelligence*, vol. 4, pp. 5–12, 2020.

[35] H. Kour, R. K. Jha, and S. Jain, "A comprehensive survey on spectrum sharing: Architecture, energy efficiency and security issues," *Journal of Network and Computer Applications*, vol. 103, pp. 29–57, 2018.

[36] H. Ding, X. Li, Y. Ma, and Y. Fang, "Energy-efficient channel switching in cognitive radio networks: A reinforcement learning approach," *IEEE Transactions on Vehicular Technology*, vol. 69, no. 10, pp. 12 359–12 362, 2020.

[37] K. Kumar, A. Prakash, and R. Tripathi, "A spectrum handoff scheme for optimal network selection in cognitive radio vehicular networks: A game theoretic auction theory approach," *Physical Communication*, vol. 24, pp. 19–33, 2017.

[38] A. A. Alotaibi and M. C. Angelides, "A serious gaming approach to managing interference in ad hoc femtocell wireless networks," *Computer Communications*, vol. 134, pp. 163–184, 2019.

[39] K. Atefi, S. Yahya, A. Rezaei, and A. Erfanian, "Traffic behavior of local area network based on m/m/1 queuing model using poisson and exponential distribution," in *2016 IEEE Region 10 Symposium (TENSYMP)*. IEEE, 2016, pp. 19–23.

[40] P. S. Bithas, A. A. Rontogiannis, and G. K. Karagiannidis, "An improved threshold-based channel selection scheme for wireless communication systems," *IEEE transactions on wireless communications*, vol. 15, no. 2, pp. 1531–1546, 2015.

[41] T. Nguyen, B. L. Mark, and Y. Ephraim, "Spectrum sensing using a hidden bivariate markov model," *IEEE Transactions on Wireless Communications*, vol. 12, no. 9, pp. 4582–4591, 2013.

[42] P. Thakur, A. Kumar, S. Pandit, G. Singh, and S. N. Satashia, "Spectrum monitoring in heterogeneous cognitive radio network: How to cooperate?" *IET Communications*, vol. 12, no. 17, pp. 2110–2118, 2018.

[43] H. R. Qavami, S. Jamali, M. K. Akbari, and B. Javadi, "A learning automata based dynamic resource provisioning in cloud computing environments," in *2017 18th International Conference on Parallel and Distributed Computing, Applications and Technologies (PDCAT)*. IEEE, 2017, pp. 502–509.

[44] P. Poornima and S. Chithra, "Optimization of sensing time in cognitive radio networks based on localization algorithm," in *International Conference on Sustainable Communication Networks and Application*. Springer, 2019, pp. 38–48.

[45] M. Gupta and K. Kumar, "Progression on spectrum sensing for cognitive radio networks: A survey, classification, challenges and future research issues," *Journal of Network and Computer Applications*, 2019.

[46] X. Wu, J. Ma, Z. Xing, C. Gu, X. Xue, and X. Zeng, "Secure and energy efficient transmission for irs-assisted cognitive radio networks," *IEEE Transactions on Cognitive Communications and Networking*, vol. 8, no. 1, pp. 170–185, 2021.

[47] Y. Molina-Tenorio, A. Prieto-Guerrero, and R. Aguilar-Gonzalez, "Real-time implementation of multiband spectrum sensing using sdr technology," *Sensors*, vol. 21, no. 10, p. 3506, 2021.

[48] S. Agarwal and S. De, "Impact of channel switching in energy constrained cognitive radio networks," *IEEE Communications Letters*, vol. 19, no. 6, pp. 977–980, 2015.

[49] C. Thakur, S. Majumdar, and S. Chatterjee, "Performance of combined rf and non-rf based energy harvesting scheme for multi-relay cooperative cognitive radio network," in *2022 First International Conference on Electrical, Electronics, Information and Communication Technologies (ICEEICT)*. IEEE, 2022, pp. 1–5.

[50] X. Liu, M. Xia, P. Hu, K. Zheng, and S. Zhang, "Optimal time allocation for energy harvesting cognitive radio networks with multichannel spectrum sensing," *Wireless Communications and Mobile Computing*, vol. 2022, 2022.

[51] A. Kumar and K. Kumar, "Energy-efficient resource optimization using game theory in hybrid noma assisted cognitive radio networks," *Physical Communication*, p. 101382, 2021.

[52] M. S. Gupta and K. Kumar, "AFSOS: An auction framework and stackelberg game oriented optimal networks resource selection technique in cognitive radio networks," *IEEE Transactions on Network and Service Management*, vol. 19, no. 1, pp. 61–72, 2021.

[53] A. Kumar and K. Kumar, "A game theory based hybrid noma for efficient resource optimization in cognitive radio networks," *IEEE Transactions on Network Science and Engineering*, vol. 8, no. 4, pp. 3501–3514, 2021.

[54] M. S. Gupta and K. Kumar, "Application aware networks' resource selection decision making technique using group mobility in vehicular cognitive radio networks," *Vehicular Communications*, vol. 26, p. 100263, 2020.

[55] N. B. Halima and H. Boujemâa, "Energy harvesting for cooperative cognitive radio networks," *Wireless Personal Communications*, pp. 1–18, 2020.

[56] Y. Gao, H. He, Z. Deng, and X. Zhang, "Cognitive radio network with energy-harvesting based on primary and secondary user signals," *IEEE Access*, vol. 6, pp. 9081–9090, 2018.

[57] P. Verma and S. Kaur, "A framework on cognitive-based green communication technology to reduce the emission of co 2 in the system," in *2021 9th International Conference on Reliability, Infocom Technologies and Optimization (Trends and Future Directions)(ICRITO)*. IEEE, 2021, pp. 1–4.

[58] S. S. Nijhawan and H. C. Rai, "Performance analysis of energy harvesting in cognitive radio networks over nakagami-m fading channels," in *2020 IEEE International Conference on Computing, Power and Communication Technologies (GUCON)*. IEEE, 2020, pp. 877–884.

[59] P. Mukherjee and S. De, "A system state aware switched-multichannel protocol for energy harvesting crns," *IEEE Transactions on Cognitive Communications and Networking*, vol. 6, no. 2, pp. 669–682, 2019.

[60] M. Waqas, S. Aslam, Z. Ali, G. A. S. Sidhu, Q. Xin, and J. W. Jang, "Resource optimization for cognitive radio based device to device communication under an energy harvesting scenario," *IEEE Access*, vol. 8, pp. 24 862–24 872, 2020.

[61] O. Abdulghafoor, M. Shaat, I. Shayea, F. E. Mahmood, R. Nordin, and A. K. Lwas, "Efficient power allocation algorithm in downlink cognitive radio networks," *ETRI Journal*, 2022.

[62] A. F. Isnawati and M. A. Afandi, "Game theoretical power control in heterogeneous network," in *2021 9th International Conference on Information and Communication Technology (ICoICT)*. IEEE, 2021, pp. 149–154.

[63] R. Amiri, M. A. Almasi, J. G. Andrews, and H. Mehrpouyan, "Reinforcement learning for self organization and power control of two-tier heterogeneous networks," *IEEE Transactions on Wireless Communications*, vol. 18, no. 8, pp. 3933–3947, 2019.

[64] A. A. El-Saleh, T. M. Shami, R. Nordin, M. Y. Alias, and I. Shayea, "Multi-objective optimization of joint power and admission control in cognitive radio networks using enhanced swarm intelligence," *Electronics*, vol. 10, no. 2, p. 189, 2021.

[65] S. Fan, H. Tian, and C. Sengul, "Self-optimized heterogeneous networks for energy efficiency," *EURASIP Journal on Wireless Communications and Networking*, vol. 2015, no. 1, pp. 1–11, 2015.

[66] S. Xia and C. Yin, "Utility function based power control scheme in femtocell network," in *2020 International Conference on Cyber-Enabled Distributed Computing and Knowledge Discovery (CyberC)*. IEEE, 2020, pp. 316–320.

[67] R. Ranjan, N. Agrawal, and S. Joshi, "Interference mitigation and capacity enhancement of cognitive radio networks using modified greedy algorithm/channel assignment and power allocation techniques," *IET Communications*, vol. 14, no. 9, pp. 1502–1509, 2020.

[68] S. S. Mohite and U. Kolekar, "Power control optimization model in femto-macro networks by cso algorithm," in *2021 International Conference on Communication information and Computing Technology (ICCICT)*. IEEE, 2021, pp. 1–5.

[69] X. Cao, R. Ma, L. Liu, H. Shi, Y. Cheng, and C. Sun, "A machine learning-based algorithm for joint scheduling and power control in wireless networks," *IEEE Internet of Things Journal*, vol. 5, no. 6, pp. 4308–4318, 2018.

[70] N.-C. Wang and W.-J. Hsu, "Energy efficient two-tier data dissemination based on q-learning for wireless sensor networks," *IEEE Access*, vol. 8, pp. 74 129–74 136, 2020.

[71] I. Ahmed, M. K. Shahid, H. Khammari, and M. Masud, "Machine learning based beam selection with low complexity hybrid beamforming design for 5g massive mimo systems," *IEEE Transactions on Green Communications and Networking*, vol. 5, no. 4, pp. 2160–2173, 2021.

[72] V. Mohanakurup, V. S. Baghela, S. Kumar, P. K. Srivastava, N. V. Doohan, M. Soni, and H. Awal, "5g cognitive radio networks using reliable hybrid deep learning based on spectrum sensing," *Wireless Communications and Mobile Computing*, vol. 2022, 2022.

[73] J. Chen, Y. Wang, Y. Li, and E. Wang, "Qoe-aware intelligent vertical handoff scheme over heterogeneous wireless access networks," *IEEE Access*, vol. 6, pp. 38 285–38 293, 2018.

[74] V.-s. Feng and S. Y. Chang, "Determination of wireless networks parameters through parallel hierarchical support vector machines," *IEEE Transactions on Parallel and Distributed Systems*, vol. 23, no. 3, pp. 505–512, 2011.

[75] V. Maglogiannis, D. Naudts, A. Shahid, and I. Moerman, "An adaptive lte listen-before-talk scheme towards a fair coexistence with wi-fi in unlicensed spectrum," *Telecommunication Systems*, vol. 68, no. 4, pp. 701–721, 2018.

[76] X. Li and S. A. Zekavat, "Traffic pattern prediction and performance investigation in cognitive radio systems," in *2008 IEEE Wireless Communications and Networking Conference*. IEEE, 2008, pp. 894–899.

[77] L.-C. Wang, C.-W. Wang, and C.-J. Chang, "Modeling and analysis for spectrum handoffs in cognitive radio networks," *IEEE Transactions on Mobile Computing*, vol. 11, no. 9, pp. 1499–1513, 2011.

[78] C.-H. Ng and S. Boon-Hee, *Queueing modelling fundamentals: With applications in communication networks*. John Wiley & Sons, 2008.

[79] A. Zanella and F. De Pellegrini, "Mathematical analysis of ieee 802.11 energy efficiency," in *Proc. WPMC*. Citeseer, 2004, pp. 1–5.

[80] G. Kaur, M. Dhamania, P. Tomar, and P. Singh, "Efficient integration of high-order models using an fdtd–tdma method for error minimization," in *International Conference on Communications and Cyber Physical Engineering 2018*. Springer, 2018, pp. 311–323.

[81] Y. Li, K. Li, W. Li, Y. Zhang, M. Sheng, and J. Chu, "An energy-efficient power control approach for ieee 802.11 n wireless lans," in *2014 IEEE International Conference on Computer and Information Technology*. IEEE, 2014, pp. 49–53.

[82] G. Kaur, P. Tomar, and P. Singh, "Design of cloud-based green iot architecture for smart cities," in *Internet of Things and Big Data Analytics Toward Next-Generation Intelligence*. Springer, 2018, pp. 315–333.

[83] M. H. Dwijaksara, W. S. Jeon, and D. G. Jeong, "User association for load balancing and energy saving in enterprise wlans," *IEEE Systems Journal*, vol. 13, no. 3, pp. 2700–2711, 2019.

[84] S. Kumar, P. S. Chauhan, P. Raghuwanshi, and M. Kaur, "Ed performance over α-η-μ/ig and α-κ-μ/ig generalized fading channels with diversity reception and cooperative sensing: A unified approach," *AEU-International Journal of Electronics and Communications*, vol. 97, pp. 273–279, 2018.

[85] J. N. Laneman, D. N. Tse, and G. W. Wornell, "Cooperative diversity in wireless networks:efficient protocols and outage behavior," *IEEE Transactions on Information theory*, vol. 50, pp. 3062–3080, 2004.

[86] S. Kumar, M. Kaur, N. K. Singh, K. Singh, and P. S. Chauhan, "Energy detection based spectrum sensing for gamma shadowed α–η–μ and α–κ–μ fading channels," *AEU-International Journal of Electronics and Communications*, vol. 93, pp. 26–31, 2018.

[87] H. Yu, "Optimal channel sensing in cognitive radio network with multiple secondary users," in *International Conference on Grid and Pervasive Computing*. Springer, 2013, pp. 838–845.

[88] A. Srivastava, M. S. Gupta, and G. Kaur, "A game theory based approach for opportunistic channel access in green cognitive radio networks," in *2019 IEEE International Conference on Advanced Networks and Telecommunications Systems (ANTS)*. IEEE, 2019, pp. 1–6.

[89] D. L. Evans, L. M. Leemis, and J. H. Drew, "The distribution of order statistics discrete random variables with applications to bootstrapping," *INFORMS Journal on Computing*, vol. 18, no. 1, pp. 19–30, 2006.

[90] R. Zhong, Y. Liu, X. Mu, Y. Chen, and L. Song, "Ai empowered ris-assisted noma networks: Deep learning or reinforcement learning?" *IEEE Journal on Selected Areas in Communications*, vol. 40, no. 1, pp. 182–196, 2021.

[91] F. Yan and Q. Gao, "Extensions and demonstrations of hölders inequality," *Journal of Inequalities and Applications*, vol. 2019, no. 1, pp. 1–12, 2019.

List of Publications

[1] Akanksha Srivastava, Gurjit Kaur, "Cooperation and Energy Harvesting based Spectrum Sensing Schemes for Green Cognitive Radio Networks," *Transactions on Emerging Telecommunications Technologies*, pp. e4714, 2022. [SCI indexed journal Impact Factor: 3.31].

[2] Akanksha Srivastava, Gurjit Kaur, "CEAR: A Cooperation based Energy Aware Reward Scheme for Next Generation Green Cognitive Radio Networks," *Physical Communication*, vol. 56, pp. 101947, 2023. [SCI indexed journal Impact Factor: 2.379]

[3] Akanksha Srivastava, Gurjit Kaur, "Resource management for traffic imbalance problem in green cognitive radio networks," *Physical Communication*, vol. 48, pp. 101437, 2021. [SCI indexed journal Impact Factor: 2.379]

[4] Akanksha Srivastava, Gurjit Kaur, "Optimal Power Control Scheme for Next Generation Multi-layer Green Cognitive Radio Networks: A Reinforcement Learning Perspective," *IEEE Transactions on Signal and Information Processing over Networks* [Under revision], [SCI indexed journal Impact Factor: 3.2]

[5] Akanksha Srivastava, Gurjit Kaur, "Blocking Probability Analysis for Energy Efficient Next Generation Green Cognitive Radio Networks," *IEEE-2nd Asian Conference on Innovation in Technology*, (ASIANCON-2022), IEEE. (Scopus)

[6] Akanksha Srivastava, Mani Shekhar Gupta, Gurjit Kaur, "Energy efficient transmission trends towards future green cognitive radio networks (5G): Progress, taxonomy and open challenges," *Journal of Network and Computer Applications*, vol. 168, pp. 102760, 2020. [SCI indexed journal Impact Factor: 8.7].

[7] Akanksha Srivastava, Mani Shekhar Gupta, Gurjit Kaur, "A Game Theory based Approach for Opportunistic Channel Access in Green Cognitive Radio Networks," *IEEE International Conference on Advanced Networks and Telecommunications Systems* , (ANTS-2019), IEEE. (Scopus)

[8] Gurjit Kaur, Yaman Parasher, Akanksha Srivastava, Prabhjot Singh, "Machine learningbased predictive modeling for failure management of optical spatial mode division multiplexing system," *International Journal of Communication Systems*, John Wiley & Sons Ltd, vol. 35, pp. e5337, 2022. [SCI indexed journal Impact Factor: 2.1]

Patent Filed

- Akanksha Srivastava, Gurjit Kaur, "OPPORTUNISTIC BANDWIDTH ACCESS USING UNLICENSED SPECTRUM AS A BACKUP RESOURCE (OBUB)," *Indian Patent Application No. 202211029217*, dated May 20, 2022.